Cairo University

5G PERFORMANCE IMPROVEMENT USING MASSIVE MIMO AND BEAMFORMING

By

Amal Samir Mohammed Mohammed

Salma Hasan Mahmoud Hasan Farghaly

Mariam Ashraf Fathy Mohamed

Mennat-Allah Mostafa Ali Mostafa Abd-Elrahman

Yomna Mohamed Abd-Elsattar Mahmoud Kandeel

A Graduation Project Report Submitted to
the Faculty of Engineering at Cairo University
in Partial Fulfillment of the Requirements for the
Degree of Bachelor of Science
in

Electronics and Communications Engineering

Faculty of Engineering, Cairo University

Giza, Egypt

August 2020

Table of Contents

List of Tables

List of Figures

List of Symbols and Abbreviations

Abbreviation	Definitions
3G	3rd Generation
3GPP	3rd Generation Partnership Project
4G	4th Generation
5G	5th Generation
ACK	Acknowledgement
ARQ	Automatic Repeat Request
BCH	Broadcast channel
BER	Bit error rate
BGN	Base graph number
BS	Base station
BW	Bandwidth
BWP	Bandwidth part
CDL	Cluster delay line
CP	Cyclic prefix
CQI	Channel quality indicator
CRC	Cyclic redundancy check
CRNTI	Cell Radio Network Temporary Identifier
CSI	Channel state information
DCI	Downlink control information
DL	Downlink
DLSCH	Downlink shared channel
DMRS	Demodulation reference signals
e-MBB	enhanced mobile broadband
FDD	Frequency division duplex
FEC	Forward error correction
FR1	Frequency range 1
FR2	Frequency range 2
GT	Guard time
HARQ	Hybrid automatic repeat request
ID	identification

IEEE	Institute of Electrical and Electronics Engineers
ITU	International Telecommunication Union
LDPC	Low density parity check
LMMSE	meast minimum meam square error
LOS	Lino of sight
LSB	Least significant bit
LTE	Long Term Evolution
MAC	Multiple access control
MMSE	Minimum mean square error
MSB	Most significant bit
mMTC	Massive Machine-Type Communications
NACK	No acknowledgement
NLOS	Non line of sight
NR	New radio
NRB	Number or resource block
OFDM	Orthogonal frequency division multiple access
PBCH	Physical broadcast shared channel
PDCCH	Physical downlink control channel
PMI	Precoding matrix indicator
PRACH	Physical random access channel
PRB	Physical resource block
PSS	Primary synchronization signals
PUSCH	Physical uplink shared channel
QAM	Quadrature amplitude modulation
QPSK	Quadrature phase modulation
RACH	Random access channel
RAR	Random Access Response
RB	Resource block
RE	Resource element
REG	Resource element group
RF	Radio frequency
RNTI	Radio Network Temporary Identifier
RRC	Radio Resource Control
RX	Receiver
SCS	Subcarrier spacing

SIB	System information block
SINR	Signal to interference noise ratio
SISO	Single input single output
SNR	Signal to noise ratio
SS	Synchronization Signal
SSB	Synchronization Signal Block
SSS	Secondary synchronization signal
SU	Single user
SVD	Singular vector deposition
TDD	Time division duplex
TDL	Tapped delay line
UE	User Equipment
UL	Uplink
URLLC	Ultra-Reliable Low-Latency Communications
VRB	Virtual resource block

Acknowledgments

Without the participation and assistance of so many people the completion of this undertaking could not have been possible. Their contributions are sincerely appreciated and gratefully acknowledged.

However, the group would like to express their deep indebtedness and appreciation to

Dr. Hassan Mostafa

Dr. Mohammed Nafei

Eng. Mohammed Abdel-Moniem

Eng. Abdulrahman Hamed

for their endless support, kind and understanding spirit.

Abstract

Fifth generation (5G) mobile communication is expected to enormously expand the capabilities of mobile networks than any of its predecessors as it provides higher network capacity, lower latency, and increased data rate. This is done using new technologies and functionalities that are introduced to 5G systems in various domains as massive MIMO (multiple-input and multiple-output) and digital beamforming.

This thesis studies the 5g system, its physical layer, and the effect of adding massive MIMO and beamforming in a multi-antenna wireless communications system using the MATLAB System Level Simulator. In simulations different subcarriers spacing and different bandwidths are evaluated.

To evaluate the effect of digital beamforming, two different precoders have been studied and compared in this thesis. These are, the Codebook based precoding and the singular vector decomposition (SVD) precoder. As for the effect of the massive MIMO an analysis of the simulation results is made for different number of transmitter antennas at the base station and receiver antennas at the user equipment besides sending up to eight data streams simultaneously. Addition comparisons are made between Line-of-Sight (LOS) and Non-Line-of-Sight (NLOS) propagation conditions accounting for fixed user, and comparisons between different channel and user parameters such as subcarrier spacing, used bandwidth and error correction usage.

All these contrasting scenarios will help the reader to understand the pros and cons of the two aforementioned precoding methods and the available parameters. Finally, an analysis of the simulation results is made to demonstrate the improvement in the system bit error rate (BER) and throughput resulted from beamforming and massive MIMO.

Chapter 1: Introduction

5G is the fifth-generation technology standards of telecommunications for cellular networks ,the 5G standard was set by the 3GPP(3rd generation partnership project) and the minimum standards are set by the ITU(international telecommunications union).Different from its predecessors,5G offers a new type of network that can connect virtually everyone and everything together including machines, objects, and devices.

5G is meant to deliver higher speed, ultra-low latency, more reliability, increased availability, and more uniform experience to more users. the increased benefits are mainly due to different factors that improve the system performance such as : the high frequency used to achieve higher data rates and lower latency ,the use of Massive MIMO (multiple-input-multiple-output) improves the penetration and coverage area and it was used on a smaller scale in 4G, 5G uses MIMO on a larger scale and can achieve higher capacity performance up to 8 times using beamforming, where the base station computes the best route for the radio waves to reach each wireless device while organizing multiple antennas to work together as phased arrays creating beams that can reach the device.

The 5G spectrum covers 3 different bands: low-band, mid-band, and high-band, all of which perform differently from each other, Low-band spectrum it offers great coverage area and wall penetration nut its peak data rate only reaches 100 Mbps. Mid-band spectrum**,** it provides faster speeds and lower latency than low band. But it doesn't penetrate buildings as effectively as low-band spectrum. Expect peak speeds up to 1Gbps on mid-band. High-band spectrum is what delivers the highest performance for 5G, as it can offer peak speeds up to 10Gbps and has really low latency but with major weaknesses such as low coverage area and poor building penetration.

The ITU has defined three main use cases for the enhanced capabilities of 5G. They are Massive machine to machine communications (mMTC) – also known as Internet of Things (IoT), Ultra-reliable low latency communications (URLLC) and enhanced mobile broadband (eMBB).

Only eMBB is deployed in 2020; URLLC and mMTC are several years away in most locations.

5G is expected to drive global economic growth as it can generate 13.2 trillion dollars of global economic output and create 22.3 million jobs, the 5G full economical effect will likely be realized by the year 2035, and as of June 2020 5G is launched in over 35 countries and more countries are expected to launch their 5G network by the end of 2020.

1.1 Background

1.1.1 USE CASES OF 5G

5G will target three use case families with very distinct features: enhanced mobile broadband (eMBB), massive machine-type communications (mMTC), and ultra-reliable low-latency communications (URLLC) the features of these three use case categories, are described during this subsection that are depicted in Fig. 1.1

- eMBB:

This use case category is taken into account the natural extension of the classic mobile connectivity scenario. That is done by providing a higher data rate across a wide coverage area and a better capacity to support peak data rates greater than 10 Gbps for end-users that are moving and in crowds.

- URLLC:

The main requirements on both reliability and latency are the distinctive features of this use case category, it provides low latency starting from 1 ms and below to few milliseconds and ultra-high reliability higher than 99.9999% for mission-critical services as smart grids, intelligent transportation and remote medical surgery.

- mMTC:

The main focus of the mMTC is on providing connectivity to an extremely massive number of devices that is not delay critical. The mMTC is a type of communication between machines that provides internet access for monitoring, sensing, and metering devices.

The number of mMTC devices is expected to exceed the number of devices carrying human-generated traffic so the growth of IoT is causing a proliferation of wirelessly connected devices carrying MTC traffic.

The unique feature of this use case is that the MTC devices will be totally heterogeneous in terms of cost, capabilities, and transmission power and energy consumption.

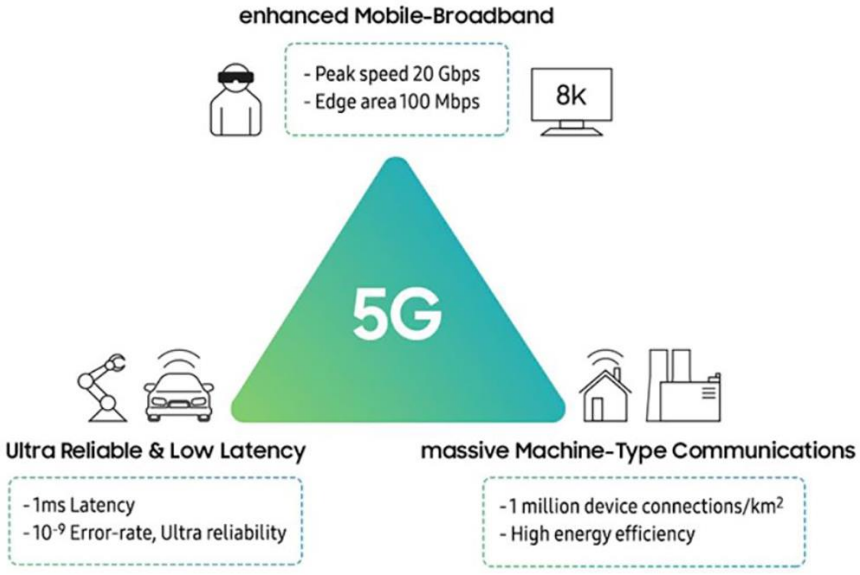

Figure 1-1: The three 5G use cases, and their main features

1.1.2 CAPABILITIES OF 5G NR

This subsection describes an overview of 5G NR key technical features and enhancements for realizing the three high level usage scenarios as mentioned in the subsection 1.1.1. The eight capabilities are shown in Fig.2.

- **Low latency**

One among the goals for every wireless generation has been to reduce latency. Latency measures how long a signal takes to travel from its source to its receiver, then back again as it will be an essential capability for the URLLC usage thus, it is going to be faster even than from human visual processing which make it possible to manage devices remotely in near-real time. It offers an ultra-low latency of 1ms and this means an instant response from the devices using that network.

- **High data rate**

One of the main advantages of the 5G network is that the huge bump in internet speeds that users would luckily enjoy, once they get access. No, it is not about 2 times increase in speeds but about 100 times more data speeds over the air as the predicted speed is up to 10Gbps.

- **High capacity**

The new 5G network will support more than 100 times more device handling capacity. This means that more and more people or devices would have the ability to connect to a given network without degrading the performance for the rest of the connected users.

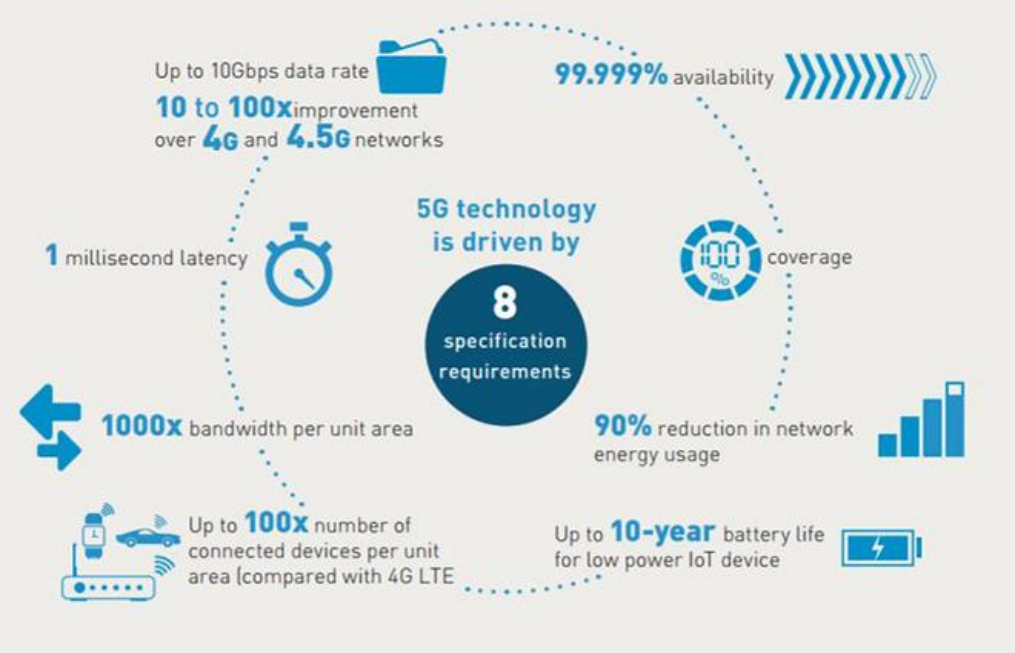

Figure 1-2: Capabilities needed for to support the 5G NR use cases

- **Long battery lifetime**

One of the worst impacts of high-speed networks is that they end up stressing the devices by consuming too much power and thus result in poor battery life but 5G is actually a mix of several technologies in one. The system, however, intelligent and knows when to make use of which technology for achieving maximum efficiency. Thereby, it allows the network to offer the best available connection to devices without searching which indeed preserves the battery life of devices such as phones.

- **Connecting massive number of devices**

5G is the key driver in creating an interconnected world. 5G and Massive IoT, this term is used to describe the world's massive number of connected sensors and devices that can communicate with each other, will be enabled in the 5G network infrastructure.

5G is expected to support up to 1 million connected devices per .38 square miles so that the network is able to handle the massive number of devices that is deployed for the IoT applications.

- **Spectrum and bandwidth flexibility**

Spectrum and bandwidth flexibility refer to the flexibleness of the system design to handle different scenarios, and particularly to the capability to operate at different frequency ranges, including wider channel bandwidths and higher frequencies than today.

- **Reliability**

Reliability relates to the capability for providing a given service with a very high level of availability.

- **Network slicing:**

5G makes it possible to implement virtual networks, which it means to create subnets, in order to provide connectivity adjusted to specific needs. The creation of sub-networks will give specific characteristics to a part of the network, being a programmable network and will allow to prioritize connections, as could be the emergencies in front of other users; therefore they can't be affected by possible overloads of the mobile network.

- **Coverage:**

From the most important benefits of 5G technologies is the better coverage for 5G users where signals will hit the places that were hard-to-reach places previously. Therefore, users will get the extraordinary quality they expect on their devices.

1.2 The Difference between 5G (NR) and 4G (LTE)

- 5G speeds will be nearly 10 times faster than 4G.
- 4G often struggled during peak hours; 5G will leave a more robust number of users to attach simultaneously.
- 5G latency will be decreased to 1 ms instead of 10 ms in 4G.
- Cell edge concept in 4G will disappear in 5G and the users will experience flat throughput.
- 5G connectivity would be stable enough to power home devices solely off the 5G network.

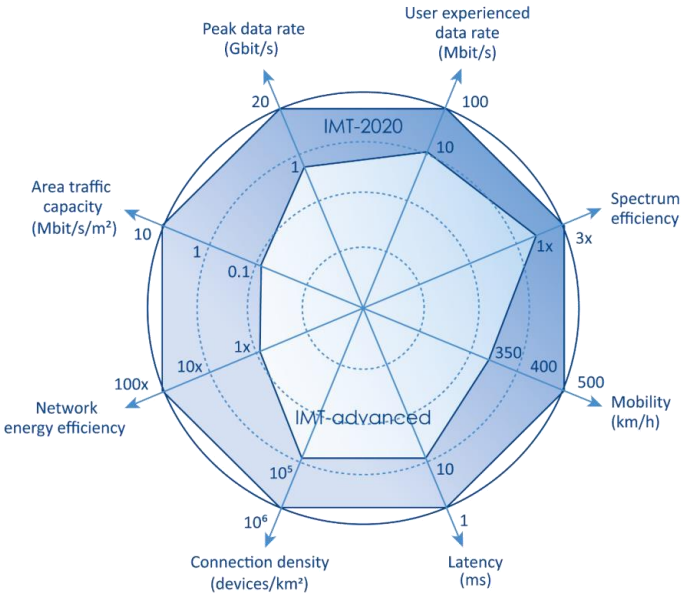

Figure 1-3: The differences between 4G and 5G

This thesis covers most of the main differences in technology between 4G and 5G such as LDPC and polar encoders, but in this section more differences between them will be explained.

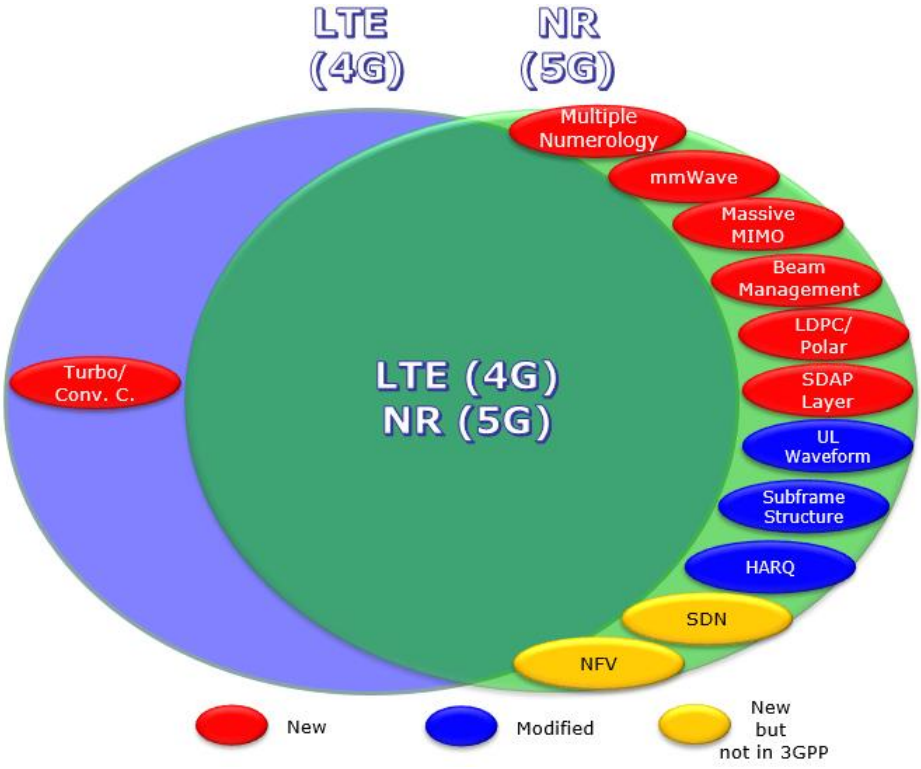

Figure 1-4 : 4G vs. 5G

1.2.1 Multiple Numerology

In LTE, there's just one numerology (subcarrier spacing) which is 15 KHz, but in NR various differing kinds of subcarrier spacing are supported; from 15 KHz to 240 KHz.

And counting on Numerology, frame structure gets different. Even more complex situation caused by this multiple numerology is that the case where different physical channels or signal use different subcarrier spacing, or different numerology is employed for various BWP even within the same gNB. And this results in complex translation between each resource elements / resource block.

1.2.2 Spectrum

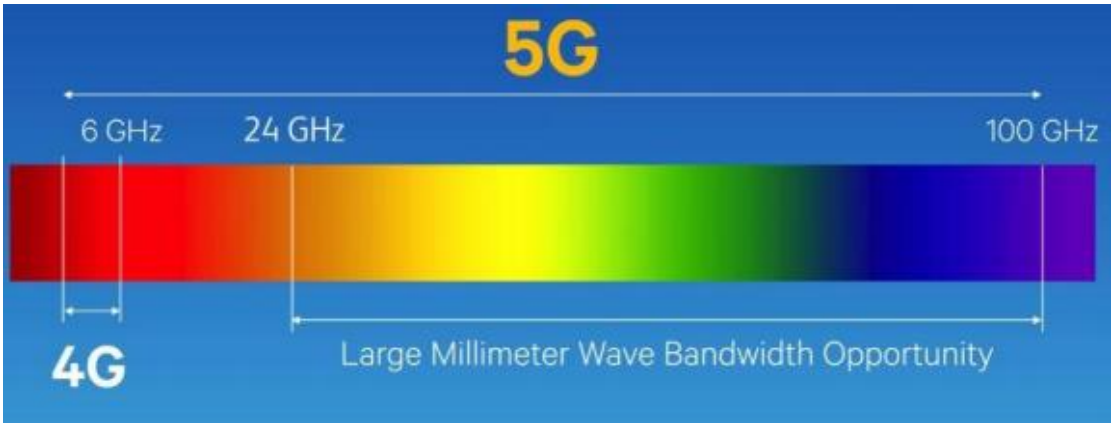

Figure 1-5:mmWave in 5G

Millimeter wave spectrum is that the band of spectrum between 30 GHz, and 300 GHz. this spectrum is used for high-speed wireless communications as seen in the newest IEE802.11ad Wi-Fi standard which operating at 60 GHz.

Even though at early phase 5G deployment in Sub 6 GHz, but the most unique aspect of NR deployment will be the support of mmWave .

1.2.3 Bandwidth part (BWP)

In 5G, BWP is a mechanism to define portions of frequency (fragment of band) region within a given band and let UE and gNB communicate within the portion. BWP in 5G is a similar concept as narrowband in LTE M1. But BWP can be described in more flexible fashion than narrowband.

Chapter 2: 5G NR Physical Layer

The physical layer is the backbone for any wireless technology and to meet the system requirements, the 5G NR physical layer has to support a wide range of frequencies from sub 1 GHz to 100 GHz and different services and deployment scenarios.

NR is the first mobile radio access technology going into mmWave frequency range targeting channel bandwidths in the GHz range and enabling massive multi-antenna systems.

3GPP NR Release 15 has developed a flexible physical layer for NR in June 2018. Any future releases of NR will be backwards compatible to the initial release.

In this chapter, we provide an overview of the NR physical layer based on the first NR release. The chapter is organized as follows. Section 1 is about the selection of the CP-OFDM of the 5G NR and how it is different from the LTE OFDM. In section 2, we describe the frame structure of the 5G NR in terms of subframes, slots and symbols configurations. In section 3, we explained why the TDD is the best choice for the eMBB use case. Section 4 is about the 5G NR spectrum and the reason why selecting the 3.5 GHz in this project. Section 5 is about the physical time-frequency resources of the 5G NR. Section 6 gives an overview of the physical channels' key technology components such as modulation and coding schemes. Also, the physical structure and the transport process of channels are explained briefly.

2.1 Waveform

CP-OFDM waveform is selected as it is compatible with multi-antenna technology, suitable for TDD and supports high spectral efficiency. CP-OFDM is also used in LTE for downlink transmissions. The LTE OFDM has fixed subcarrier spacing of 15 KHz while the 5G NR OFDM supports multiple numerologies as given by table 2-1 where μ and the cyclic prefix for a BWP are obtained from the higher-layer parameters of the subcarrier spacing and cyclic prefix respectively.

Note: The following table is taken from the 5G standard 3GPP TR 38.211 section 4.2

Table 2-1: Supported Transmission Numerologies

μ	Subcarrier spacing Δf	Cyclic-Prefix
0	15	Normal
1	30	Normal
2	60	Normal, Extended
3	120	Normal
4	240	Normal

Where: $\Delta f = 2^{\mu}.15\ KHz$

For all numerologies, the number of active subcarriers is 3300. Considering 3300 active subcarriers, the maximum bandwidth depends on the numerology and given by table 2-2 below:

Table 2-2: Maximum bandwidth enabled by different numerologies

Subcarrier spacing	15 KHz	30 KHz	60 KHz	120 KHz
Maximum bandwidth	50 MHz	100 MHz	200 MHz	400 MHz

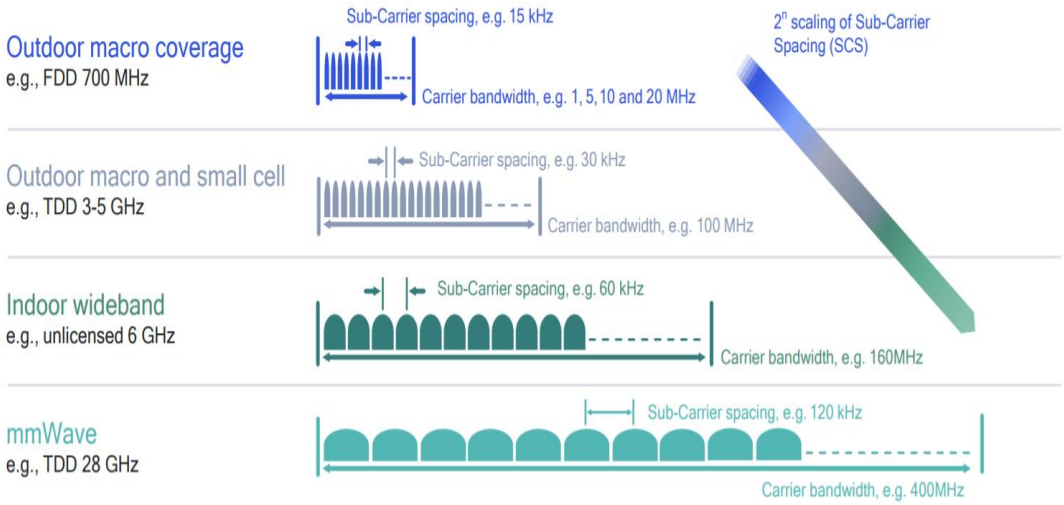

Figure 2-1:5G NR Scalable numerologies

Figure 2-1 above shows that the scalable numerology of the 5G NR OFDM enables diverse services on a wide range of frequencies and deployments.

2.2 Frame structure

The 5G NR Frame structure includes subframes, slots and symbol configurations. NR Frame structure is specified in the 3GPP specification TR 38.211 as shown in the following sections.

2.2.1 Subframes

A frame consists of 10 subframes having equally 1 ms duration. Each frame can have a number of slots as given in tables 2-3 and 2-4. Each slot occupies either 14 OFDM symbols or 12 OFDM symbols based on CP type.

Each 5G NR frame is divided into two half frames of equal size of 5 subframes in each. Half-frame 0 consists of subframes 0 to 4 and half-frame 1 consists of subframes 5 to 9.

2.2.2 Slot length

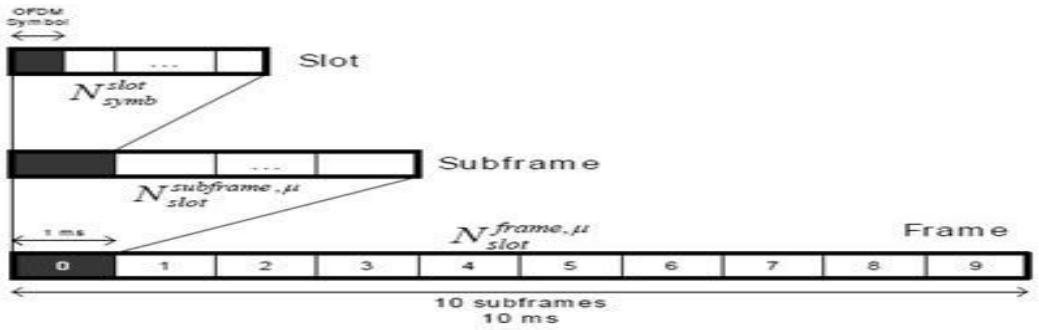

Figure 2-2: Frame Structure in 5G NR

A subframe has a fixed duration of 1 ms whereas the slot length varies depending on subcarrier spacing and the number of slots per subframe as given in tables 2-3 and 2-4 below:

Note: The following tables are taken from the 5G standard 3GPP TR 38.211 section 4.3.2

Table 2-3: Number of Symbols per Slot, Slots per Frame and Slots per Subframe for Normal CP

μ	Number of symbols per slot	Number of slots per frame	Number of slots per subframe
0	14	10	1
1	14	20	2
2	14	40	4
3	14	80	8
4	14	160	16

Table 2-4: Number of Symbols per Slot, Slots per Frame and Slots per Subframe for Extended CP

μ	Number of symbols per slot	Number of slots per frame	Number of slots per subframe
2	12	40	4

As shown in tables 2-3 and 2-4:

- Slot length is 1 ms for 15 KHz spacing, 500 μs for 30 KHz and so on.
- Subcarrier spacing of 15 KHz occupy 1 slot in subframe, Subcarrier spacing of 30 KHz occupy 2 slots in subframe and so on.

In this thesis, we are using normal cyclic prefix and simulating with different values of subcarrier spacing to determine its effect on throughput and bit error rate.

2.2.3 Symbols per slot

Number of symbols per slot depends on scheduling. In slot-based scheduling, slot consists of 14 OFDM symbols while in non-slot-based scheduling, slot consists of 2, 4 or 7 OFDM symbols. This mini slot is used for shorter transmission. Therefore, low-latency data can be sent without any waiting for all slot duration.

2.3 Spectrum

5G NR spectrum is divided to three bands: low-band, mid-band and high-band.

- Low band (sub 1 GHz): supports widespread coverage across urban, suburban and rural areas.
- Mid-band (from 1 GHz up to 6 GHz): offers good mixture of coverage and capacity benefits.

- High band (from 6 GHz up to 100 GHz): mmWave is needed to meet the ultra-high broadband speeds envisioned for 5G.

In our simulations, the 3.5 GHz band is selected as majority of commercial 5G networks depend on spectrum between 3.3 and 3.8 GHz.

In release 15, the operating bands are divided into two frequency ranges FR1 and FR2 as shown in table 2-5:

Note: The following table is taken from the 5G standard 3GPP TR 38.101 section 5.1

Table 2-5: Frequency Ranges in 5G NR

Frequency range	Corresponding range of frequencies
FR1	**450 MHz – 6000 MHz**
FR2	**24.25 GHz – 52.6 GHz**

In FR1, the supported subcarrier spacings are 15, 30 and 60 KHz. The supported bandwidth and the number of resource blocks for each bandwidth and subcarrier spacing are as shown in table 2-6:

Note: The following tables are taken from the 5G standard 3GPP TR 38.101 section 5.3.2

Table 2-6: Maximum transmission bandwidth configuration NRB for FR1

SCS/BW	5 MHz	10 MHz	15 MHz	20 MHz	25 MHz	40 MHz	50 MHz	60 MHz	80 MHz	100 MHz
15 KHz	**25**	**52**	**79**	**106**	**133**	**216**	**270**	**N/A**	**N/A**	**N/A**
30 KHz	**11**	**24**	**38**	**51**	**65**	**106**	**133**	**162**	**217**	**273**
60 KHz	**N/A**	**11**	**18**	**24**	**31**	**51**	**65**	**79**	**107**	**135**

In FR2, the supported subcarrier spacings are 60 and 120 KHz. The supported bandwidth and the number of resource blocks for each bandwidth and subcarrier spacing are as shown in table 2-7:

Table 2-7: Maximum transmission bandwidth configuration NRB for FR2

SCS/BW	50 MHz	100 MHz	200 MHz	400 MHz
60 KHz	66	132	264	N/A
120 KHz	32	66	132	264

NR is designed to operate in the operating bands defined by tables 2-8 and 2-9 below:

Note: The following tables are taken from the 5G standard 3GPP TR 38.104 section 5.2

Table 2-8:NR operating bands in FR1

NR *operating band*	Uplink (UL) *operating band* BS receive / UE transmit $F_{UL,low}$ – $F_{UL,high}$	Downlink (DL) *operating band* BS transmit / UE receive $F_{DL,low}$ – $F_{DL,high}$	Duplex Mode
n1	1920 MHz – 1980 MHz	2110 MHz – 2170 MHz	FDD
n2	1850 MHz – 1910 MHz	1930 MHz – 1990 MHz	FDD
n3	1710 MHz – 1785 MHz	1805 MHz – 1880 MHz	FDD
n5	824 MHz – 849 MHz	869 MHz – 894 MHz	FDD
n7	2500 MHz – 2570 MHz	2620 MHz – 2690 MHz	FDD
n8	880 MHz – 915 MHz	925 MHz – 960 MHz	FDD
n12	699 MHz – 716 MHz	729 MHz – 746 MHz	FDD
n20	832 MHz – 862 MHz	791 MHz – 821 MHz	FDD
n25	1850 MHz – 1915 MHz	1930 MHz – 1995 MHz	FDD
n28	703 MHz – 748 MHz	758 MHz – 803 MHz	FDD
n34	2010 MHz – 2025 MHz	2010 MHz – 2025 MHz	TDD
n38	2570 MHz – 2620 MHz	2570 MHz – 2620 MHz	TDD
n39	1880 MHz – 1920 MHz	1880 MHz – 1920 MHz	TDD
n40	2300 MHz – 2400 MHz	2300 MHz – 2400 MHz	TDD
n41	2496 MHz – 2690 MHz	2496 MHz – 2690 MHz	TDD
n50	1432 MHz – 1517 MHz	1432 MHz – 1517 MHz	TDD
n51	1427 MHz – 1432 MHz	1427 MHz – 1432 MHz	TDD
n65	1920 MHz – 2010 MHz	2110 MHz – 2200 MHz	FDD
n66	1710 MHz – 1780 MHz	2110 MHz – 2200 MHz	FDD
n70	1695 MHz – 1710 MHz	1995 MHz – 2020 MHz	FDD
n71	663 MHz – 698 MHz	617 MHz – 652 MHz	FDD
n74	1427 MHz – 1470 MHz	1475 MHz – 1518 MHz	FDD
n75	N/A	1432 MHz – 1517 MHz	SDL
n76	N/A	1427 MHz – 1432 MHz	SDL
n77	3300 MHz – 4200 MHz	3300 MHz – 4200 MHz	TDD
n78	3300 MHz – 3800 MHz	3300 MHz – 3800 MHz	TDD
n79	4400 MHz – 5000 MHz	4400 MHz – 5000 MHz	TDD
n80	1710 MHz – 1785 MHz	N/A	SUL
n81	880 MHz – 915 MHz	N/A	SUL
n82	832 MHz – 862 MHz	N/A	SUL
n83	703 MHz – 748 MHz	N/A	SUL
n84	1920 MHz – 1980 MHz	N/A	SUL
n86	1710 MHz – 1780 MHz	N/A	SUL

Table 2-9:NR operating bands in FR2

NR *operating band*	Uplink (UL) and Downlink (DL) *operating band* BS transmit/receive UE transmit/receive $F_{UL,low}$ – $F_{UL,high}$ $F_{DL,low}$ – $F_{DL,high}$	Duplex Mode
n257	26500 MHz – 29500 MHz	TDD
n258	24250 MHz – 27500 MHz	TDD
n260	37000 MHz – 40000 MHz	TDD
n261	27500 MHz – 28350 MHz	TDD

In this thesis, the operating frequency is 3.5 GHz in the n78 operating band.

2.4 Duplex mode

Time division duplex (TDD) is chosen over frequency division duplex (FDD) for the following reasons:

- TDD is more spectrum efficient since it requires only one frequency channel for DL and UL.
- Physical layer features such as precoding and beamforming depend on channel state information (CSI) measurements. Therefore, TDD makes it possible to use the uplink channel estimation data to determine the downlink precoding and beam directions.
- There is no need for duplexer.
- In TDD, it is possible to assign different amount of band for UL and DL based on system requirements. Therefore, most portion of band is allocated for DL in DL data centric networks such as internet browsing and streaming. And most portion of band is allocated for UL in UL data centric networks such as camera surveillance.

This is applicable for our use case (eMBB), while FDD is more suitable for other use cases such as URLLC as it provides low latency due to simultaneous transmission and reception.

In addition to the FDD and TDD bands, other bands have been allocated to provide supplementary uplink and downlink capacity. The bands marked SDL are for supplementary downlinks and SUL are for supplementary uplinks.

In supplementary uplink (SUL), when channel condition is good, Network tell UE to use the original UL frequency and when channel condition gets poor than a certain criteria, Network directs UE to use the supplementary UL frequency where the supplementary UL frequency is a low frequency to guarantee larger cell coverage.

NR bands that are dedicated for the SUL and SDL are defined in table 2-8 where all dedicated bands are under 2 GHz which is lower than the operating band in this project.

2.5 Physical time-frequency resources

The smallest time-frequency resource is the resource element (RE) which consists of one subcarrier in one OFDM symbol. A resource element (RE) is uniquely identified by (k, l) where k is the index in frequency domain and l refers to the symbol position in the time domain.

Transmissions are scheduled in groups of 12 subcarriers called the resource blocks (RB) and a set of RBs form a BWP.

The 5G NR resource grid is defined for each numerology and carrier as shown in figure 2-3. There is one set of resource grids per transmission direction (DL or UL).

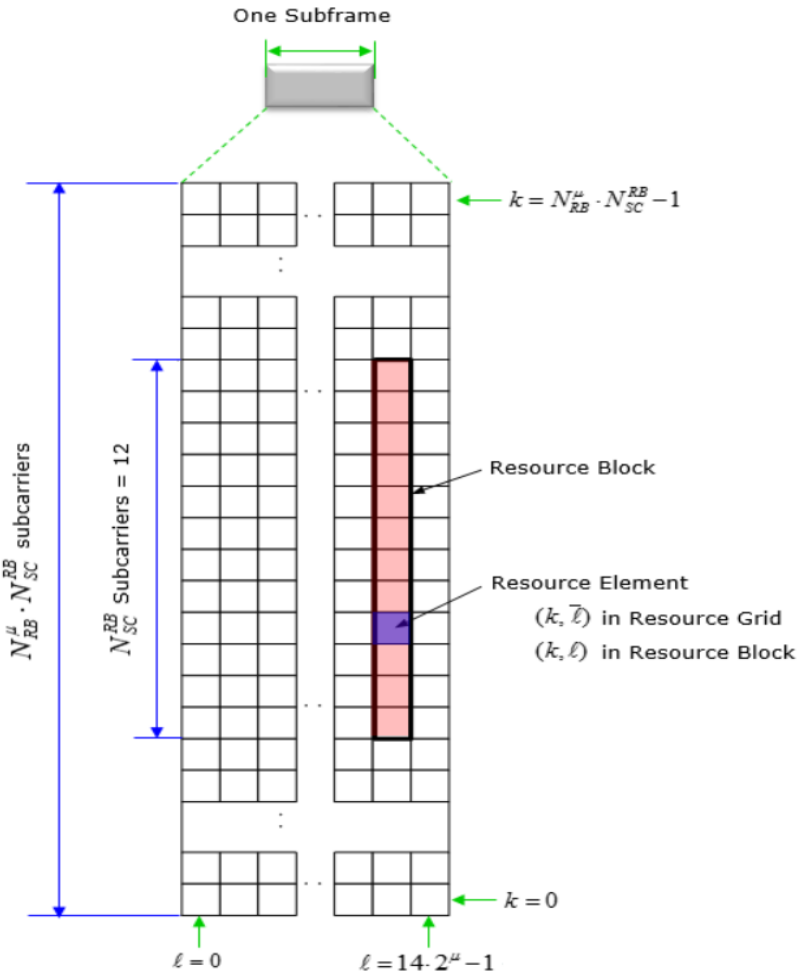

Figure 2-3:5G NR Resource Grid

2.5.1 Bandwidth part

A bandwidth part (BWP) is subset of contiguous resource blocks for a given numerology (SCS and CP) as shown in Figure 2-4. A UE can be configured with up to 4 DL BWPs and up to 4 UL BEPs for each serving cell. Per serving cell, only one BWP in DL and one in UL are active at a given time.

UEs cannot transmit or receive anything outside the frequency range for the active BWPs.

2.5.1.1 Why BWP?

Although 5G NR has a flexible mechanism of changing bandwidth dynamically by changing NRB, we need BWP concept to help low-end user-equipment (UEs) which cannot handle the full operating wideband of 5G NR. Therefore, we can say that BWP concept is more important for UE than for network.

This problem was not stated in LTE the maximum bandwidth was up to 20 MHz which can be handled by UEs unlike the 200 MHz maximum bandwidth of the 5G NR.

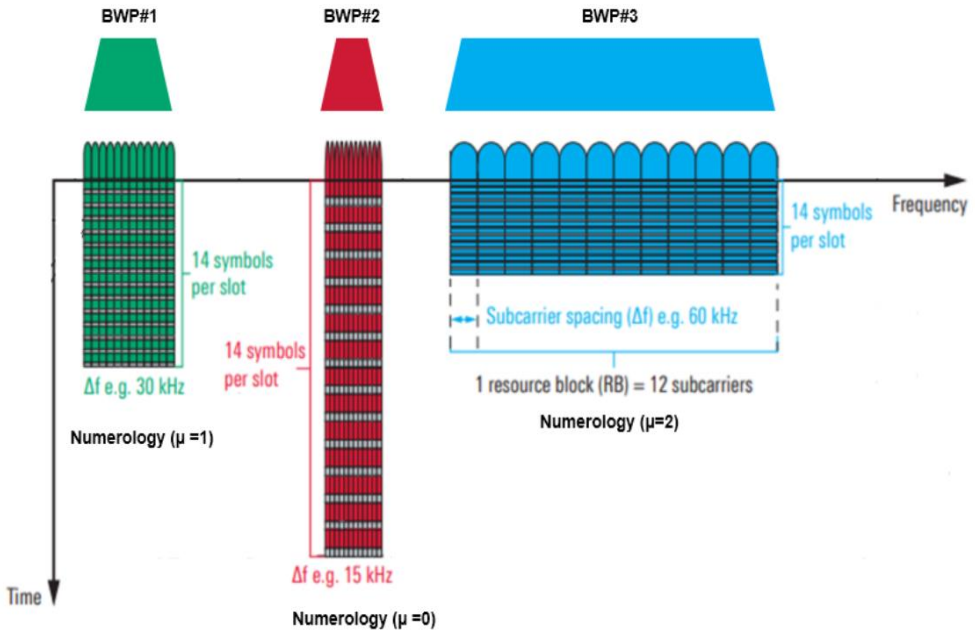

Figure 2-4: Bandwidth Part defined for different numerologies

2.6 Physical channels

2.6.1 Downlink shared channels

The downlink shared channel (DL-SCH) carries user data and the system information block (SIB). Data is coded by LDPC encoder then it is mapped to the physical downlink shared channel (PDSCH).

2.6.1.1 DL-SCH

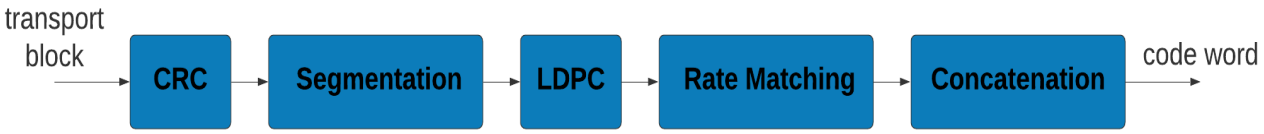

Figure 2-5:5G NR Downlink Shared Channel

Figure 2-5 shows the downlink shared channel in the physical layer and it contains , CRC block, segmentation block, LDPC (low density parity check) block, rate matching and concatenation blocks .the input of this chain is the transport block and the output is the code word.

2.6.1.1.1 CRC

Cyclic Redundancy Check is an error detection technique which adds a check value to the input data based on the remainder of polynomial division of the data. Then the received data is divided by the same polynomial. If the result is zero, then data is correct. If else, action can be taken to correct data.

The length of added check value (L) is based on length of the input data (A) as shown in table 2-8 below:

Table 2-10: Length of the added check value of CRC

L	Input data length
24	A > 3824
16	O.W

CRC polynomial in 5G NR can be specified as '6', '11', '16', '24A', '24B', or '24C'.

2.6.1.1.2 Segmentation

Segmentation occurs only when the input length is greater than the maximum code block size (CBS) which is determined based on the base graph number (BGN) as shown in table 2-9 below:

Table 2-11: Maximum code block size based on the BGN

BGN	Max Code Block Size
1	8448
2	3840

2.6.1.1.3 LDPC Encoder

Forward Error Correction (FEC) codes -such as Low-Density Parity Check (LDPC) codes- its main usage is to control errors in data transmissions over unreliable or noisy communication channels.

The LDPC codes theory is based on a branch of mathematics called graph theory, and these codes are linear block codes which use overlapping parity check sets where the amount of overlap is large enough to protect each bit but not so large that the correction problem becomes complex (low-density).

Channel coding in 5G must achieve the requirement of the 5G user such as, better flexibility, low latency, and high reliability in communication. In 3G and 4G, other channel coding schemes was used such as:

- Convolutional codes which are widely used in many standards because of the advantages, like low complexity encoding, and possibility of simple rate adaption.
  But also, they have problems, like when the message length increased, the bit error performance didn't improve. Therefore, they are not suitable for the message with long length.
  Convolutional codes are used in 2G, and 3G to transmit the control signals.

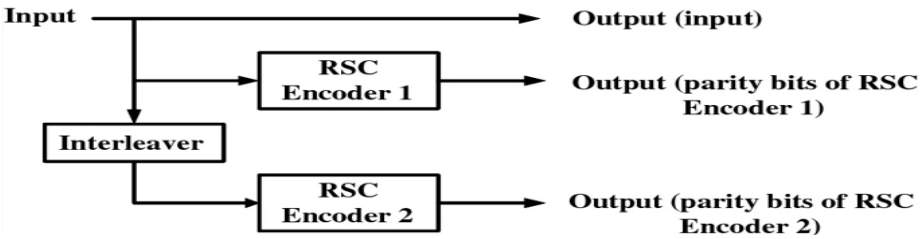

Figure 2-6: Turbo codes based on convolutional codes

- Turbo codes are based on convolutional codes but with interleaver between them, and because of this turbo codes took all the advantages from convolutional codes and solve the problem of the bit error performance which made them the channel coding schemes for 3G and 4G. However, turbo codes have some issues like high decoding complexity.

2.6.1.1.3.1 Why LDPC?

- LDPC codes computations is decomposed into larger number of smaller independent atomic units compared to turbo codes. This parallelism is more effectively achieved in hardware.
- LDPC codes have already been adopted in other wireless standards such as IEEE 802.11 and DVB.
- 5G LDPC codes are QC-LDPC codes which belong to a family of protograph codes. These codes have a rate-compatible structure that makes them suitable for HARQ protocols.
- LDPC codes can offer higher coding gains and have lower error floors compared to turbo codes.
- Consequently, the throughput of the LDPC decoder increases as the code rate increases.
- LDPC code shows inferior performance for short block lengths (< 400 bits) and at low code rates (< 1/3) which is typical scenario for URLLC and mMTC use cases.

2.6.1.1.4 Rate Matching

Rate matching is to match the number of bits of the transport block to the number of bits that can be transmitted in the given allocation. Rate matching operation of 5G LDPC codes is controlled by redundancy version value (rv) from 0 to 3, the modulation scheme and the number of transmission layers.

Rate matching includes bit selection, interleaving and code block concatenation.

2.6.1.2 PDSCH

Figure 2-7 shows the PDSCH (physical downlink shared channel), it consists of 5 blocks, they are: scrambling, modulation, layer mapping ,MIMO precoding and resource mapping. The input of the PDSCH is the output of the DLSCH which is the code word and the output of the PDSCH is the resource grid.

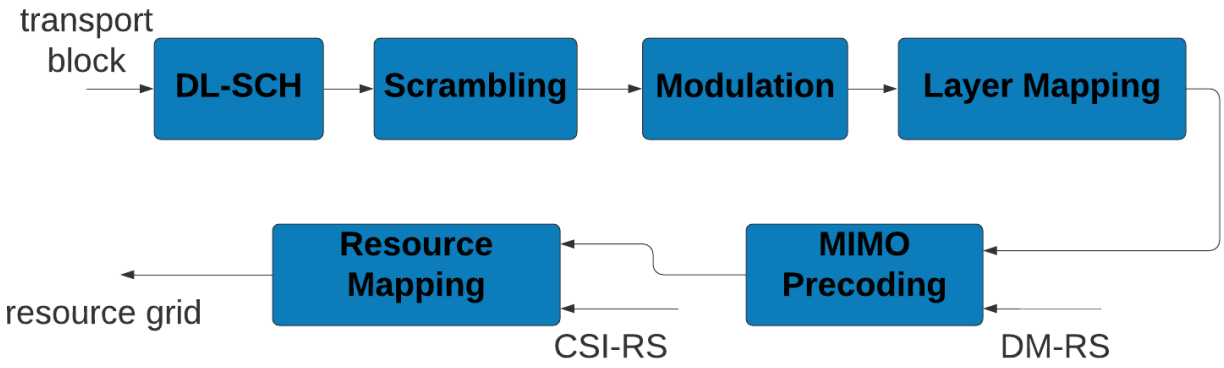

Figure 2-7:5G NR Physical downlink Shared Channel

2.6.1.2.1 Scrambling

Scrambling is converting an input bit stream into seemingly random output of the same length to avoid long sequences of bits of the same value. Scrambling is done based on the identity number (NID) and the RNTI of the UE.

Where the NID is a higher layer parameter (0 to 1023) or can be specified as the physical layer cell identity number (0 to 1007).

RNTI is the radio network temporary identifier (0 to 65535) which is used to differentiate users from each other, and each DCI message is scrambled by a specific RNTI value.

2.6.1.2.2 Modulation

Modulation is the process of mixing the signal with a carrier to produce a new signal based on the modulation scheme used. Modulation scheme for the data can be QPSK, 16-QAM, 64-QAM or 256-QAM.

2.6.1.2.3 Layer mapping

Mapping one or two codewords into a given number of transmission layers where:

Anything up to 4 layers uses a single codeword, anything beyond 4 layers uses a second codeword.

2.6.1.2.4 MIMO precoding

Precoding is the operation that maps the layers to antenna ports using a multiplication matrix. Mapping one layer to multiple antennas enables beamforming while mapping several layers to multiple antennas is called spatial multiplexing.

In this thesis, two methods of precoding are discussed in chapter 6.

2.6.1.2.5 Resource mapping

Resource mapper function is to map the output of the precoder to the virtual resource blocks (VRB) then to the physical resource blocks (PRB) where frequency is mapped first then time is mapped.

Mapping VRBs to PRBs can be either interleaved or non-interleaved. In the non-interleaved mapping, the VRB is directly mapped to the same position in physical resource grid while in the interleaved mapping, frequency diversity is applied by distributing VRBs over the whole BWP.

2.6.2 Downlink control channel

As the other radio access techniques, 5G NR has a physical downlink control channel (PDCCH) to perform physical layer control functions and carry downlink control information (DCI).

One from the questions about the transmission and the reception in each radio access technique is that, how can the receiving side figure out exactly where in the slot and in which modulation scheme that the transmitter transmit the data, it is DCI which carries those detailed information.

Therefore, to understand how the information is transmitted over 5G NR it is very important to understand how PDCCH operates.

The design should ensure good coverage for NR PDCCH transmission, due to path loss and channel conditions corresponding to different transmission environments.

2.6.2.1 NR PDCCH physical structure

A PDCCH refers to a set of resource elements carrying DL control information (DCI), twelve resource elements; nine for the PDCCH payload and three for demodulation reference signal (DMRS) REs in frequency domain make a one resource block, which equals a resource element group (REG), and an NR control channel element (CCE) consists of 6 REGs. NR PDCCH candidate consists of a set of NR CCEs, i.e., 1, 2, 4, 8, or 16.

Important parameters such as frequency and time domain resources are configured to the user-equipment through the control resource set (CORESET).

A CORESET is defined as a set of REGs under a given numerology. Particularly, a CORESET is a set of 250 resource blocks (PRBs) configured using a 6-PRB granularity, within which the UE tries to blindly decode the DCI. The UE can be configured with up to 12 CORESETs on a serving cell.

2.6.2.2 NR PDCCH transport process

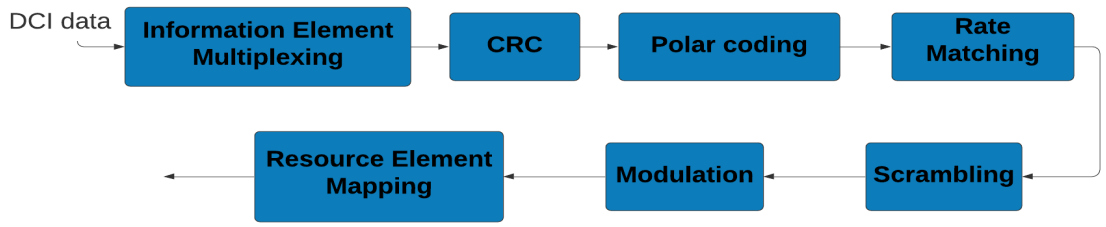

Figure 2-8:5G NR PDCCH transport process

Figure 2-8 shows the PDCCH (physical downlink control channel), it consists of 5 blocks, they are: IEM(information element multiplexing) ,CRC ,polar coding ,rate matching ,scrambling ,modulation ,and resource element mapping. The input of the PDCCH is the DCI data.

2.6.2.2.1 Information element multiplexing

In this stage a bit string of DCI carrying various control and signaling information is generated. The size of DCI will be zero padded until the payload size equals 12 bits if it is less than 12 bits.

2.6.2.2.2 CRC attachment

CRC is used to allow the UE to detect errors in the decoded DCI bits.

After CRC Attachment, the last 16 bits is masked with the radio network temporary identifier (RNTI). Using this RNTI, UE figures out the UE which the DCI is for and distinguish sets of DCI with different usage which have the same payload size.

Then the interleaving process is done, where the data is interleaved so that CRC bits are distributed among information bits. The max input size of the interleaver is 164 bits, which means that DCI without CRC can be max 140 bits. The next process will be the encoding; the bits are encoded by the Polar encoder to protect the DCI against errors during transmission.

2.6.2.2.3 Polar coding

One of linear error-correction codes is the polar code that introduced by Erdal Arikan.

Polar code is important as it has proven the capacity-achieving performance of Shannon capacity with acceptable complexity algorithms in both encoding and decoding.

The theory of polar coding is to transform a pair of identical binary-input channels into two distinct channels of different qualities: one better and one worse than the original binary-input channel. Therefore, Polar code is constructed as a result of the channel polarization transform, and the encoder function almost is a polarization transform.

Polar codes are used in 5G NR because of simple decoding schemes with modest complexity and memory requirements, also polar codes can achieve high throughput and better BER performance with less complex methods of puncturing.

2.6.2.2.3.1 5G NR polar codes

After many discussions and trials, polar codes are the suitable coding scheme for channel coding in 5G NR. Because of the presence of error floor and high complexity decoding algorithms, Turbo codes are not suitable for reliable communication and cannot achieve a high throughput.

Polar Code is considered to be suitable for the 5G URLLC and mMTC use cases as it offers excellent performance with variety in code rates and code lengths.

Polar codes can support up to 99.999% reliability which is a must for the ultra-high reliability requirements of 5G applications. It also has lower SNR requirements than the other codes for equivalent error rate and hence, provides higher coding gain and increased spectral efficiency.

2.6.2.2.4 Rate matching

The output of the encoder then is rate matched to fit the DCI allocated resource elements.

2.6.2.2.5 Scrambling

Each DCI bits are scrambled by a scrambling sequence generated from the length-31 Gold sequence. This sequence is initialized by either the physical layer cell identity of the cell or by a UE specific scrambling identity and a UE specific cell RNTI (C-RNTI).

2.6.2.2.6 Modulation

The modulation scheme that is used for NR PDCCH is QPSK.

2.6.2.2.7 Resource element mapping

The modulated symbols are mapped to physical resources, which is the control channel elements (CCEs). With QPSK modulation scheme, a CCE contains 54 REs and therefore can carry 108 bits.

Chapter 3: Channel model

The 3GPP standard body has agreed on two types of propagation channels for simulations of 5G systems with frequencies in the range from 0.5 GHz to 100 GHz and bandwidth up to 2 GHz defined in the document TR 38.901:

- CDL (Clustered Delay Line).
- TDL (Tapped Delay Line).

The CDL model is designed as a signal arriving at the receiver antenna dispersed into many signals as it passes through each cluster in the channel. At this time, the delay, power and four kinds of angles are defined. In case of the TDL model, instead of defining each cluster parameter in the channel, only the power delay profile of each tap is defined for the entire channel. Therefore, TDL is a simplified form of CDL in which the process of distributing signals passing through each cluster to many signals is not modeled.

In our simulation, tapped delay line channel with different parameters is applied. Then, Noise is added with:

$$N_0 = \frac{1}{SNR * \sqrt{2 * nRxAnts * Nfft}}$$

Equation 3-1: noise figure

3.1 Important Properties of the TDL channel:

3.1.1 Delay profile

In Multipath fading, same signal is received through different paths with different delays or phase shifts, the Delay profile of a channel provides multiple versions of the transmitted signal at the receiver.

Fig.1. below illustrates a TDL model with two internal taps located at delays of $\mathbf{M_1}$ and $\mathbf{M_2}$ samples.

The output signal is a linear combination of the input signal $x(n)$, the delay line output $x(n-M_3)$ and the two tap signals $x(n-M_1)$ and $x(n-M_2)$.

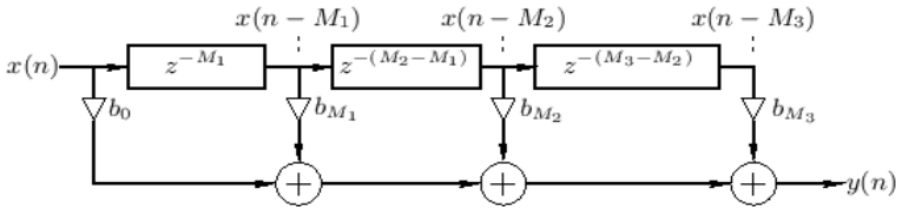

Figure 3-1: Tapped delay line with two internal taps

The difference equation of TDL model is:

$$y(n) = b_o x(n) + b_{M_1} x(n-M_1) + b_{M_2} x(n-M_2) + b_{M_3} x(n-M_3) \quad \text{Equation 3-2}$$

Corresponding to the transfer function:

$$H(z) = b_o + b_{M_1} Z^{-M_1} + b_{M_2} Z^{-M_2} + b_{M_3} Z^{-M_3} \quad \text{Equation 3-3}$$

When number of taps increases, the channel is expected to perform better as there are more reflections and in the multipath channels, reconstruction of the transmitted signal at receiver is higher as probability of having constructive interference is higher.

The Delay profile has the following types:

- TDL-A, TDL-B and TDL-C for non-line-of-sight channels.
- TDL-D and TDL-E for line-of-sight channels.
- Custom.

If the Delay profile is set to ‘Custom’, the delay profile type is configured using other properties such as Path delays, Average Path gains, Fading distribution and K Factor of the first tap.

Table 3-1 below shows number of taps of different delay profile types.

Table 3-1: Number of taps of different delay profile types

Delay profile type	# Taps
TDL-A	**23**
TDL-B	**23**
TDL-C	**24**
TDL-D	**13**
TDL-E	**14**

In this thesis, Performance of TDL is studied with delay profile types of C for NLOS channels and E for LOS channels as they have more taps than other types.

3.1.2 Fading distributions

Fading Distribution is mainly the distribution probability of the signal fading relative to a reference point. Fading Distribution can be specified as:

- Rayleigh Fading.
- Rician Fading.

Both of Rayleigh and Rician are caused by multipath propagation. Rayleigh fading occurs in environments where there is NLOS between transmitter and receiver. However, Rician fading occurs when one of the paths is wrongly LOS.

3.1.3 Delay spread

Delay spread is the certain variation of values of multiple different arrival timings at the receiver antenna due to the multipath fading and the delay spread value can be specified from table 3-2:

Note: The following table is taken from the 5G standard 3GPP TR 38.901 section 7.7.3-1

Table 3-2: Delay spread values of different delay spread models

Delay Spread Model	Delay Spread Value
Very short delay spread model	**10 ns**
Short delay spread model	**30 ns**
Nominal delay spread model	**100 ns**
Long delay spread model	**300 ns**
Very long delay spread model	**1000 ns**

In this thesis, Long delay spread model is assumed (300 ns).

3.1.4 Sample rate

Sample rate is the average number of samples obtained in one second. The default value is 30.72 MHz

3.1.5 Maximum Doppler Shift

Doppler shift is the change in the frequency due to Tx, Rx or scatterer movement. If max Doppler shift is set to 0, the channel remains static for the entire input.

Max Doppler Shift default value is 5 Hz.

Chapter 4: Initial access procedures

4.1 Initial Attach Sequence

In this section the Stand-Alone initial attach process will be explained.

4.1.1 SS Block

SS Block (SSB) stands for Synchronization Signal Block and it refers to Synchronization/PBCH block because Synchronization signal and PBCH channel are packed as one block that always moves together.

Even though it is a tiny low package sitting in a very radio frame, it has many various components in it such as are PSS (Primary Synchronization Signal), and SSS (Secondary Synchronization Signal). Therefore, the way it works is complicated.

The components of this block Each of SS Block components (PSS, SSS, PBCH DMRS, PBCH) are allocated in SS Block Resource Grid in several cases that are illustrated in Figure 4-1.

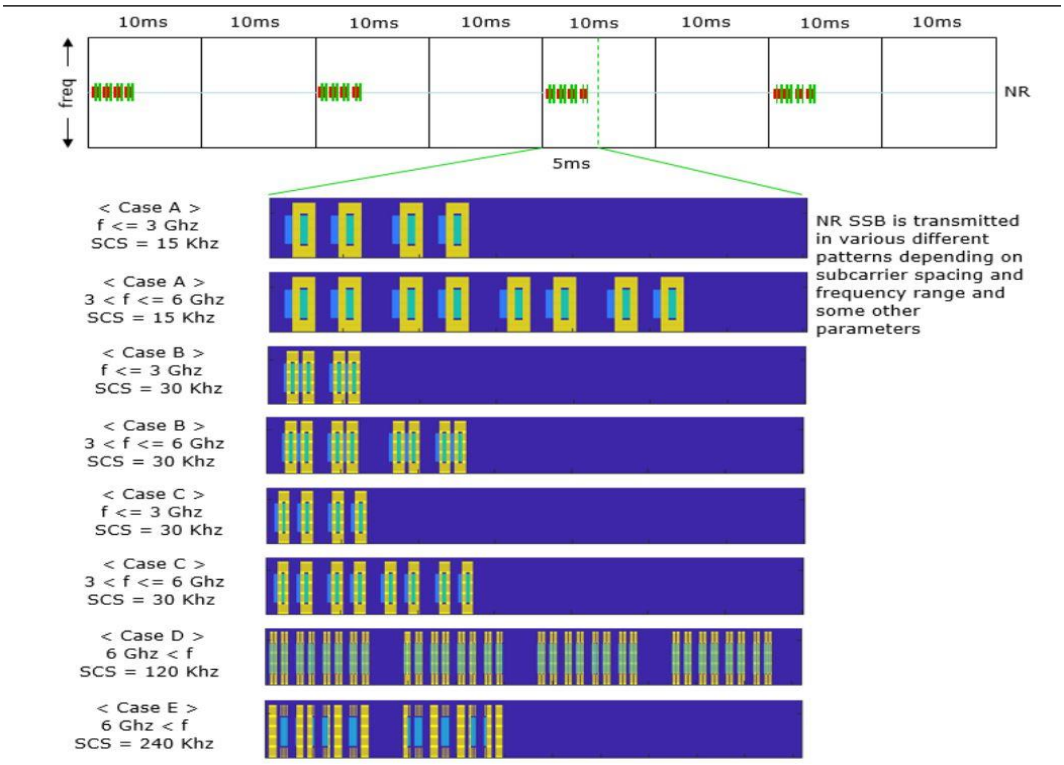

Figure 4-1: SS Block Resource Grid in several cases

4.1.1.1 SSB measurements

The SSB measurements are essential in 5G NR due to many reasons such as:

1. The UE uses the SSB for 5G NR cell search and synchronization.
2. The UE measurements on the various SSBs are essential to work out the correct beam configuration for data transmission (based on a UE / CPE / gNB internal algorithm).

4.1.1.2 Generation of PSS, and SSS:

PSS could be a specific physical layer signal that's used for radio frame synchronization. Its characteristics as listed below:

- Mapped to 127 active sub carriers round the lower end of the system bandwidth (subcarrier 80~206).
- Used for Downlink Frame Synchronization.
- One of the critical factors determining Physical Cell ID.

SSS could be a specific physical layer signal that's used for radio frame synchronization. Its characteristics as listed below:

- Mapped to 127 active sub carriers round the lower end of the system bandwidth (subcarrier 80~206).
- Made of 127 m-Sequence Values.
- Used for Downlink Frame Synchronization.
- One of the critical factors determining Physical Cell ID.

4.1.1.3 PBCH DMRS (Demodulation Reference Signal)

PBCH DMRS may be a special kind of physical layer signal, which functions as a reference signal for decoding PBCH. The main purpose of PBCH is to hold broadcast MIB (Master Information Block).

4.1.2 Master Information Block (MIB):

The overall characteristics of MIB (Master Information Block) are as follow:

- Transmitted over (BCH / PBCH) as PBCH is transmitted as an element of SSB. So, it'll be beneficial to grasp on SSB the maximum amount as possible.
- Transmitted with the periodicity of 80 ms and within these 80 ms repetitive transmission happens.
- For initial cell selection, a UE may assume that half frames with SS/PBCH blocks occur with a periodicity of two frames.
- Includes the parameters that are required to decode SIB1 (System InformationType1).

4.2 5G standalone access registration procedure

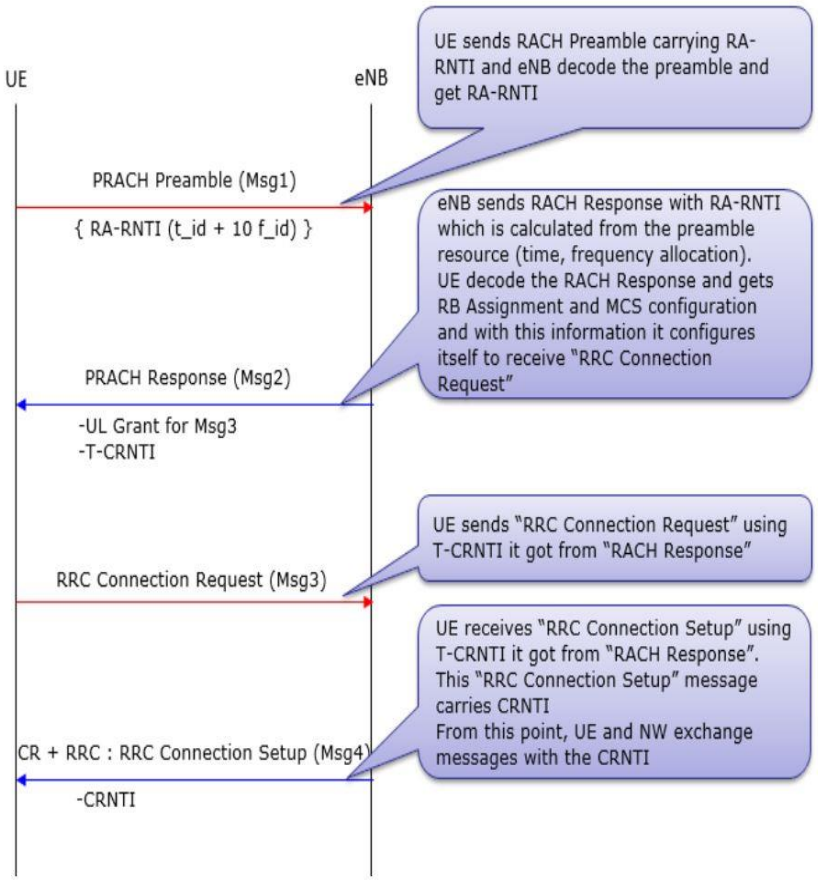

Figure 4-2 : Messages in 5G standalone access registration

4.2.1.1 - Message 1

This is the first message from UE to gNB when the mobile is powered on. A preamble is sent over PRACH channel in order to:

- Obtain the UL synchronization as the UE can perform uplink transmission only when it obtains UL synchronization with the cell.
- Obtain the resource from Msg3 (obtain uplink grant, the uplink resource request).
- Assign CRNTI (unique identity) to Device (TCRNTI will promote as CRNTI once contention resolved).

4.2.1.1.1 Preamble format

In 5G NR there are 13 types of preamble format supported known as Format 0, Format 1, Format 2, Format 3, Format A1, Format A2, Format A3, Format B1, Format B2, Format B3, Format B4, Format C0, Format C1 where the differences of preamble formats includes different CP length, Sequence Length , GP length and number of repetitions. There are 64 preambles available for each cell and UE has to be able to generate the 64 preambles for the cell it want to camp on. You can easily generate 64 different preambles just by cyclically shifting an existing sequence, but there is a condition for this. All the preamble sequences should be orthogonal to each other. Otherwise, various preambles from multiple UEs within the same cell can interfere each other.

The PRACH preamble consists mainly of:

1. Cyclic prefix: the use of an OFDM transmission with cyclic prefix allows for an efficient frequency domain-based receiver in the gNB to perform PRACH detection
2. Guard period: The guard period allows for timing uncertainty due to the distance between the UE and gNB, therefore the size of the guard period determines the cell radius. Where any propagation delay exceeding the guard time would cause the random-access preamble to overlap the following sub frame at the gNB receiver.
3. Preamble Sequence: longer T_SEQ would help decoding PRACH under noised condition because it provide longer correlation window to detect PRACH.

In case of using long preamble sequence length the PRACH Signal Structure will be as the following:

1- Preamble Length in Frequency Domain is amount to 6 RBs (72 sub-carrier in the frequency domain) of UL Sub frame, which is 1.08 MHz .
2- Preamble Length in Time Domain including Guard Time (= CP Length + sequence Length + GT Length) can be 1 or 2 or 3 depending on Preamble Format.
3- Sub-carrier spacing for long preambles can be either 1.25 KHz or 5 KHz.
4- Network knows when UE will transmit the RACH even before UE sends it as Network tells (using PRACH Configuration Index) UE when the UE is supposed to transmit the RACH.
5- UE transmit PRACH Preamble with RA-RNTI if all the condition for PRACH transmission is met.
6- RA-RNTI is calculated by the following equation according to 38.321-5.1.3:
7- RA-RNTI = RA-RNTI= 1 + s_id + 14 × t_id + 14 × 80 × f_id + 14 × 80 × 8 × ul_carrier_id , where s_id is the index of the first OFDM symbol of the specified PRACH (0 <= s_id < 14) , t_id is the index of the first slot symbol of the specified PRACH in a system frame (0 <= t_id < 80) , if_id is the index of the specified PRACH in the frequency domain(0 <= s_id < 8) , and ul_carrier_id is UL carrier used for Msg1 transmission .

4.2.1.2 - Message 2

Message 2 consists of UL Grant for msg3, and Temporary Cell RNTI (TC-RNTI), each one of them will be illustrated below.

- UL Grant for msg3: as a response to a PRACH transmission, a UE attempts to detect a DCI format 1_0 with CRC scrambled by a corresponding RA-RNTI during a window controlled by higher layers.

The window starts at the primary symbol of the earliest control resource set the UE is configured to receive PDCCH for Type1-PDCCH common search space, that's a minimum of one symbol, after the last symbol of the PRACH occasion corresponding to the PRACH transmission,

where the symbol duration corresponds to the subcarrier spacing for Type1- PDCCH common search space.

If the UE detects the DCI format 1_0 with CRC scrambled by the corresponding RA-RNTI and a transport block during a corresponding PDSCH within the window, the UE passes the transport block to higher layers.

If the UE doesn't detect the DCI format 1_0 with CRC scrambled by the corresponding RA-RNTI within the window, or if the UE doesn't correctly receive the transport block within the corresponding PDSCH within the window, the upper layers can indicate to the physical layer to transmit a PRACH. If the UE detects a DCI format 1_0 with CRC scrambled by the corresponding RA-RNTI and receives a transport block in a corresponding PDSCH, the UE may assume same DM-RS antenna port quasi co-location properties, as for a SS/PBCH block or a CSI-RS resource the UE used for PRACH association, irrespective of whether or not the UE is provided higher layer parameter TCI States for the control resource set where the UE receives the PDCCH with the DCI format 1_0. If the UE attempts to detect the DCI format 1_0 with CRC scrambled by the corresponding RA-RNTI in response to a PRACH transmission initiated by a PDCCH order that triggers a non-contention based random access procedure, the UE may assume that the PDCCH that has the DCI format 1_0 and also the PDCCH order have same DM-RS antenna port quasi colocation properties. A RAR UL grant schedules a PUSCH transmission from the UE (Msg3 PUSCH). The contents of the RAR UL grant, starting with the MSB and ending with the LSB. If the worth of the frequency hopping flag is 0, the UE transmits Msg3 PUSCH without frequency hopping; otherwise, the UE transmits Msg3 PUSCH with frequency hopping.

4.2.1.2.1 Temporary Cell RNTI (T-CRNTI)

it is used during Random Access procedure, the gNB’s MAC generates Random Access Response (RAR) as a response to the Random-Access Preamble transmitted by the UE. The MAC RAR contains Temporary C-RNTI. During contention based random access procedure, the UE stores received Temp C-RNTI (received in RAR) and uses it during random access procedure.

The UE shall use Temp C-RNTI for scrambling of msg3 (PUSCH cherish RAR grant) and its retransmissions. During contention-based RA procedure, the UE monitors PDCCH scrambled with

Temp C-RNTI. The Temp C-RNTI is promoted to C-RNTI for a UE which detects RA success and does not have already a C-RNTI.

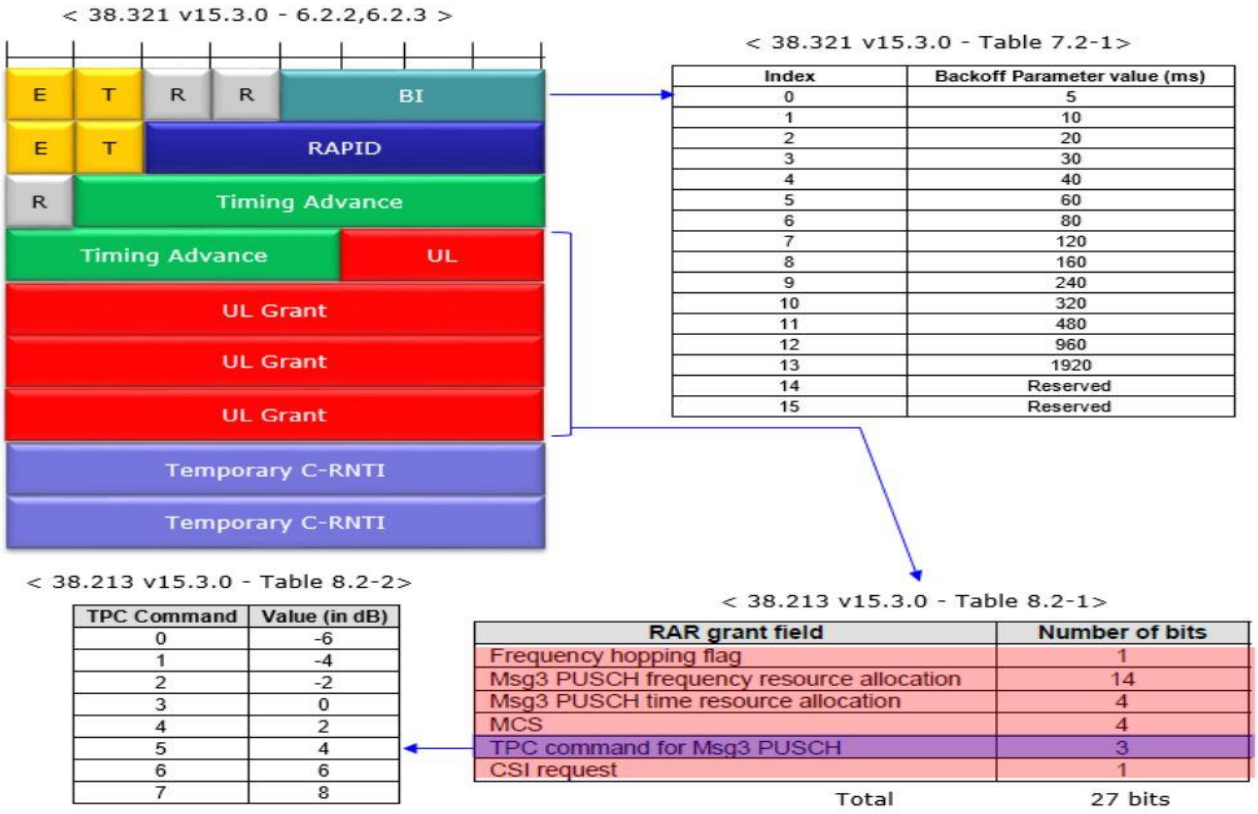

Figure 4-3:The data structure of MAC PDU that carries RAR(Random Access Response

4.2.1.3 -Message 3

In message 3 the UE sends RRC connection request to the gNB using T-CRNTI by following the steps:

- UE shall determine whether it'll apply transform precoding for Message3 PUSCH or not, supported the RRC parameter called message3-tp, where it indicates to whether or not the UE shall apply transform precoding for an Msg3 PUSCH transmission.

  If the UE applies transform precoding to an Msg3 PUSCH transmission with frequency hopping, the frequency offset for the second hop will be determined according to the below table.

Table 4-1:Frequency offset for second hop for Msg3 PUSCH transmission with frequency hopping

Number of PRBs in initial active UL BWP	Value of $N_{UL,hop}$ Hopping Bits	Frequency offset for 2nd hop
$N_{BWP}^{size} < 50$	0	$\lfloor N_{BWP}^{size}/2 \rfloor$
	1	$\lfloor N_{BWP}^{size}/4 \rfloor$
$N_{BWP}^{size} \geq 50$	00	$\lfloor N_{BWP}^{size}/2 \rfloor$
	01	$\lfloor N_{BWP}^{size}/4 \rfloor$
	10	$-\lfloor N_{BWP}^{size}/4 \rfloor$
	11	Reserved

- UE shall determine the subcarrier spacing for Msg3 PUSCH from the RRC parameter called msg3-scs (Subcarrier Spacing.
- UE shall transmit Msg3 PUSCH on the identical serving cell to which it sent PRACH.

To determine msg3 location in the time slot A UE transmits an UL-SCH in an exceedingly in Msg3 PUSCH scheduled by a RAR grant in a corresponding RAR message using redundancy version number 0.

Retransmissions, if any, of the UL-SCH in an Msg3 PUSCH are scheduled by a DCI format 0_0 with CRC scrambled by a TC-RNTI provided within the corresponding RAR message. If in slot a UE receives a PDSCH with a RAR message for a corresponding preamble transmission from the UE, the UE transmits a Msg3 PUSCH in slot, where is provided within the standard. The UE may assume a minimum time between the last symbol of a PDSCH reception conveying a RAR and therefore the first symbol of a corresponding Msg3 PUSCH transmission scheduled by the RAR within the PDSCH for a UE is adequate to msec. NT,1 may be a time duration of N1 symbols cherish a PDSCH reception time for PDSCH processing capability 1 when additional PDSCH DM-RS is configured and, NT,2 may be a time duration of N2 symbols cherish a PUSCH preparation time for PUSCH processing capability 1.

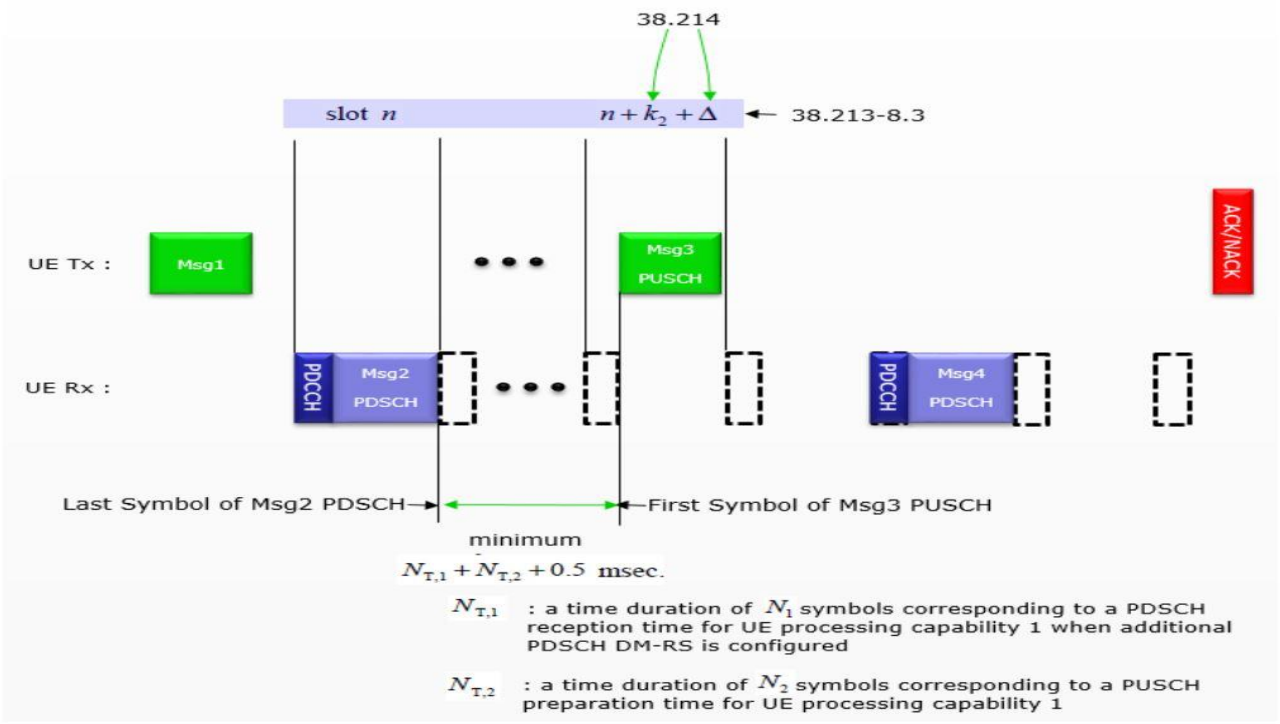

Figure 4-4:Msg3 location in the time slot

4.2.1.4 - Message 4

At this step right after sending Msg3, the following steps will happen:

- Monitor to decode PDCCH with TC-RNTI While ra-Contention Resolution Timer is running, UE looks for DCI within the search space.
- If PDCCH is successfully decoded, - decode PDSCH carrying the MAC CE – Set

  C-RNTI = TC-RNTI: as Cell RNTI may be a unique identification used for identifying RRC Connection and scheduling which is devoted to a selected UE. The gNB assigns different C-RNTI values to different UEs.

  The gNB uses C-RNTI to allocate a UE with uplink grants, downlink assignments, etc. C-RNTI is employed by gNB to differentiate uplink transmissions (e.g. PUSCH, PUCCH) of a UE from others.
- Discard ra-Contention Resolution Timer .
- consider this Random Access Procedure successfully completed Once UE successfully decode Msg4 (Contention Resolution), UE sends HARQ ACK for the data (PDSCH carrying Msg4). In response to the PDSCH reception with the UE contention resolution identity, the UE transmits HARQ-ACK information during a PUCCH.

Chapter 5: Massive MIMO in 5G NR

5.1 Multiple-Input Multiple-Output (MIMO):

MIMO is a wireless technology that uses multiple transmitting and receiving antennas to increase the capacity of data. The basic principle of MIMO is that when the received quality is high, it is better to receive multiple data streams with reduced power per stream than receiving one stream with the full power.

In a MIMO system, multiple data streams are transmitted using the same time and frequency resources. Therefore, each signal reaches the receiving antenna through a different path which in turn results in more reliable data. Receiver in MIMO systems can recognize the time difference between receptions of the signal, noise and interference.

5.2 SU-MIMO vs MU-MIMO:

The main difference between SU-MMO and MU-MIMO is that MU-MIMO allows multiple wireless devices to simultaneously receive the multiple data streams. While in the SU-MIMO, only one device is allowed at a time.

In single-user MIMO, both of the base station and UE have multiple antenna ports and antennas. Multiple data streams (Layers) are transmitted simultaneously to the UE using same time and frequency resources. The number of layers that can be supported depends on the radio channel. UE needs to have at least as many receiver antennas as the number of layers in order to distinguish between DL layers.

In multi-user MIMO, the base station has multiple antenna ports and one port is needed in each UE. Base station sends multiple data streams simultaneously, one per UE, using same time and frequency resources. Therefore, the total throughput increases.

Beamforming is used in MU-MIMO to direct signals toward the intended device where the antenna array simultaneously sends different layers in separate beams to different users. The interference between users should be low to guarantee the efficient MU-MIMO. This can be achieved using

beamforming with null forming such that when layer is sent to one user, nulls are formed in directions of the other users.

As the number of the simultaneous users increases, the power for each user decreases. Therefore, the network capacity improves as the number of MIMO layers increases to the point at which power sharing and interference between users result in diminishing gains.

5.3 Massive MIMO (mMIMO):

MIMO has been used in wireless communications for a long time. Now, with the design of 5G NR, MIMO becomes massive. Massive MIMO concept is to add much higher number of antennas –it can be up to hundreds of antennas- on the base station to improve throughput and efficiency.

Since massive MIMO uses many more antennas than the number of UEs, the beam is much narrower. Therefore, RF energy can be delivered to the UE more precisely. Using large number of base station antennas increases the signal-to-noise ratio in cell which in turn increases the cell capacity and throughput.

5.3.1 Beamforming vs massive MIMO:

Beamforming concept is simply steering a lobe of power in a particular direction toward a user where relative amplitudes and phase shifts are applied to each antenna element to add the output signals from the array together for a particular user angle and cancel each other for other users.

Massive MIMO is considered a form of beamforming in the general concept where the multiple spatially separated users are served by the antenna array in same time and frequency resources.

In massive MIMO, data transmitted from antenna to user terminal can be affected by the surrounding environment. Signal can suffer from many reflections due to buildings and other obstacles.

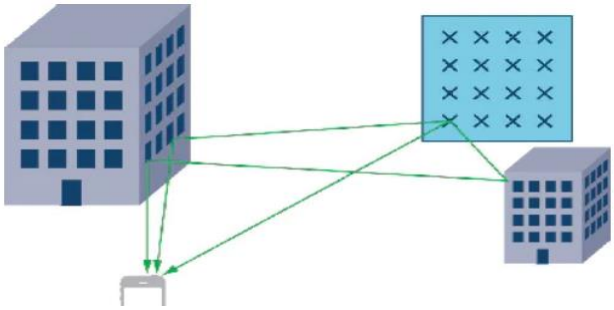

Figure 5-1:MIMO illustration

Therefore, it is necessary to characterize the spatial channel between antenna elements and user terminals to take advantage of these multiple paths. A collection of spatial transfer functions between each antenna and user terminal is gathered in a matrix and called the channel state information (CSI). The CSI is used for encoding and decoding data.

5.3.2 Characterizing the spatial channel between base station and user:

In TDD mode, both of uplink and downlink transmissions use the same frequency resource. Therefore, reciprocity assumes that the channel needs to be characterized in only one direction. The uplink channel is the choice such that one pilot signal is sent from the user terminal and received by all antenna elements.

Therefore, channel estimation and signal processing is done at the base station and affected by number of user terminals not the number of antennas in the array.

5.3.3 Signal processing that enables massive MIMO:

There are a number of methods for calculating precoding matrix based on CSI which includes important information such as channel quality information (CQI) and precoding matrix indicator (PMI). Such methods of precoding are discussed in chapter 6.

5.3.4 Advantages of massive MIMO:

Massive MIMO network can multiply the cell capacity without the need to more spectrum. It is also more responsive to devices transmitting in higher frequency bands, which improves coverage.

The massive number of antennas guarantees more possible signal paths which results in better performance in terms of data rate and link reliability. Also, it makes the network more resistant to interference than current networks.

Using beamforming with massive MIMO makes data speed and latency far more uniform across the network.

Chapter 6: Precoding

6.1 Methodology

Spatial multiplexing has two modes of operation: closed Loop Spatial Multiplexing and open Loop Spatial Multiplexing. Mainly, the main difference between them is that in the latter, the optimum precoding matrix information is additionally fed back by the UE to the gNB.

In this chapter, two types of precoding will be discussed SVD for the open loop spatial multiplexing and the codebook based precoding for the closed loop spatial multiplexing.

6.1.1 Codebook based precoding

The codebook-based precoding is a promising technology that is adopted by LTE, it fixes a common codebook comprising a set of predefined matrices and vectors at both BS and the UE. In order to support various different numbers of data streams and antenna configurations and flexibility and lower feedback overhead are a mandatory for designing precoding techniques.

The selection procedure of which of these matrices to take or which entry of codebook to select is taken at the gNB according to the decision based on the regularly received feedback from the UE to the gNB. This feedback is called PMI where the user is actually pointing to one of these entries.The UE receives the CSI-RS sent by the gNB in order to estimate the radio channel and the quality of the received signal and based on that the UE recommends the optimum precoding matrix out of the codebook and feeds back it to the gNB. After that the gNB applies the spatial domain precoding on the signal transmitted taking into consideration the PMI so that the transmitted signal matches with the channel that is experienced by the UE and after the precoding operation done by the gNB, the UE receives the information on what precoding matrix is used, that is utilized by the UE for the demodulation of the data. The following tables list the available precoders for 4,8,16 and 32 antennas.

Note: The following tables are taken from the 5G standard 3GPP TS 38.214 section 5.2.2.2

Table 6-1:5G codebook for p transmit antennas

Layers (v)	Precoder codebook
1	$w_{l,m,n}^{(1)} = \frac{1}{\sqrt{P}}\begin{bmatrix} v_{l,m} \\ \phi_n v_{l,m} \end{bmatrix}$
2	$w_{l,l',m,m',n}^{(2)} = \frac{1}{\sqrt{2P}}\begin{bmatrix} v_{L,m} & v_{l',m'} \\ \phi_n v_{L,m} & -\phi_n v_{l',m'} \end{bmatrix}$
4	If p < 16 $w_{l,l',m,m',n}^{(4)} = \frac{1}{\sqrt{4P}}\begin{bmatrix} v_{L,m} & v_{l',m'} & v_{L,m} & v_{l',m'} \\ \phi_n v_{L,m} & \phi_n v_{l',m'} & -\phi_n v_{L,m} & -\phi_n v_{l',m'} \end{bmatrix}$ If p > 16 $w_{l,m,p,n}^{(4)} = \frac{1}{\sqrt{4P}}\begin{bmatrix} \widetilde{v_{l,m}} & \widetilde{v_{l,m}} & \widetilde{v_{l,m}} & \widetilde{v_{l,m}} \\ \theta_p \widetilde{v_{l,m}} & -\theta_p \widetilde{v_{l,m}} & \theta_p \widetilde{v_{l,m}} & -\theta_p \widetilde{v_{l,m}} \\ \phi_n \widetilde{v_{l,m}} & \phi_n \widetilde{v_{l,m}} & -\phi_n \widetilde{v_{l,m}} & -\phi_n \widetilde{v_{l,m}} \\ \phi_n \theta_p \widetilde{v_{l,m}} & -\phi_n \theta_p \widetilde{v_{l,m}} & -\phi_n \theta_p \widetilde{v_{l,m}} & \phi_n \theta_p \widetilde{v_{l,m}} \end{bmatrix}$
6	$w_{l,l',l'',m,m',m'',n}^{(6)} = \frac{1}{\sqrt{6P}}\begin{bmatrix} v_{l,m} & v_{l,m} & v_{l',m'} & v_{l',m'} & v_{l'',m''} & v_{l'',m''} \\ \phi_n v_{l,m} & -\phi_n v_{l,m} & \phi_n v_{l',m'} & -\phi_n v_{l',m'} & v_{l'',m''} & -v_{l'',m''} \end{bmatrix}$
8	$w_{l,l',l'',l''',m,m',m'',m''',n}^{(8)} = \frac{1}{\sqrt{8P}}\begin{bmatrix} v_{l,m} & v_{l,m} & v_{l',m'} & v_{l',m'} & v_{l'',m''} & v_{l'',m''} & v_{l''',m'''} & v_{l''',m'''} \\ \phi_n v_{l,m} & -\phi_n v_{l,m} & \phi_n v_{l',m'} & -\phi_n v_{l',m'} & v_{l'',m''} & -v_{l'',m''} & v_{l''',m'''} & -v_{l''',m'''} \end{bmatrix}$

The number of columns in the precoding matrices refers to the number of layers while the number of rows refers to the number of antenna ports.

The quantities ϕ_n, θ_p,u_m, $v_{L,m}$ and $\tilde{v}_{L,m}$ are given by:

$$\phi_n = e^{\frac{j\pi n}{2}}$$

$$\theta_p = e^{\frac{j\pi p}{4}}$$

$$v_{L,m} = \begin{bmatrix} u_m & e^{\frac{j2\pi l}{O_1 N_1}} u_m \dots\dots\dots\dots\dots\dots e^{\frac{j2\pi l(N_1-1)}{O_1 N_1}} u_m \end{bmatrix}^T$$

$$\tilde{v}_{L,m} = \begin{bmatrix} u_m & e^{\frac{j2\pi l}{O_1 N_1}} u_m \dots\dots\dots\dots\dots\dots e^{\frac{j4\pi l\left(\frac{N_1}{2}-1\right)}{O_1 N_1}} u_m \end{bmatrix}^T$$

$$u_m = \begin{cases} \begin{bmatrix} 1 & e^{\frac{j2\pi m}{O_2 N_2}} \dots\dots\dots\dots\dots\dots e^{\frac{j2\pi m(N_2-1)}{O_2 N_2}} \end{bmatrix} & if\ N_2 > 1 \\ 1 & if\ N_2 = 1 \end{cases}$$

The values of $N_1$and $N_2$are configured with the higher layer parameter n1-n2, respectively. The supported configurations of (N_1,N_2) for a given number of CSI-RS ports and the corresponding values of (O_1, O_2) are shown in the following Table 2.

Table 6-2: Supported configurations of(N_1, N_2) and (O_1, O_2)

Number of ports	(N_1,N_2)	(O_1,O_2)
4	(2,1)	(4,1)
8	(4,1)	(4,1)
16	(8,1)	(4,1)
32	(16,1)	(4,1)

Each PMI value corresponds to three codebook indicesi_{12}, i_{11} andi_2.

- i_{11} is defined from the user feedback, using a linear minimum mean squared error (LMMSE) SINR metric where the CSI-RS are sent on some resource elements for the user to estimate

the channel and by precoding each resource element containing these predefined reference signals with each matrix and return with the value of i_{11} that achieves the highest SINR.

- $i_{12} = 0$ always $as\ N_2 = 1$

- $i_2 = \begin{Bmatrix} [0,1] \\ [0,1,2,\dots\dots 7] \\ [0,12,\dots\dots\dots 15] \end{Bmatrix} \begin{matrix} for\ 4,6,8\ layers \\ for\ 2\ layers \\ for\ 1\ layer \end{matrix}$

6.1.2 SVD precoding technique

In MIMO systems, one from the precoding schemes that could be used is the singular value decomposition of the channel matrix H**,** with the assumption that almost always ideal radio channel knowledge at the gNB and/or UE.

Generally, the technique of SVD precoding decomposes the matrix into three components. The diagonal component indicates the Eigen values and the unitary matrix parts indicate the basis of each component as the non- zero element in matrix S indicates the rank how many parallel layers can be transmitted in this channel conditions. Depending on the nature of the original matrix M, U, V and D can be interpreted in many different ways.

.

$\mathrm{M} = \mathrm{U}\,\mathrm{D}\,V^H$

U and V are Unitary Matrices while D is the diagonal matrix.

After this decomposition, three transformations will be performed:

- First rotation in the input space.
- Simple positive scaling that takes a vector in the input space to the output space.
- Another rotation in the output space.

The base station is supposed to have N transmit antennas while the UE is with K receiving-antennas. The channel to the k_{th} antenna is described by which is N×1 vector, h_k of channel coefficients and its i[th] element describes the channel response between the transmit antenna and the receive antenna.

$$y_k = h^H{}_k x + n_k, \quad k = 1, 2, \ldots K.$$

The previous equation mathematically represents the received signal Y, which is distorted by the air path and noise, but the target is to extract the original data x which can be achieved by multiplying the received signal with inverse of the channel information matrix H but unfortunately the inverse of the channel information matrix H is not always easy to get because of some mathematical issues, so the SVD method will solve this issue.

$$y = Hx, \ by\ SVD\ H = (UDV)^H$$

$$y = U^H \mathrm{U}\,\mathrm{D}\,V^H V\ x$$

$$y = IDI\ x$$

$$y = \sum x$$

The quantity U represents the receiver matrix while V represents the precoding matrix at the transmitter side.

Chapter 7: Determining user position and estimating the channel simulation results

7.1 SS-Burst Beamforming experimental results

Before a User Equipment (UE) device can communicate with the network, it must perform cell search and selection procedures and obtain initial system information.

The BS performs a beam sweep over an angular sector that covers the entire cell by transmitting ss-burst in each beam so that to give an initial, coarse estimate of the best beam direction and an initial estimate of the UE position.

7.1.1 Simulation steps

1) *Burst generation:* 8 bursts are generated via a specific beam radiated in a certain direction

2) *Beam sweep:* The OFDM resource grid for the SS burst is beamformed onto a set of physical transmission antennas, with each SS/PBCH block in the burst having a different beamforming vector as shown below in Figure 7-1below
3) *Propagation channel:* The transmitted waveform is passed through a TDL propagation channel model.

4) UE decides on best beam based on received SS/PBCH Block signal strength by measuring and displaying the received RMS EVM upon receiving each beam.

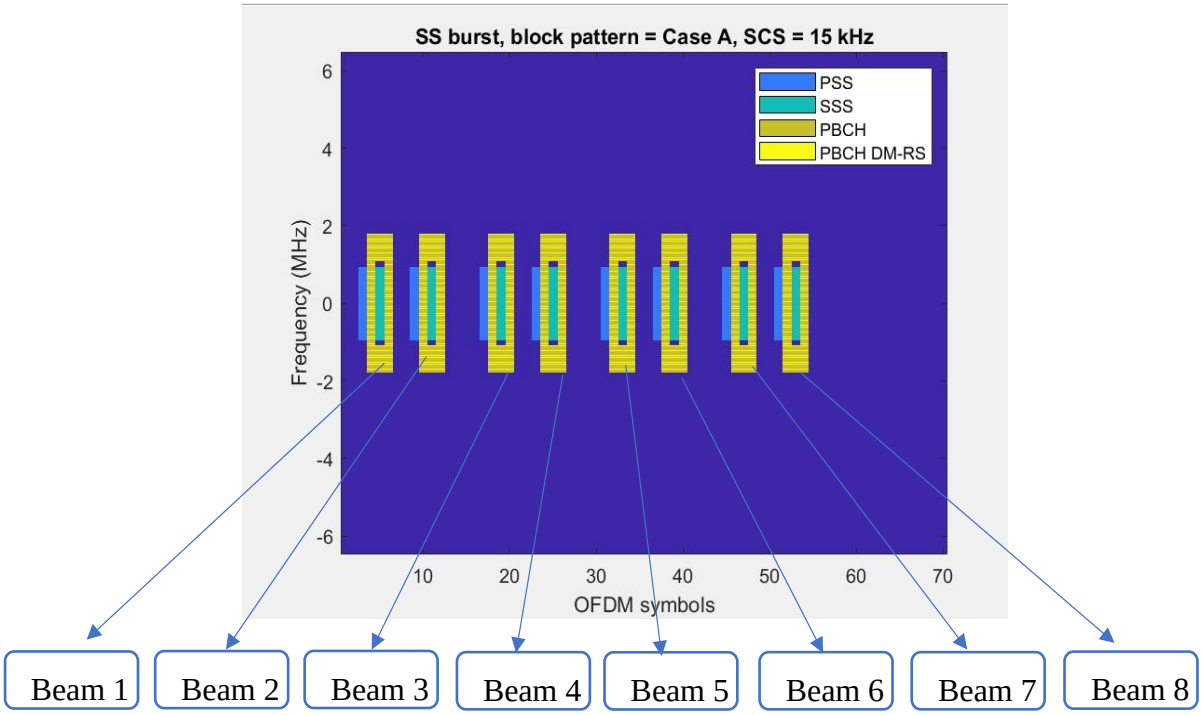

Figure 7-1: SS burst pattern

7.2 SS-Burst Beamforming Results

In this subsection measurements on receiving SS-Burst signals are discussed. The parameters of the ss-burst signals are summarized in table 7-1.

Table 7-1:Parameters of SS Burst signal

Access mode	**TDD**
Block Pattern	Case B
Bandwidth	10MHz
Subcarrier spacing	15KHz
Number of SS-Block per SS-Burst	8
Periodicity	20ms
Frequency	3GHz

Each ss-block within the burst is directed and beamformed at a certain defined angle. Table 7-2 shows the angle of each ss- block within each ss-burst.

Table 7-2: Angle of each ss-block

SSB index 0	**-52.5°**
SSB index 1	-37.5°
SSB index 2	-22.5°
SSB index 3	-7.5°
SSB index 4	7.5°
SSB index 5	22.5°
SSB index 6	37.5°
SSB index 7	52.5°

Figure 7-2, Figure 7-3, Figure 7-4, Figure 7-5, Figure 7-6, Figure 7-7, Figure 7-9 and Figure 7-8 shows the beam sweep strategy used in the numerical simulation according Table 7-2.

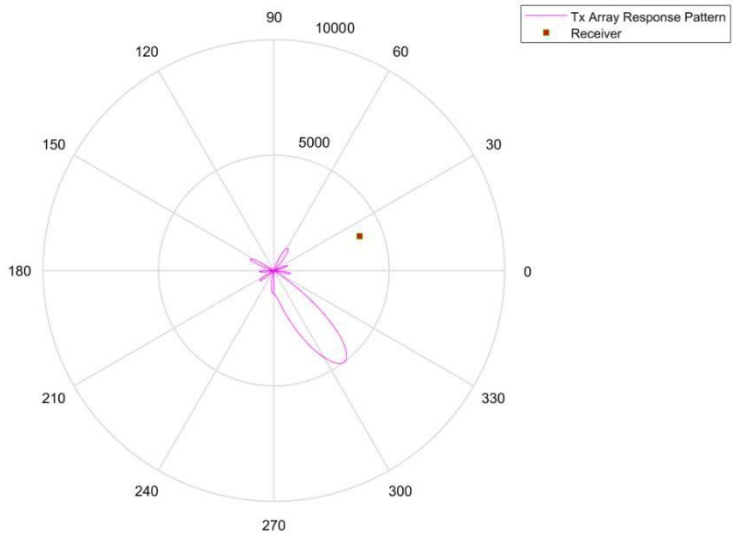

Figure 7-2:SS-Burst beamformed at angle -52.5°

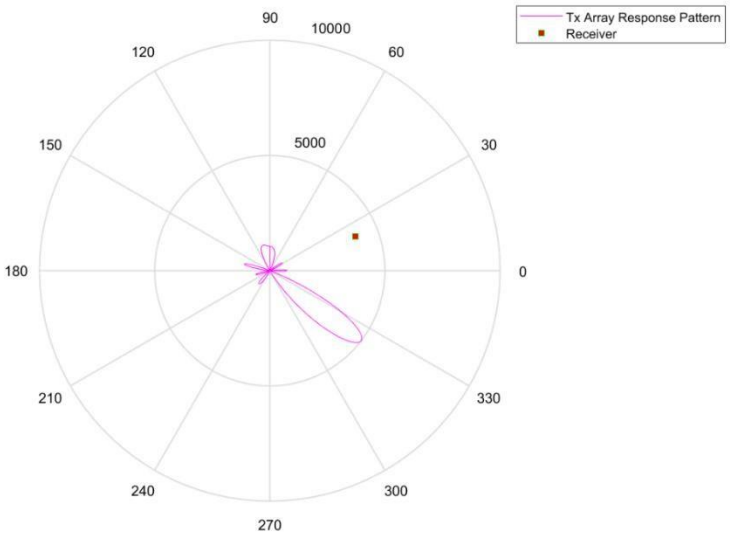

Figure 7-3:SS-Burst beamformed at angle -37.5°

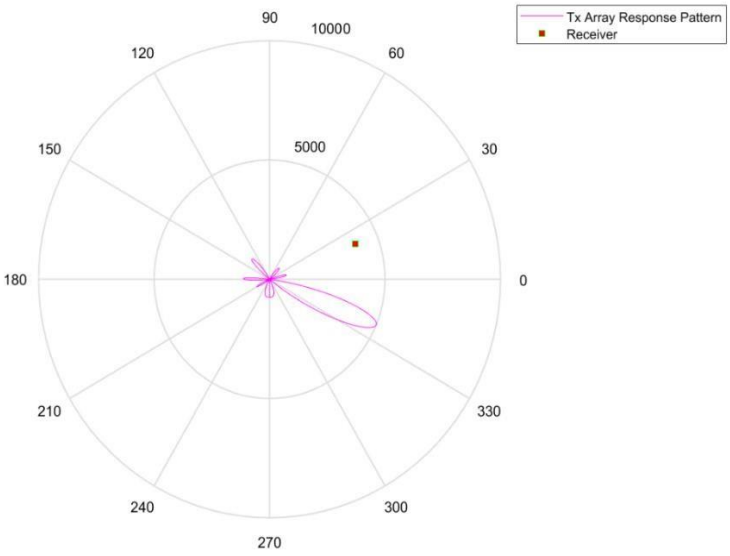

Figure 7-4:SS-Burst beamformed at angle -22.5°

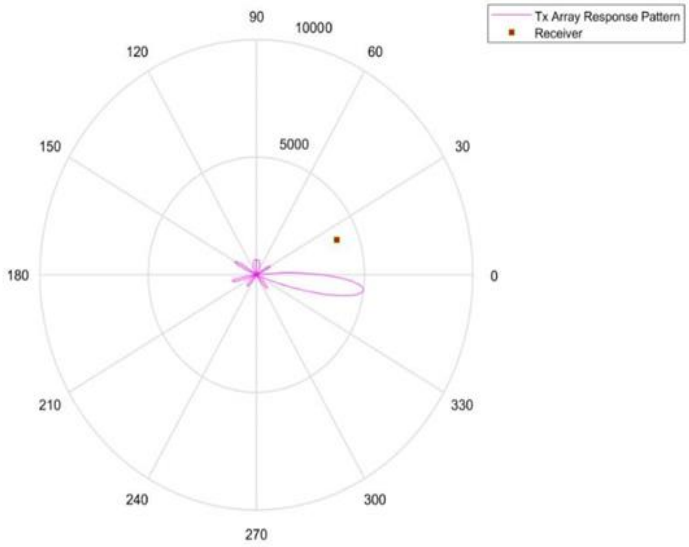

Figure 7-5: :SS-Burst beamformed at angle -7.5°

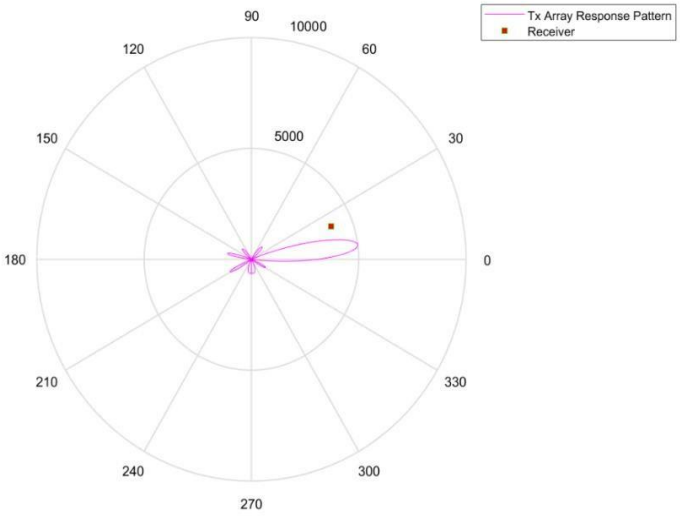

Figure 7-6:SS-Burst beamformed at angle 7.5°

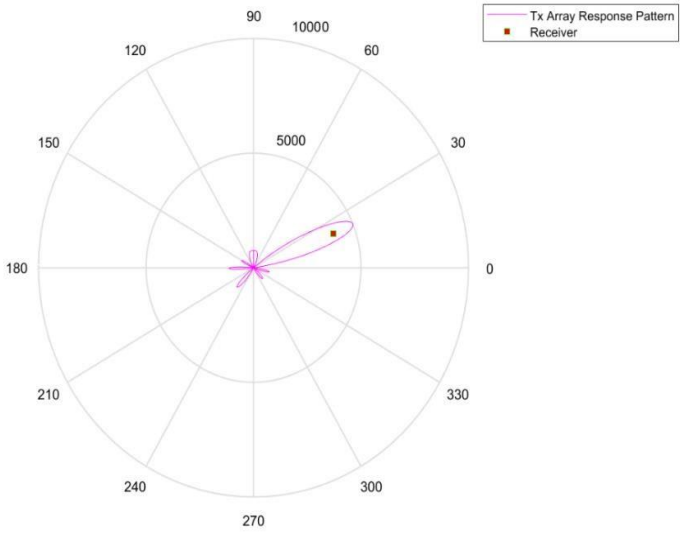

Figure 7-7: SS-Burst beamformed at angle 22.5°

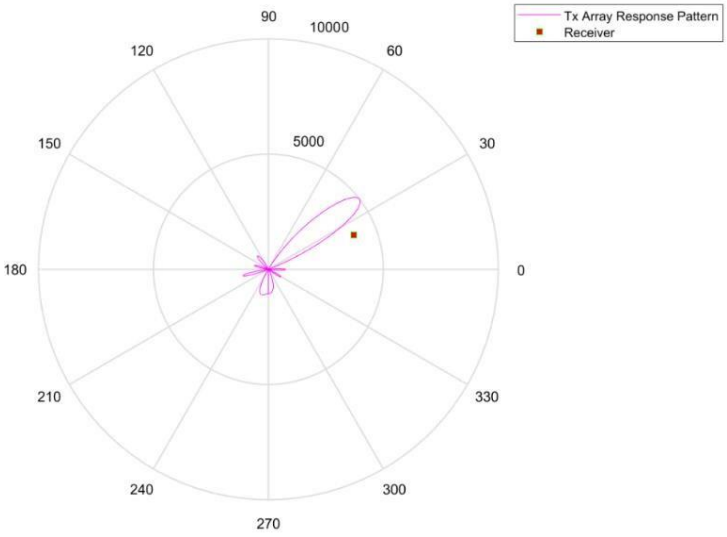

Figure 7-9: SS-Burst beamformed at angle 37.5°

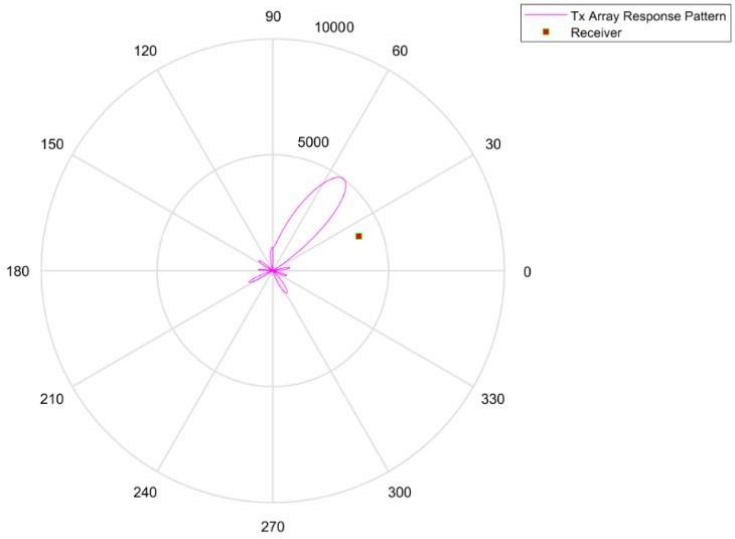

Figure 7-8:SS-Burst beamformed at angle 52.5°

7.2.1 Identification of SSB index

In this subsection the SSB index will be detected as the quality metric used for beam selection for SSB is the measured RMS EVM (error vector magnitude) from each transmitted SS-Block. The UE measures the EVM from all BS Tx beams using a wide Rx beam and reports to the BS the strongest of the beams.

Hence, it was found that the least measured EVM is from the SSB index5 that is beamformed at angle 22.5 degrees, these results conform with the user position as it was located at angle 22 degrees.

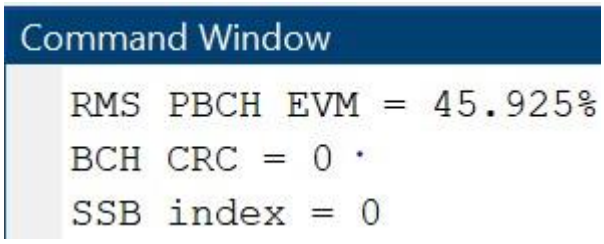

Figure 7-10: measured EVM of burst index 5 at angle -52.5°

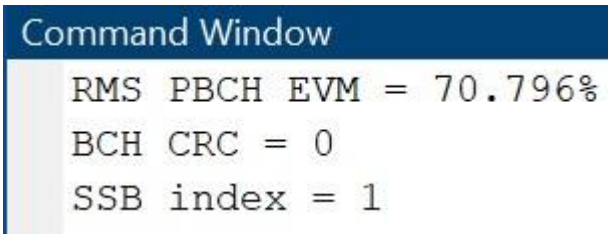

Figure 7-11: measured EVM of burst index 5 at angle -37.5°

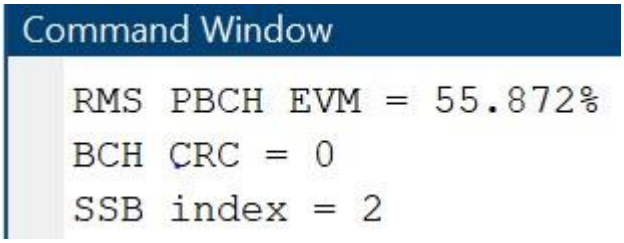

Figure 7-12:measured EVM of burst index 5 at angle -22.5°

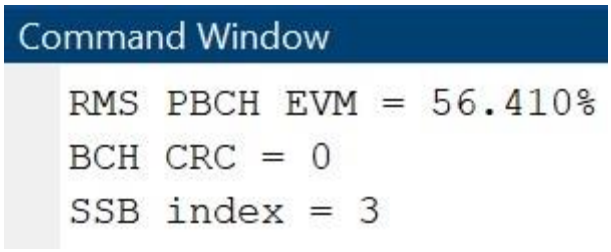

Figure 7-13: measured EVM of burst index 5 at angle -7.5°

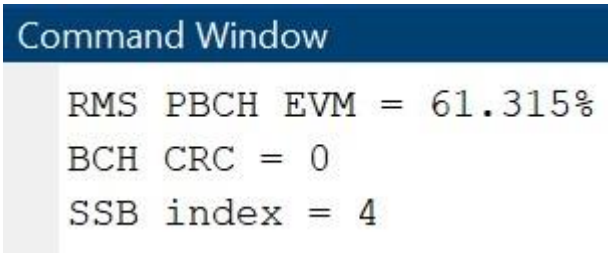

Figure 7-14: measured EVM of burst index 5 at angle 7.5°

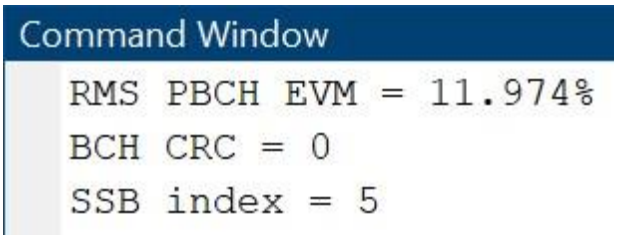

Figure 7-15: measured EVM of burst index 5 at angle 22.5°

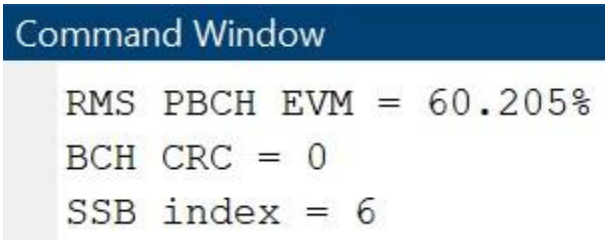

Figure 7-16: measured EVM of burst index 5 at angle 37.5°

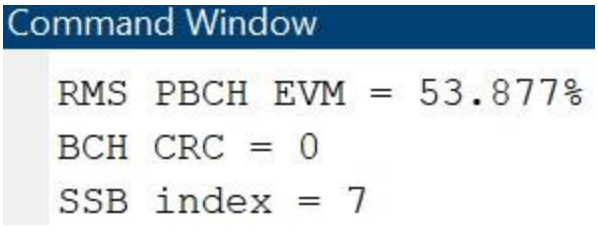

Figure 7-17: measured EVM of burst index 5 at angle 52.5°

7.3 CSI Beamforming Experimental Results

This section shows the results for beam refinement of the BS Tx beams by performing a beam sweep in a narrower angular sector than the beam sweeping in the ss-burst.

The results demonstrate the exact acquisition of the UE position with the effectiveness of beamforming after knowing the best beam of ss-burst with the least EVM and so determining the best beam for the data to be sent over.

Aperiodic CSI-RS reference signals were transmitted sequentially in an angular sector around the best beam reported by the UE from the ss-burst where a UE measures the average received power **(RSRP)**and the quality of the received signal **(RSRQ)** of the reference signals for the all 8 beams.

The CSI-RS grid is depicted in Figure 7-18 Where 8 aperiodic CSI-RS reference signals were transmitted sequentially.

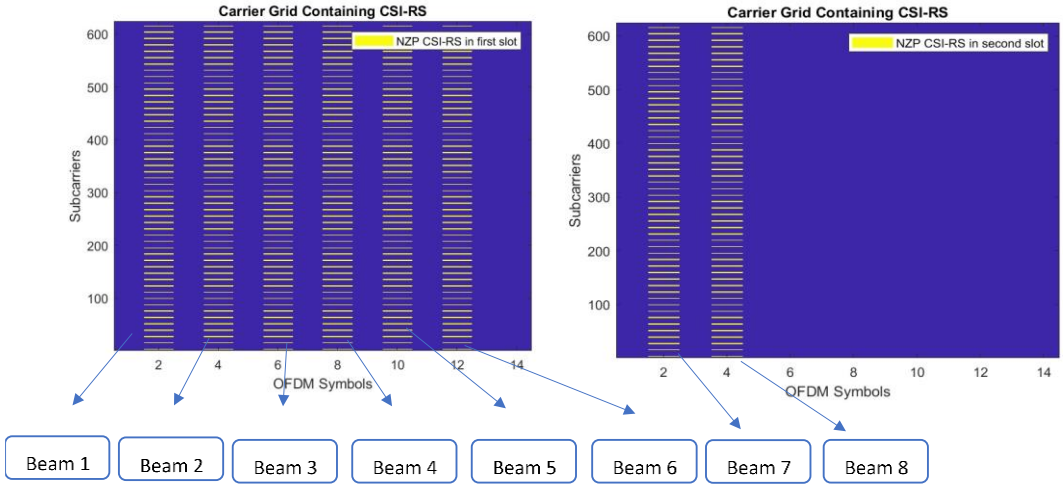

Figure 7-18:aperiodic CSI-RS reference signals

7.3.1 Beamforming of CSI-RS

Given that the UE is almost around 22 degrees from the ss-burst simulation, therefore each CSIRS resource will be beamformed at certain defined angle from 16 degrees to 30 degrees in order to get the accurate location of the UE as shown in the following figures.

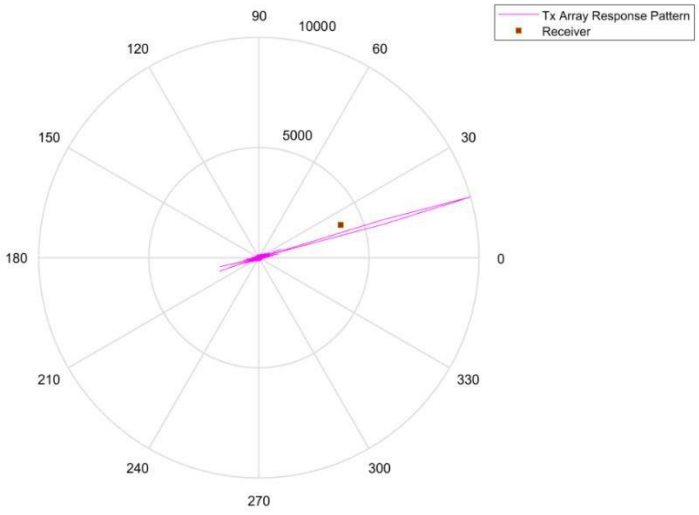

Figure 7-22:CSI-RS beamformed at angle 16°

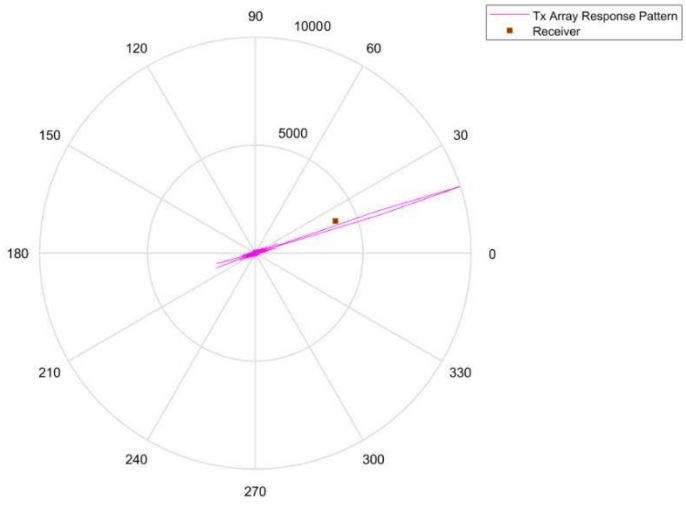

Figure 7-21:CSI-RS beamformed at angle 18°

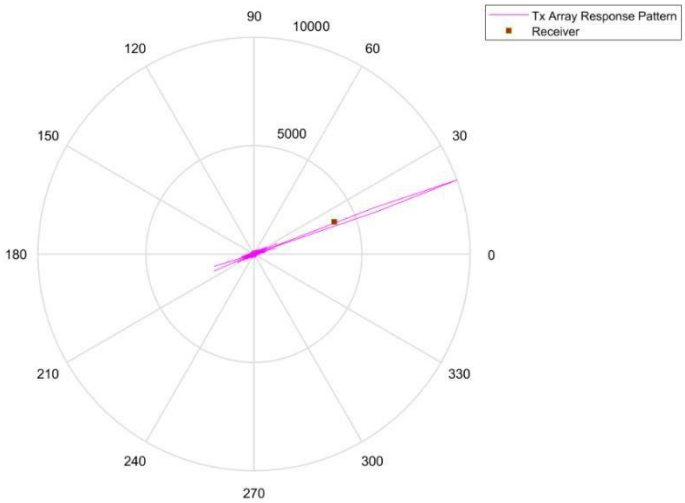

Figure 7-20: CSI-RS beamformed at angle 20°

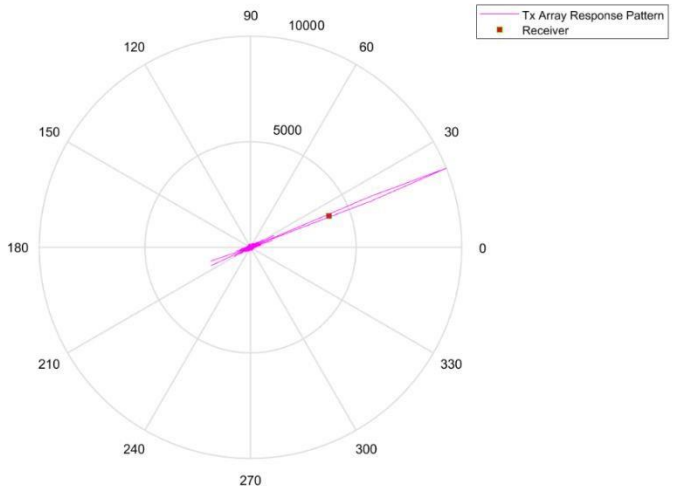

Figure 7-19:CSI-RS beamformed at angle 22°

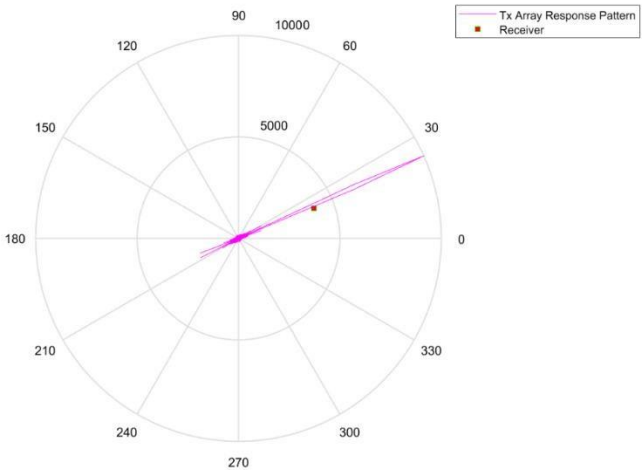

Figure 7-24:CSI-RS beamformed at angle 24°

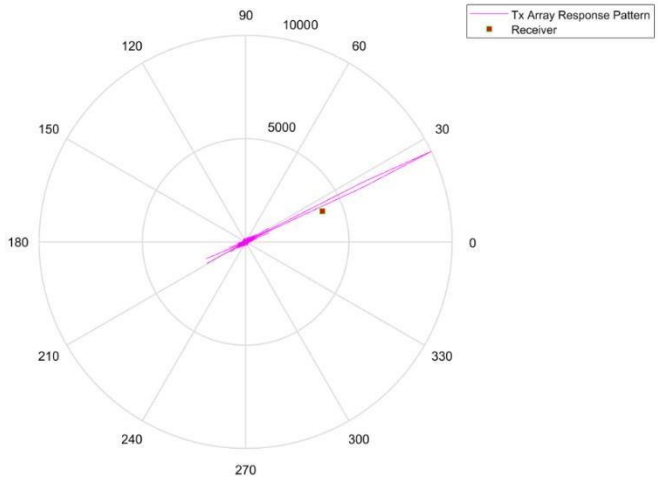

Figure 7-23:CSI-RS beamformed at angle 26°

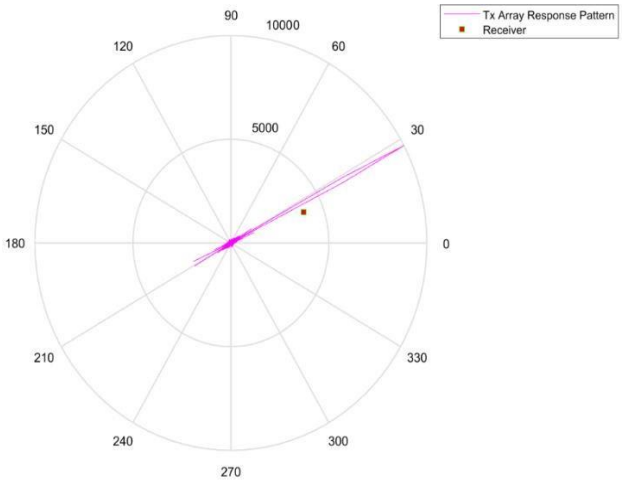

Figure 7-26:CSI-RS beamformed at angle 28°

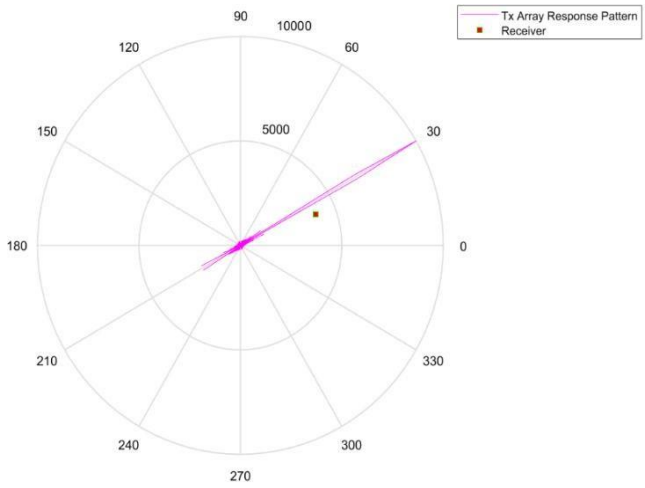

Figure 7-25:CSI-RS beamformed at angle 30°

7.3.2 CSI-RS measurements

Upon receiving the 8 beams by the UE, RSRP and RSRQ measurements are calculated as shown in Table 7-3

Table 7-3 summarize the RSRQ and RSRP measurements of each beam and so, the table shows the best received power and quality is from beam number 4.

Thus, the radiation pattern when sending the data to the UE will be beamformed at the user's position which is estimated to be at 22 degrees.

Table 7-3:RSRQ and RSRP measurements of each beam

Beam Number	Transmitted angle	RSRQ (dB)	RSRP (dBm)
1	16°	-5.76	-80.25
2	18°	-5.85	-80.20
3	20°	-5.73	-80.18
4	22°	-5.70	-80.17
5	24°	-5.79	-80.26
6	26°	-5.84	-80.32
7	28°	-5.85	-80.33
8	30°	-6.02	-80.49

Chapter 8: SISO simulation results and analysis

In this chapter we show the results of SISO (single-input-single-output) simulations and discuss and analyze these results focusing on the BER (bit error rate) and throughput.

8.1 SISO simulation steps

The simulation was done on the PDSCH (physical downlink shared channel) which is the channel responsible for transferring the data to the user, different parameters were changed during the simulation to determine their effect on the bit error rate and the throughput which are:

1. Allowing HARQ transmission and seeing the effect on the overall bit error rate and throughput if retransmission took place, the number of HARQ processes was fixed (10 HARQ consecutive process)
2. Changing the modulation scheme; we tested 3 modulation schemes: 16QAM, 64QAM, and 256QAM.
3. The subcarrier spacing and the bandwidth were also changed according to table 1 and subsequently changing the number of resource blocks.
4. The operating SNR, changing the values of the signal to noise ratio to simulate different noise levels in the operating cell, the simulation values ranges between 0 and 40 with a step of four.
5. We also measured the BER before and after error correction (using LDPC) to measure the improvement in the BER values.

The following table shows a summary of the changing and fixed parameters and their values:

Table 8-1: SISO simulation parameters

Parameter	value
Channel bandwidth (in MHz)	5, 10, 15, 20, 25, 30, 40, 50, 60, 70, 80, 90, 100
Channel type	TDL
Delay spread	300 n sec
Modulation scheme	16QAM, 64QAM, 256QAM
Number of frames	12 (for scs =15KHz) 6 (for scs =15KHz) 3 (for scs =60KHz)
Cyclic prefix	Normal
Subcarrier spacing	15, 30, 60
Number of HARQ retransmissions	No HARQ, 10 HARQ
Operating SNR	0 -> 40
Antenna Diversity	SISO

8.1.1 Performance analysis of different HARQ retransmissions

HARQ protocol is a retransmission technique used in the 5G to reduce the effect of multipath fading and enhance the BER and throughput performance. It is a combination of Automatic Repeat Request (ARQ) and Soft Combining. The function of ARQ is to check the CRC of the previous transmission to determine whether a retransmission is required. Soft Combining is an error correction technique where signals that are not received properly are stored in a buffer to be combined with next retransmissions. Therefore, a combined signal which is more reliable than its constituents is obtained.

The HARQ is based on stop and wait procedure where at the beginning the UE decode the packet which is transmitted from the gNB and send the ACK if it was wrongly decoded it sends a NACK so as a result the GNB will send a retransmission. The UE will combine the retransmission with the original transmission and will decode again. For successful decoding the UE will send positive acknowledgement (ACK) to the GNB, then the GNB will send a new packet for that HARQ process. It is worth to mention that due to the stop-and-wait way of operating, one needs to have multiple HARQ procedure to enable a continuous data flow.

Number of HARQ processes is a higher layer parameter which has a maximum value of 16 processes per cell for downlink. If there is no provided configuration, UE assumes a default value of 8 processes.

- ***BER of different modulation schemes after error correction with and without HARQ at SCS 15 KHz***

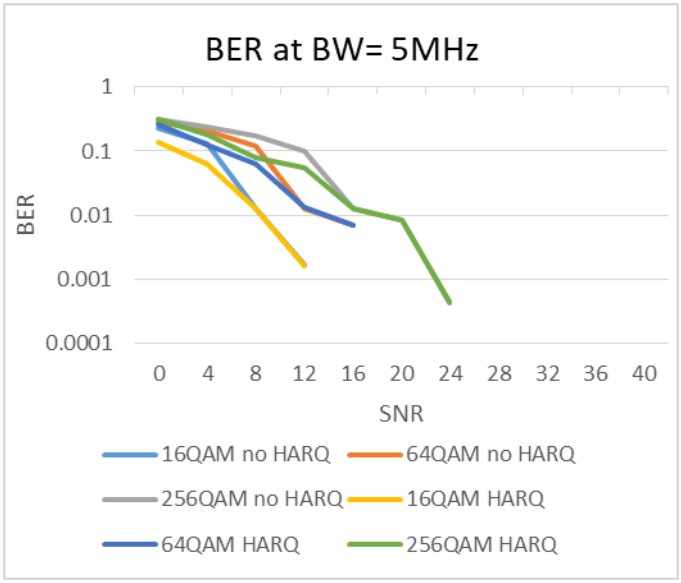

a) BER at BW= 5 MHz

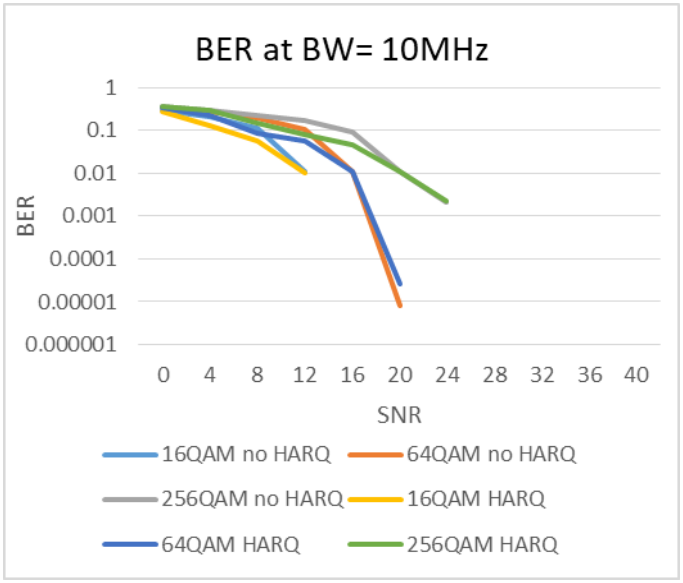

b) BER at BW= 10 MHz

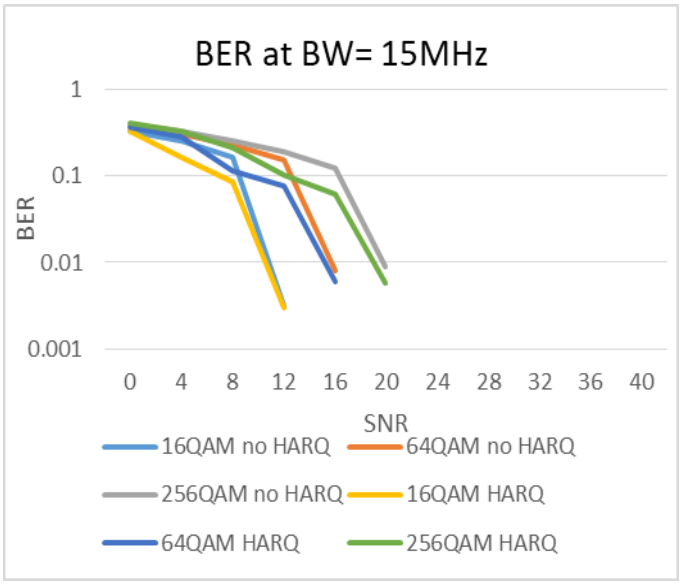

c) BER at BW= 15 MHz

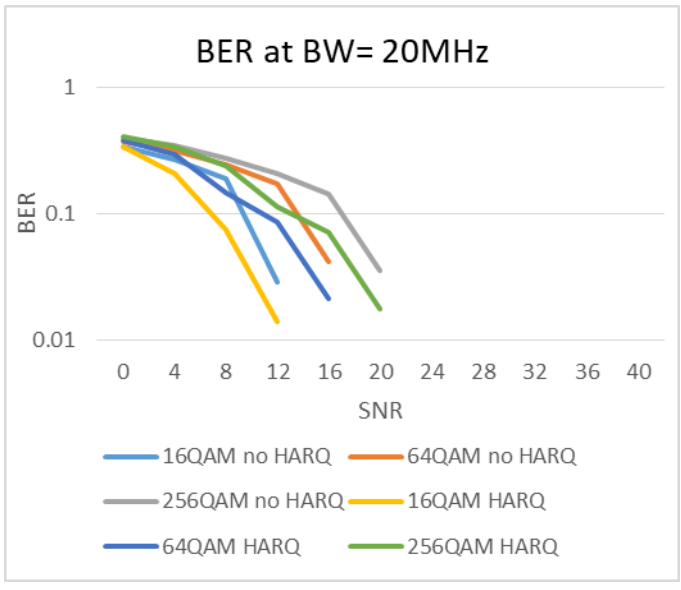

d) BER at BW= 20 MHz

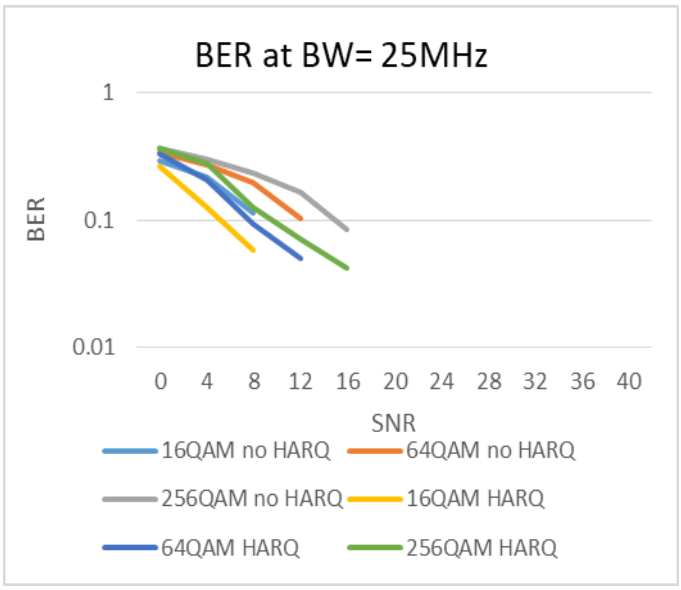

e) BER at BW= 25 MHz

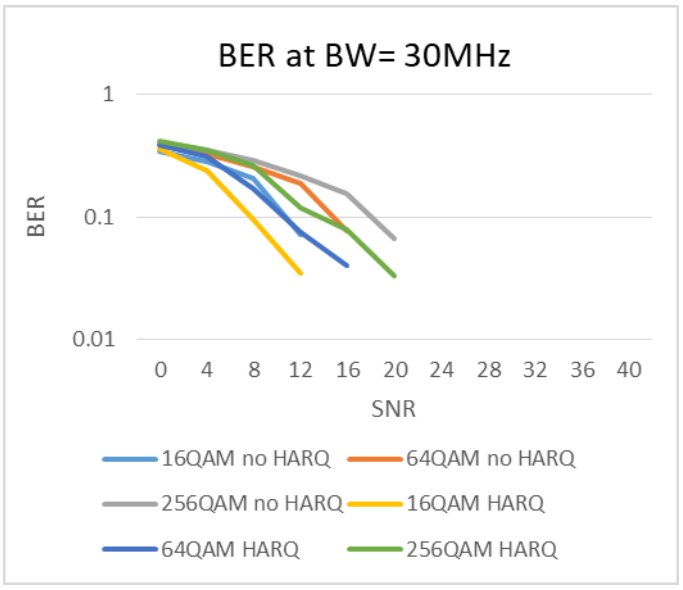

f) BER at BW= 30 MHz

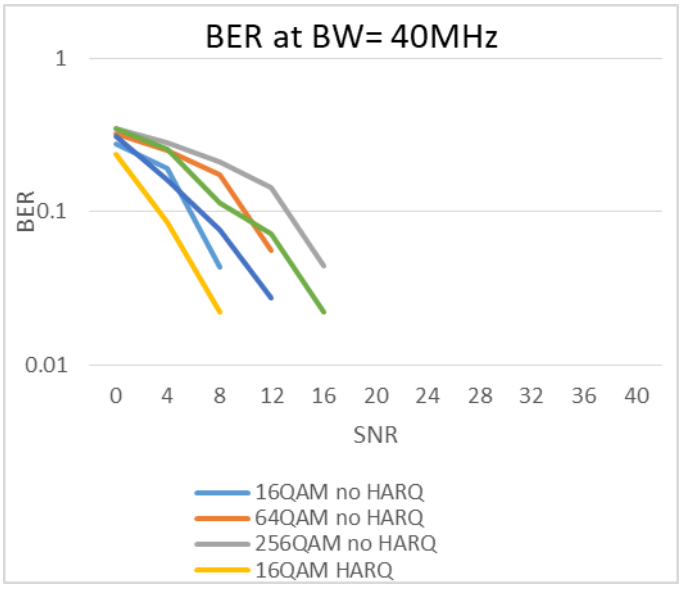

g) BER at BW= 40 MHz

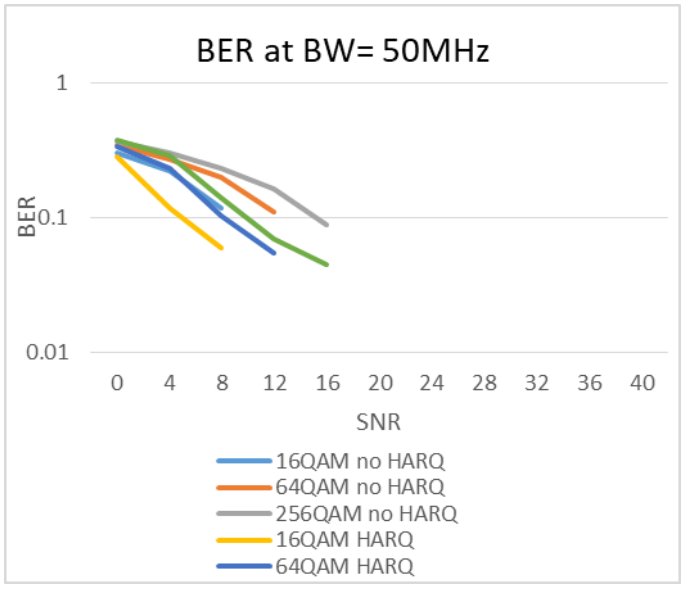

h) BER at BW= 50 MHz

Figure 8-1: BER versus SNR for different modulation schemes after error correction with and without HARQ at SCS=15 KHz

- ***BER of different modulation schemes after error correction with and without HARQ at SCS 30 KHz***

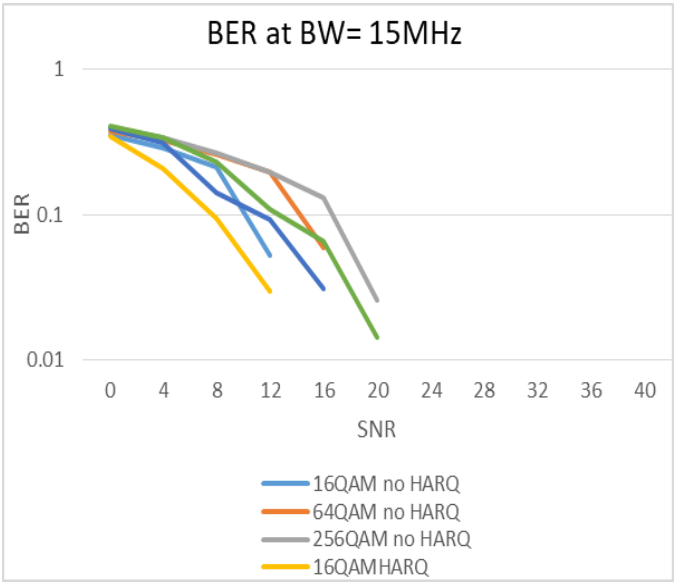

a) BER at BW= 15 MHz

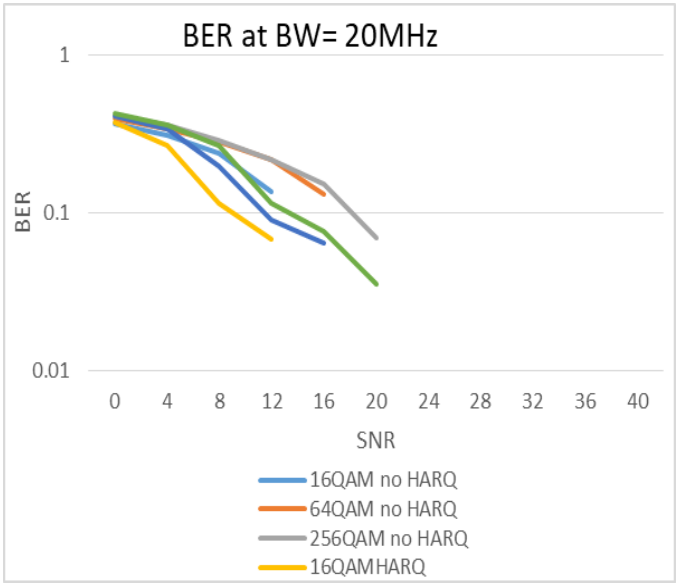

b) BER at BW= 20 MHz

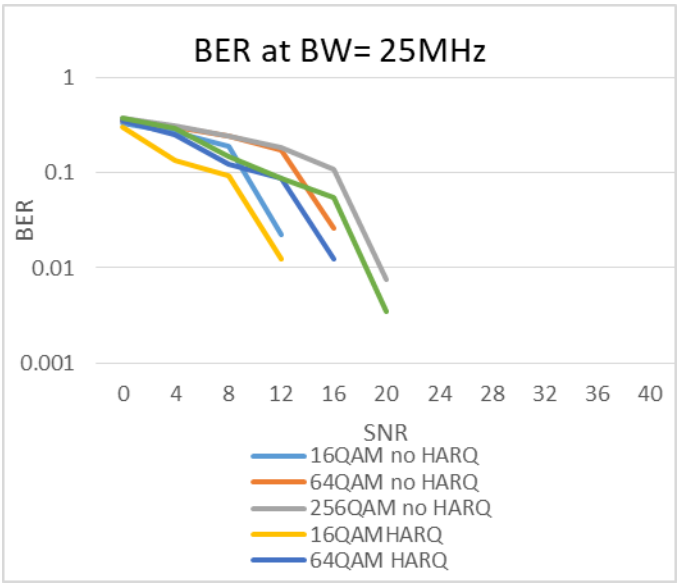

c) BER at BW= 25 MHz

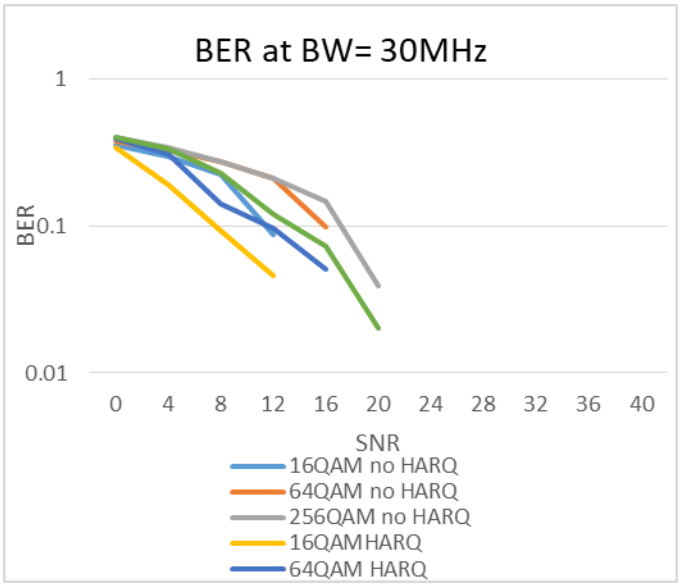

d) BER at BW= 30 MHz

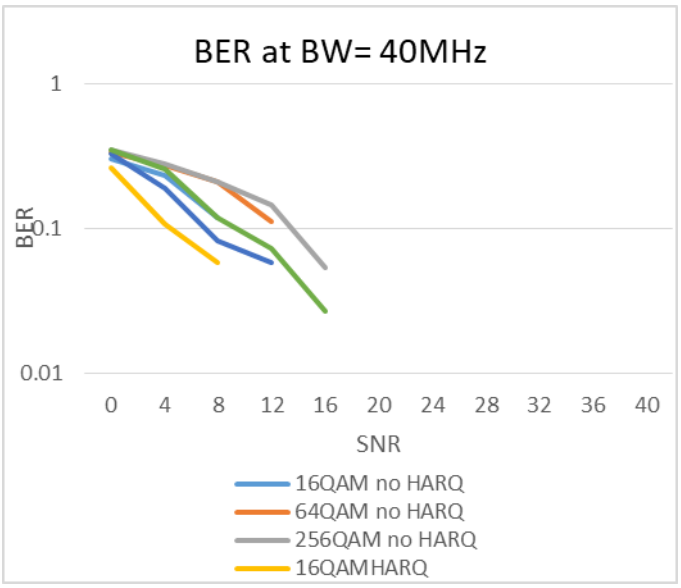

e) BER at BW= 40 MHz

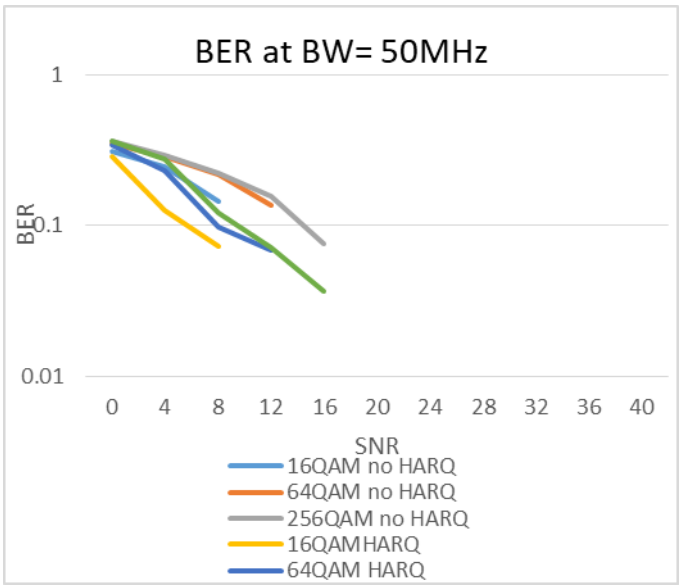

f) BER at BW= 50MHz

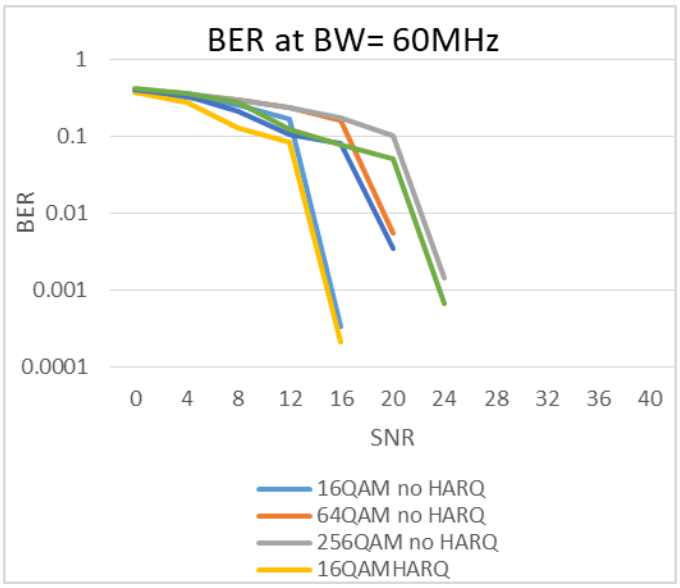

g) BER at BW= 60 MHz

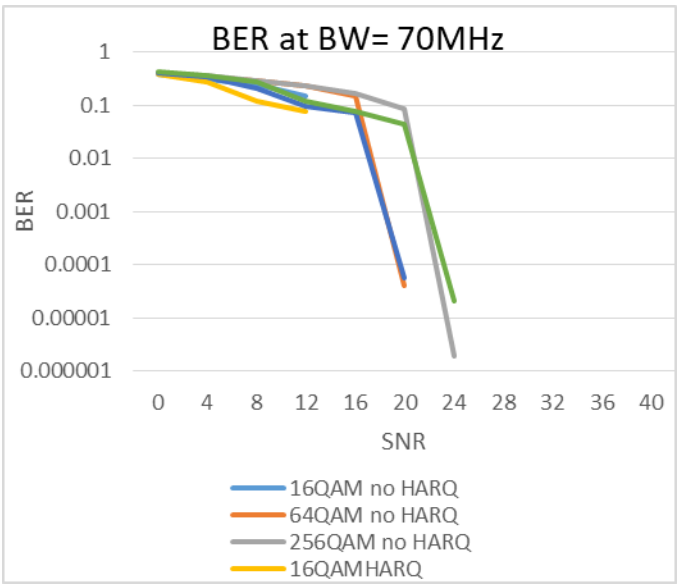

h) BER at BW= 70 MHz

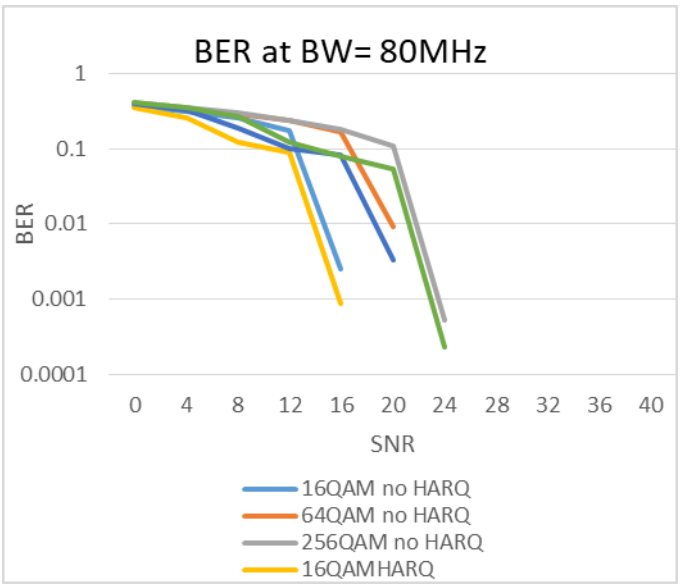

i) BER at BW= 80 MHz

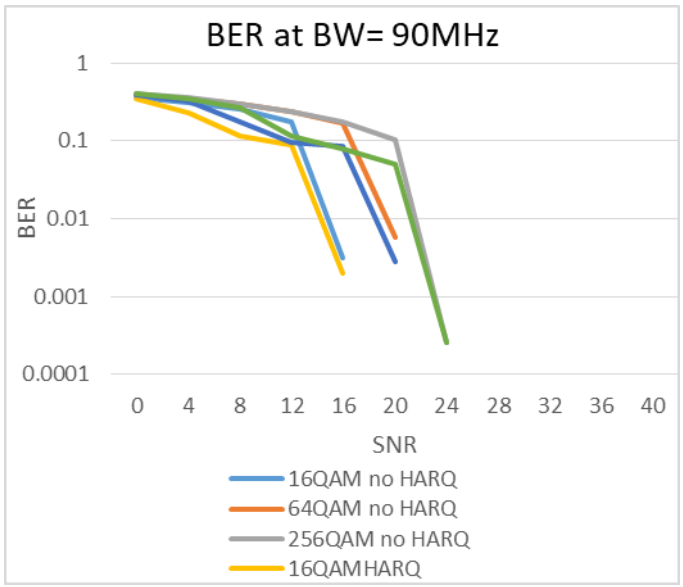

j) BER at BW= 90 MHz

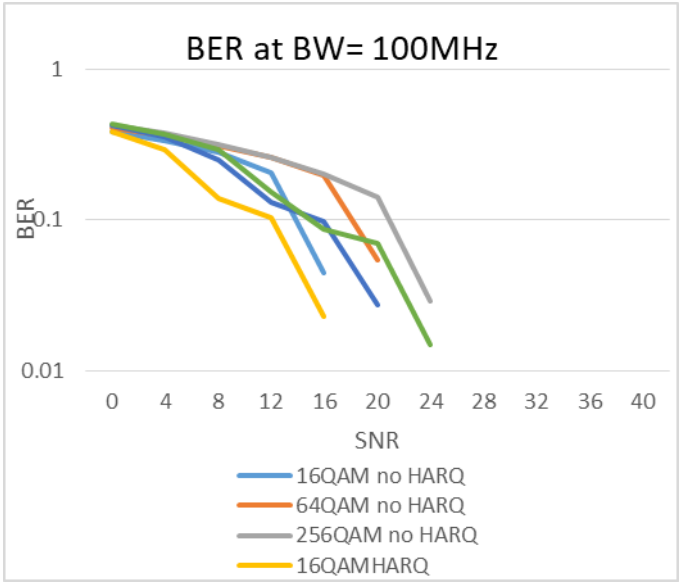

k) BER at BW= 100 MHz

Figure 8-2: BER versus SNR for different modulation schemes after error correction with and without HARQ at SCS=30 KHz

- ***BER of different modulation schemes after error correction with and without HARQ at SCS 60 KHz***

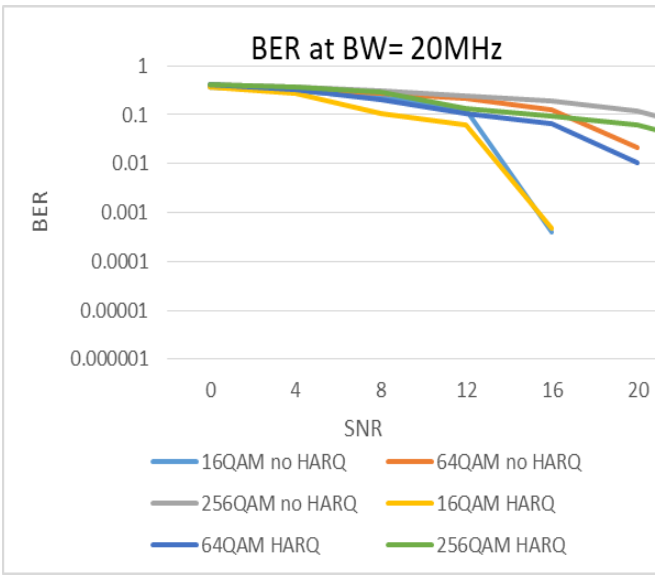

a) BER at BW= 20 MHz

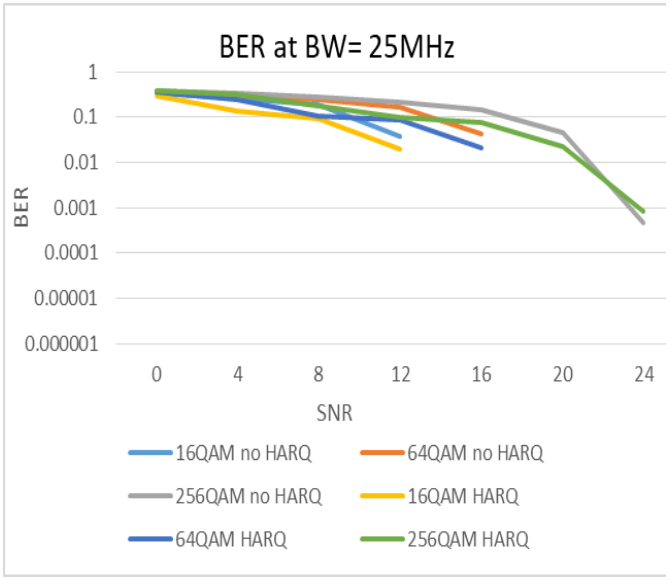

b) BER at BW= 25 MHz

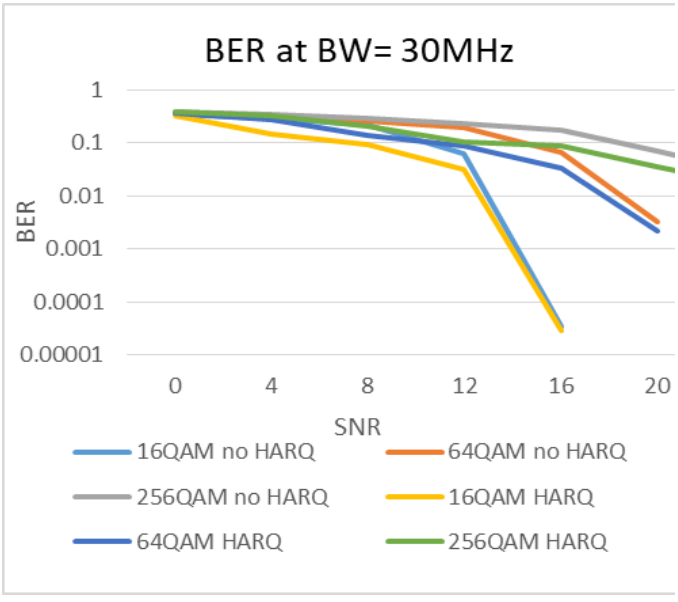

c) BER at BW= 30 MHz

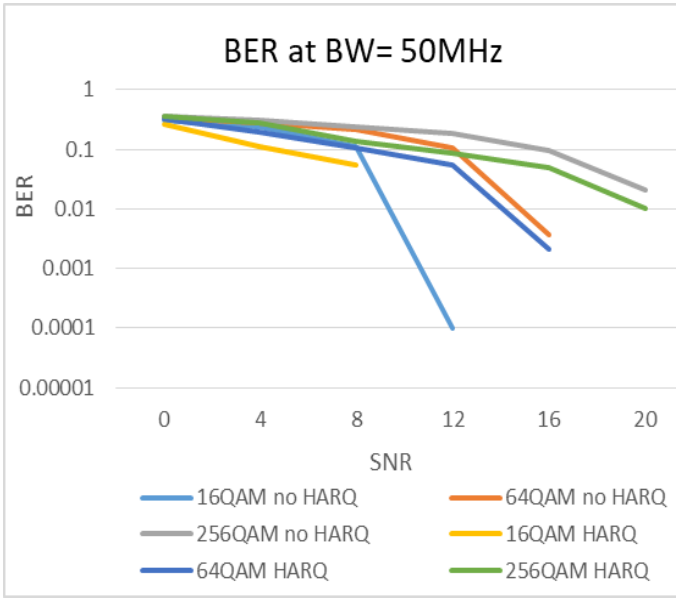

d) BER at BW= 50 MHz

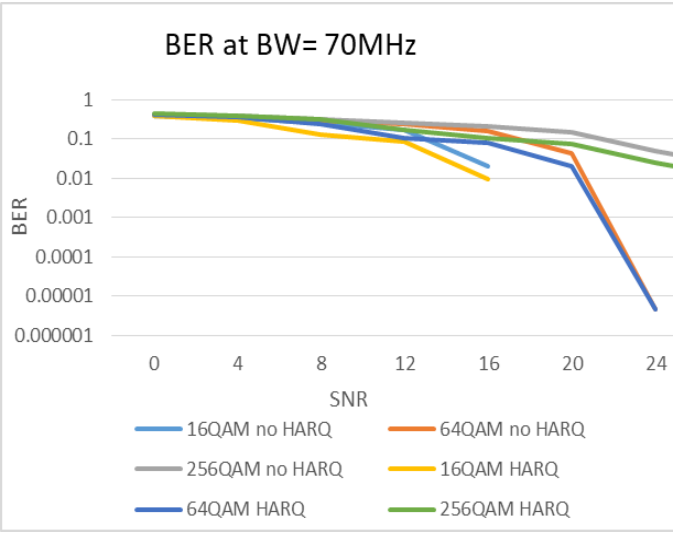

e) BER at BW= 70 MHz

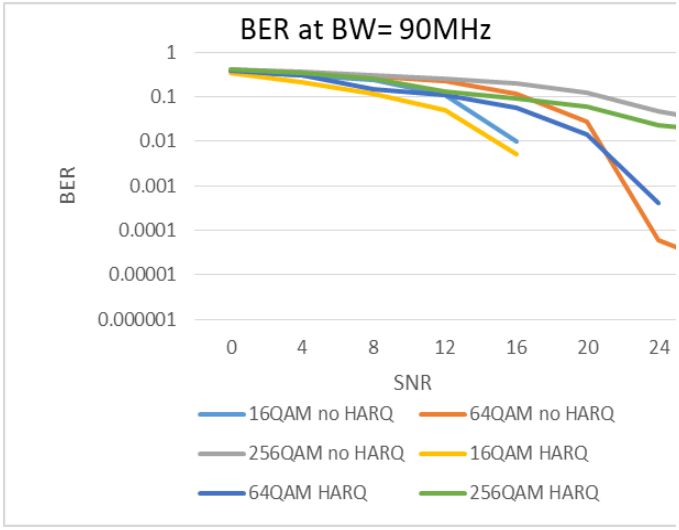

f) BER at BW= 90 MHz

Figure 8-3: BER versus SNR for different modulation schemes after error correction with and without HARQ at SCS=60 KHz

From Figure 8-1, Figure 8-2 and Figure 8-3, it is obvious that by activating the HARQ retransmissions the system BER decreases as the system uses different versions of the data to correct the previously received data ,so the overall error in the system is decreasing significantly as the system is given multiple chances (up to 4) to correct the error in the data.

The improvement due to HARQ differs with different SNR values, as for higher SNR and lower SNR there isn't much improvement as the BER nears zero for SNR values around 20 dB or higher and for lower SNR values the error is hard to overcome for both HARQ and no HARQ processes .

The following figure shows the average improvement across different bandwidths (the percentage of decrease in BER) due to HARQ for 30 KHz subcarrier spacing and 256QAM modulation scheme, the rest of the cases showed similar improvement behavior with SNR.

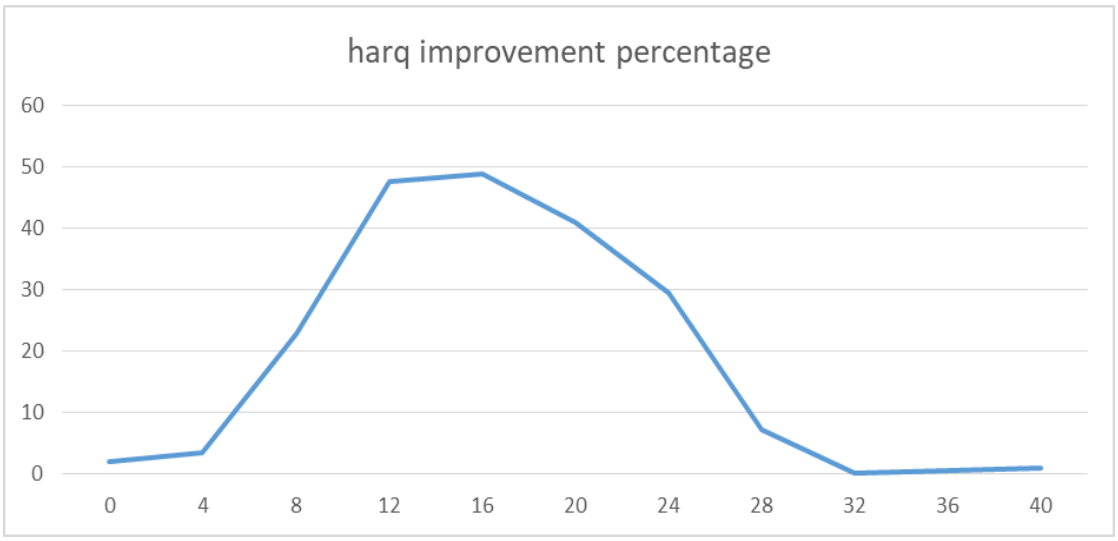

Figure 8-4:BER improvement due to HARQ for 30 KHz, 256QAM

It is clear that for the middle SNR values (4–28) dB the HARQ retransmissions technique improves the system BER performance moderately better than no HARQ retransmissions technique. But for higher SNR values both methods perform alike. Therefore, there is no point of using HARQ retransmissions technique for high channel SNR values.

When simulating on different subcarrier spacing, the only clear difference was the value of SNR that makes the performance of using HARQ almost the same as without HARQ, the following table shows these values:

Table 8-2: Average SNR values at which no significant improvement happens

Subcarrier spacing	Average SNR value
15	20dB
30	24-28dB
60	28-32dB

Also, it was found that at certain bandwidths such as 60MHz, 80MHz and 100MHz at SCS 60 the BER with HARQ remains less than without HARQ even at good channel conditions (at 36 SNR). The effect of the Bandwidth on the BER will be discussed in another section.

8.1.2 Performance analysis with and without error correction without HARQ

8.1.2.1 BER with and without error correction at SCS 15 KHz

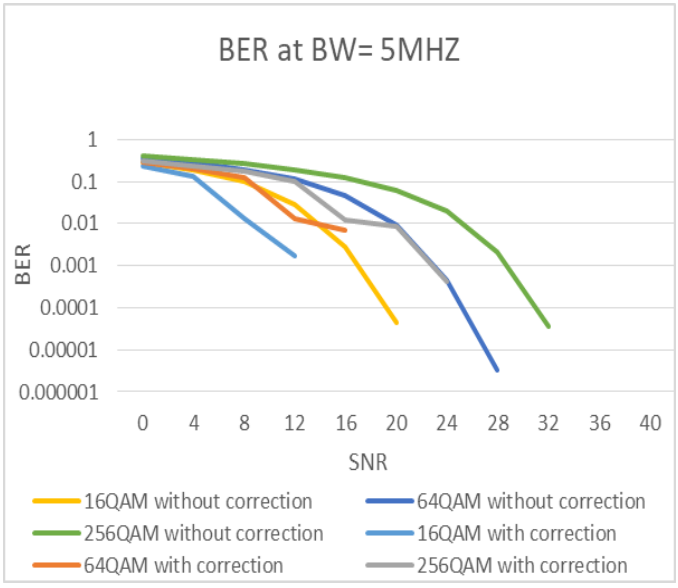

a) BER at BW= 5 MHz

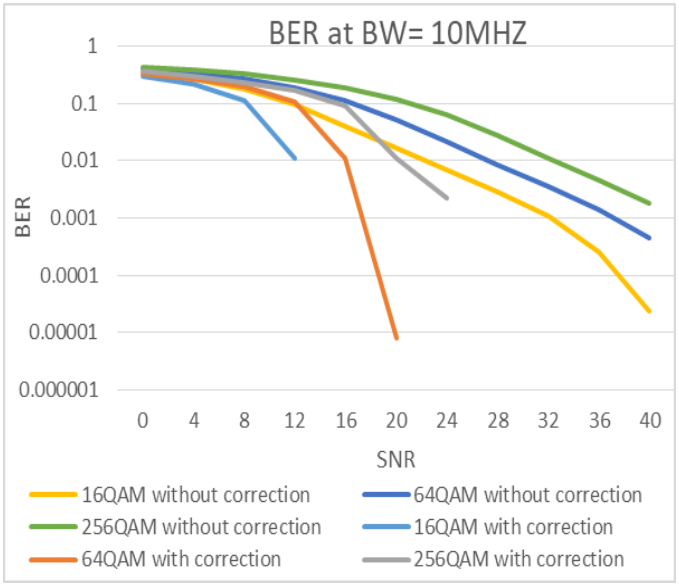

b) BER at BW= 10 MHz

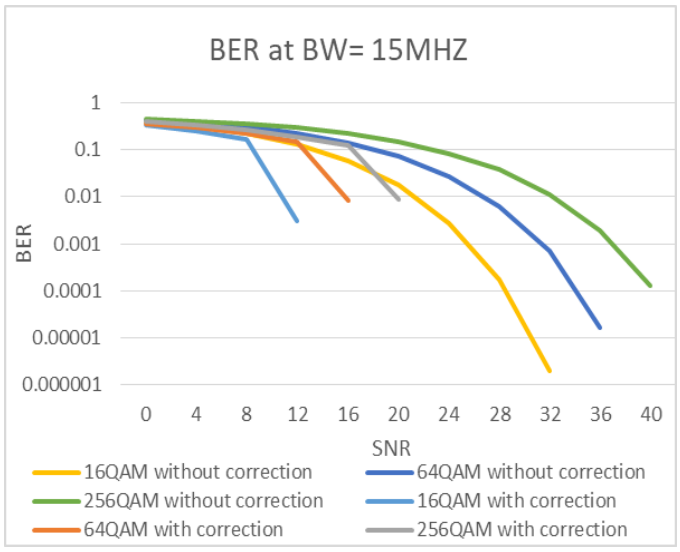

c) BER at BW= 15 MHz

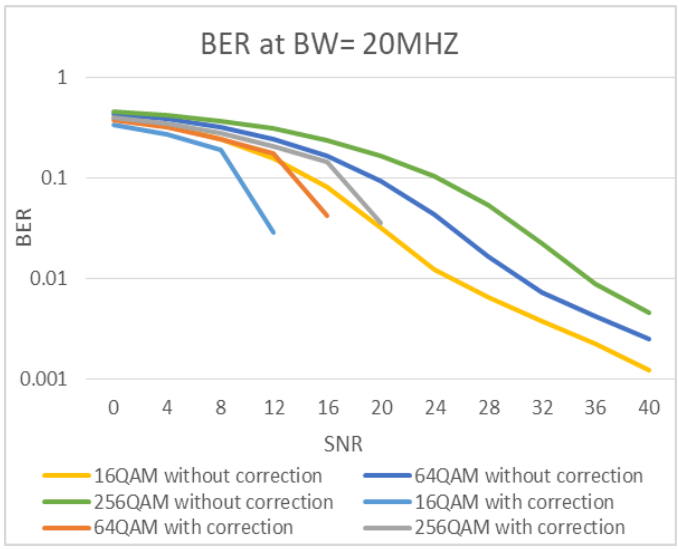

d) BER at BW= 20 MHz

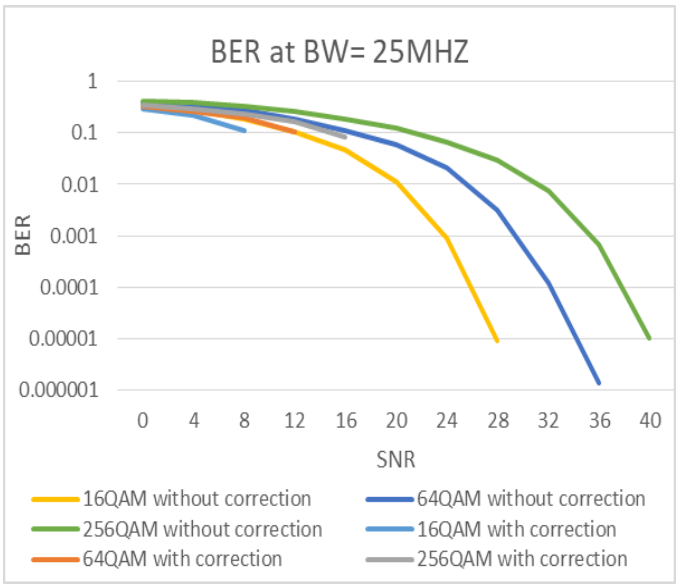

e) BER at BW= 25 MHz

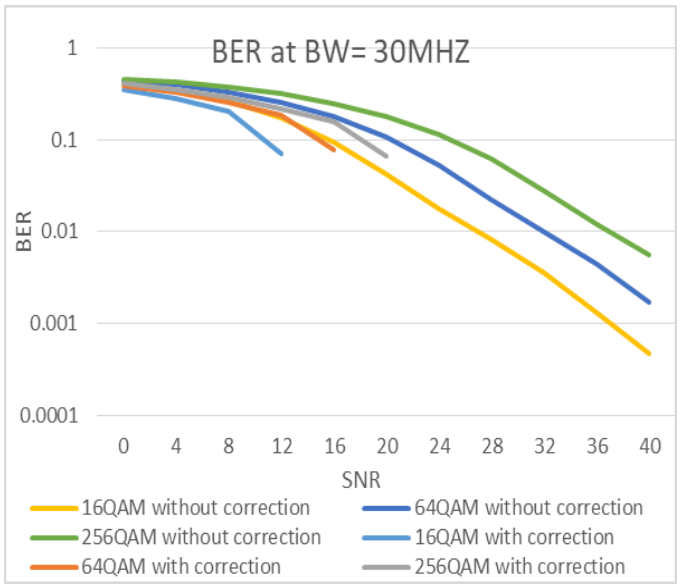

f) BER at BW= 30 MHz

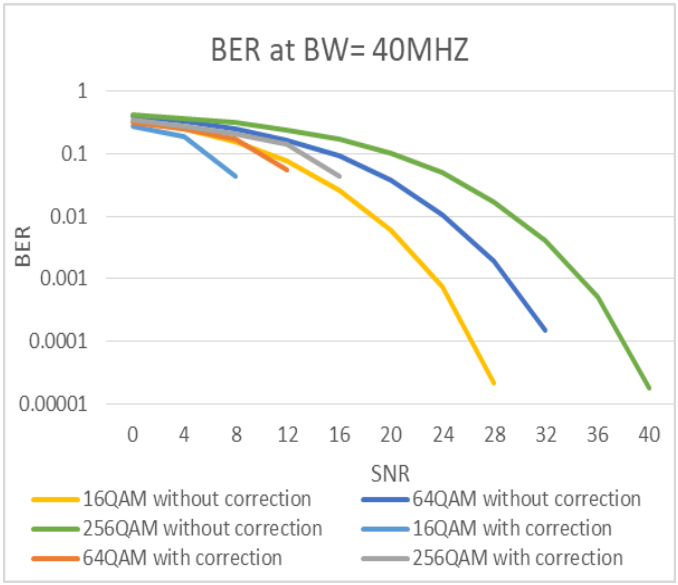

g) BER at BW= 40 MHz

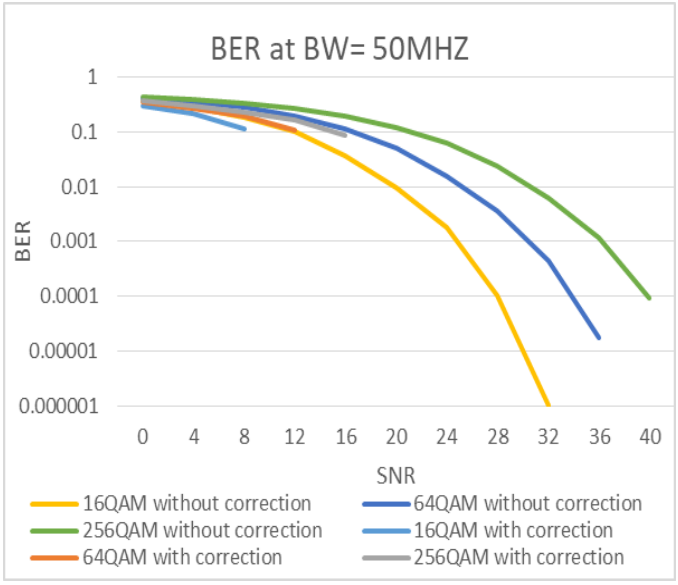

h) BER at BW= 50 MHz

Figure 8-5: BER versus SNR for Performance analysis with and without error correction without the use of HARQ at SCS=15

8.1.2.2 -BER with and without error correction at SCS 30 KHz

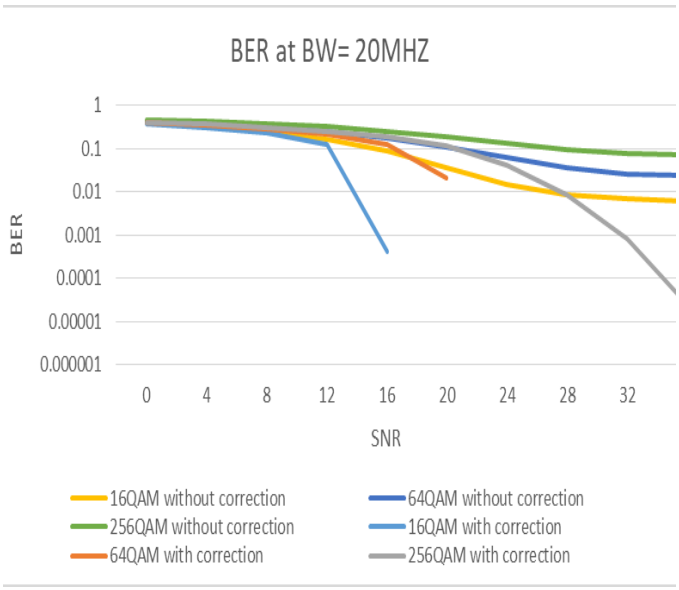

a) BER at BW= 20 MHz

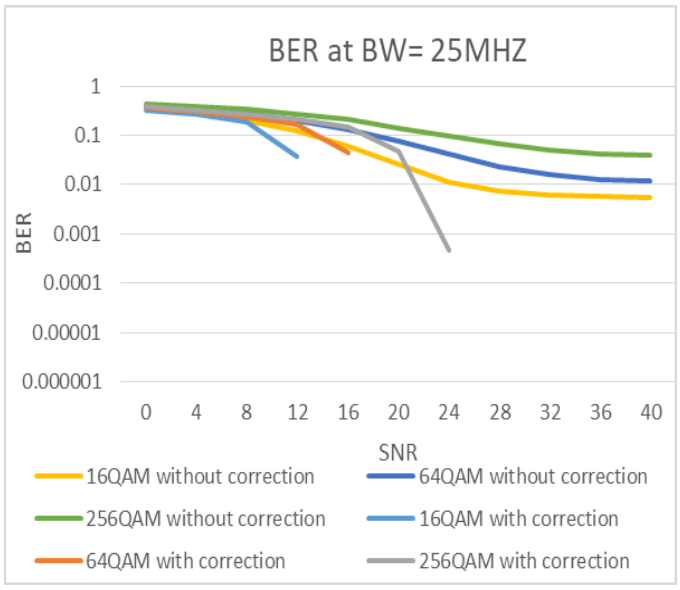

b) BER at BW= 25 MHz

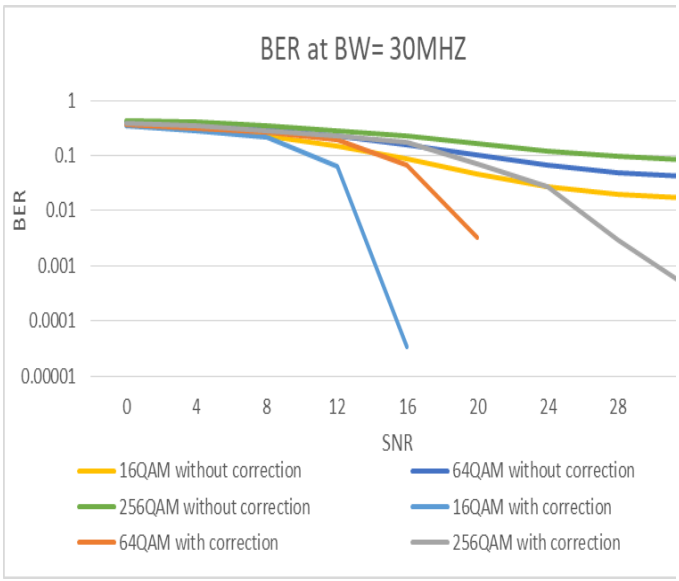

c) BER at BW= 30 MHz

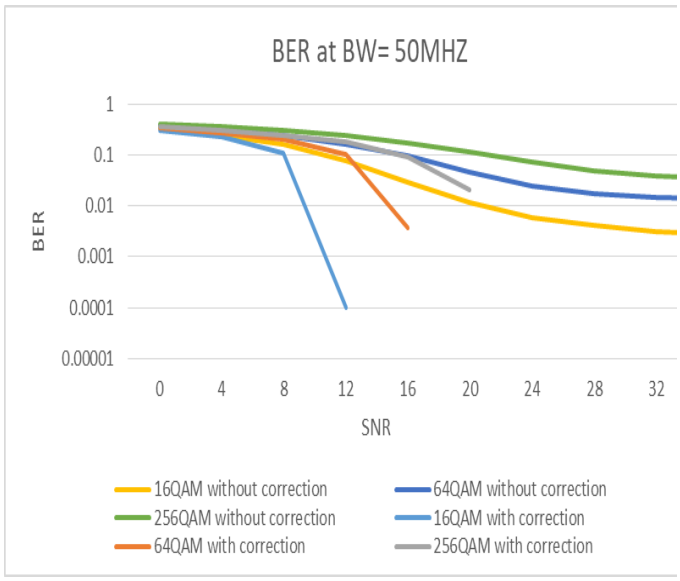

d) BER at BW= 50 MHz

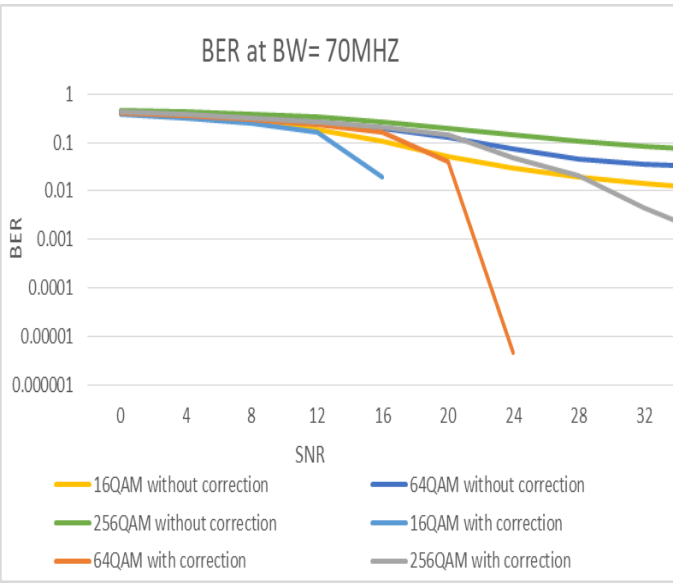

e) BER at BW= 70 MHz

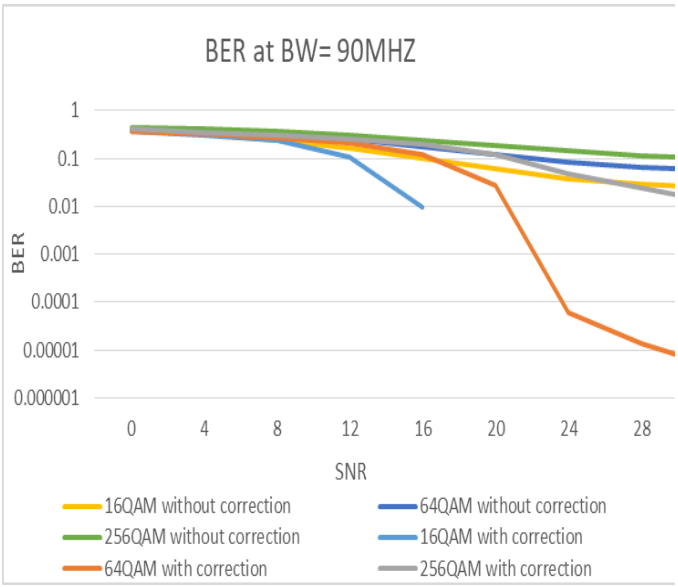

f) BER at BW= 90 MHz

Figure 8-6: BER versus SNR for Performance analysis with and without error correction without the use of HARQ at SCS=30

8.1.2.3 -BER with and without error correction at SCS 60 KHz

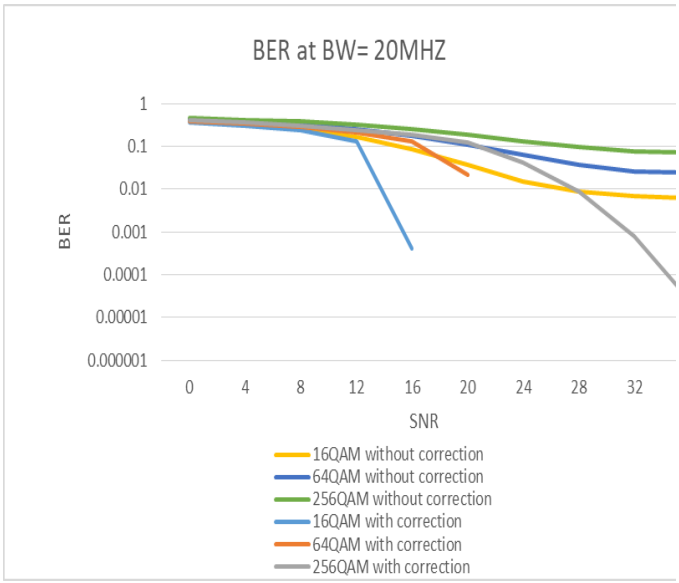

a) BER at BW= 20 MHz

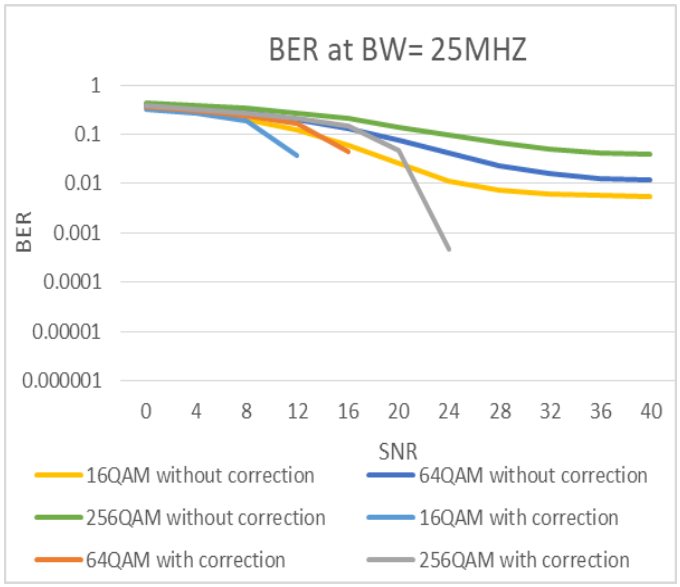

b) BER at BW= 25 MHz

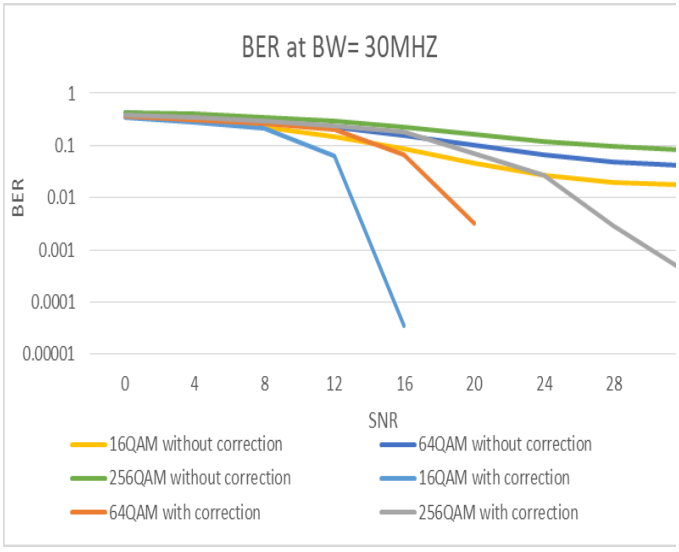

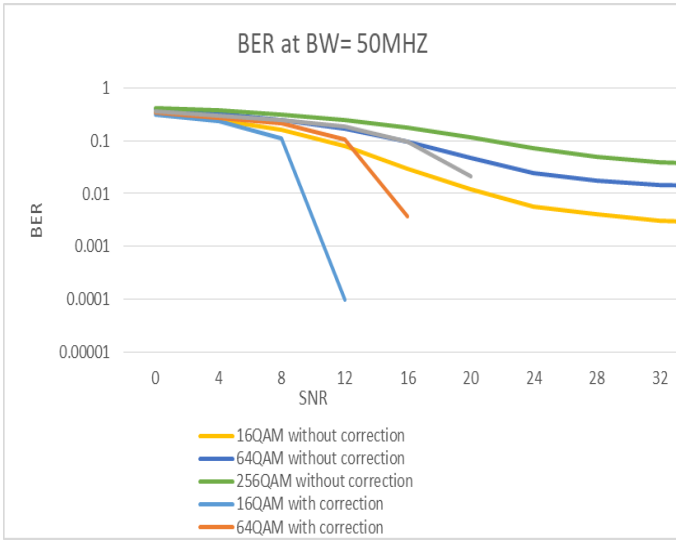

c) BER at BW= 30 MHz

d) BER at BW= 50 MHz

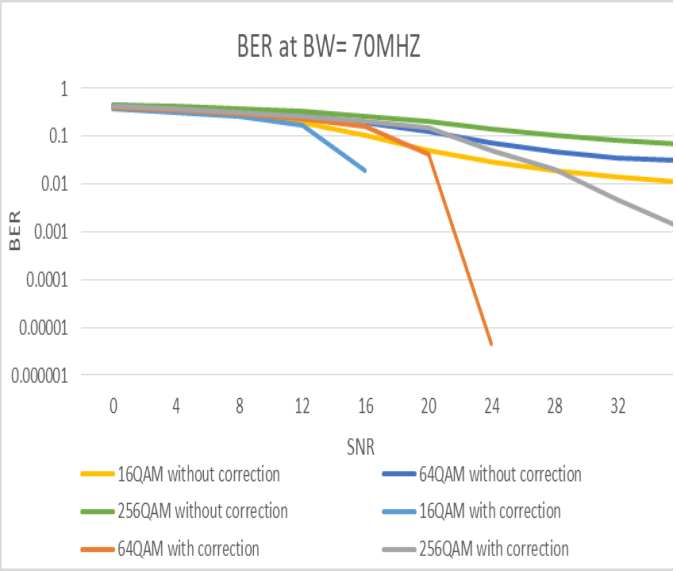

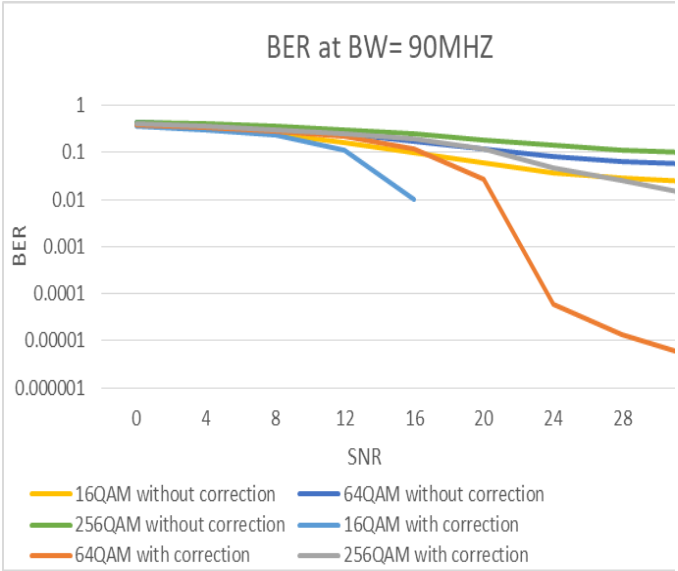

e) BER at BW= 70 MHz

f) BER at BW= 90 MHz

Figure 8-7: BER versus SNR for Performance analysis with and without error correction without the use of HARQ at SCS=60

The used coding technique is the LDPC. The LDPC adds redundancy to the un-coded input signal to make it more immune to the channel impairments such as noise and fading and thus it was clear that the BER after error correction for the 3 modulation schemes is smaller than the BER before correction, this coupled with the use of HARQ process can improve the average BER drastically.

For example:

- At 50 MHz bandwidth, using 64QAM at SNR =4:

SCS	BER before correction	BER after correction	Improvement percentage
15	0.353	0.271	23.2%
30	0.345	0.284	17.5%
60	0.330	0.276	16.3%

8.1.3 Performance analysis of different modulation schemes

The average values of the BER for subcarrier spacing 15 KHz and different modulation schemes can be seen in the following table:

Modulation schemes	BER for SNR 0:12 dB	BER for SNR 16:28 dB
16-QAM	0.35 : 0.10	0.05 : 0.002
64-QAM	0.41 : 0.2	0.12 : 0.007
256-QAM	0.43 : 0.26	0.2 : 0.03

The average values of the BER for subcarrier spacing 30 KHz and different modulation schemes can be seen in the following table:

Modulation schemes	BER for SNR 0:12 dB	BER for SNR 16:28 dB
16-QAM	0.38 : 0.14	0.08 : 0.009
64-QAM	0.42 : 0.22	0.15 : 0.02
256-QAM	0.44 : 0.29	0.22 : 0.06

The average values of the BER for subcarrier spacing 60 KHz and different modulation schemes can be seen in the following table:

Modulation schemes	BER for SNR 0:12 dB	BER for SNR 16:28 dB
16-QAM	0.37 : 0.14	0.08 : 0.016
64-QAM	0.42 : 0.23	0.15 : 0.04
256-QAM	0.44 : 0.29	0.23 : 0.09

- N.B: these values were calculated from the average values of BER across the different bandwidth values

Comment:

- As we go up the order of modulation BER increases for a given SNR value. obviously 16-QAM should have less BER with respect to other modulation schemes in same bandwidth as the order of modulation increases more number of bits are combined to make a symbol and these bits are packed more closely in signal constellation causing the increase in the bit error rate where the distance between the constellation points gets smaller and it becomes difficult for the receiver to decode correctly the sent bits.
- As we go on increasing SNR value for a given modulation technique BER goes on decreasing till the performance of all modulation schemes is almost the same (except in the case of SCS 60, where the BER doesn't reach zero at higher SNR)

8.1.4 Performance analysis of different subcarrier spacing values

8.1.4.1 -BER at modulation scheme 64QAM for different values of subcarrier spacing at different bandwidth values

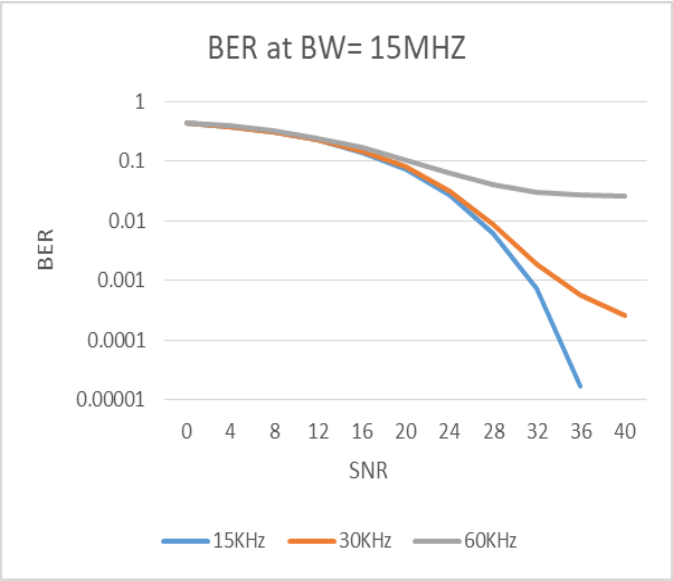

a) BER at BW= 15 MHz

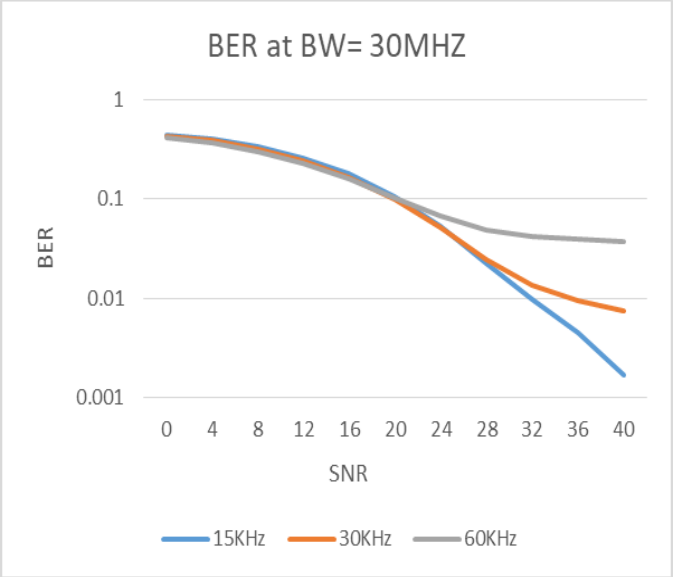

b) BER at BW= 30 MHz

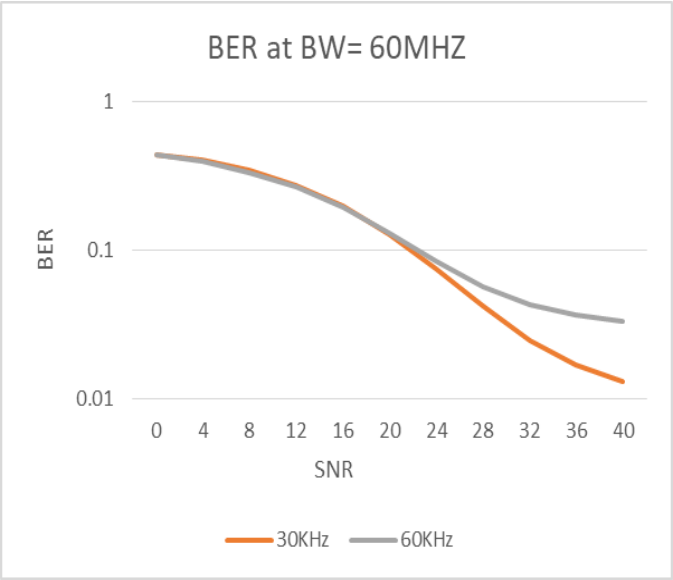

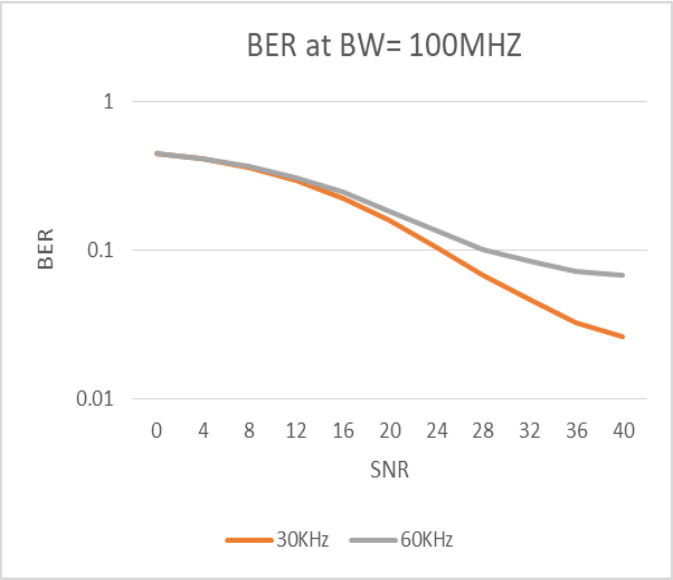

c) BER at BW= 60 MHz

d) BER at BW= 100 MHz

Figure 8-8: BER versus SNR for Performance analysis of different subcarrier spacing values

As shown in the figures the BER values for different subcarrier spacing doesn't vary that much for lower values of SNR ,but as the SNR gets higher we can see that at subcarrier spacing 60KHz the BER values start to derail from the rest of the SCS results ,this cause the success percentage of the entire to succumb as if the block have only 1 error bit ,the whole block is considered corrupted ,this can be seen in the following figures that show the percentage of successful blocks sent .and we can also see that even if HARQ is used the not that much improvement takes place.

8.1.4.2 -Throughput for different values of SCS for different bandwidth values

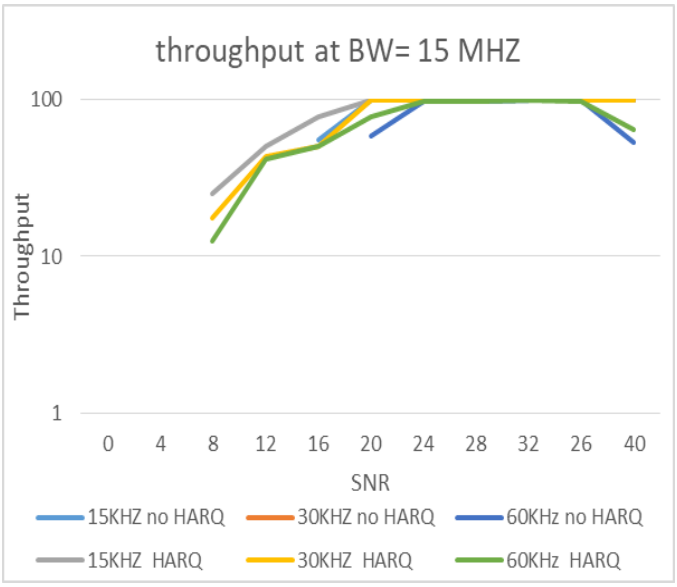

a) Throughput at BW= 15 MHz

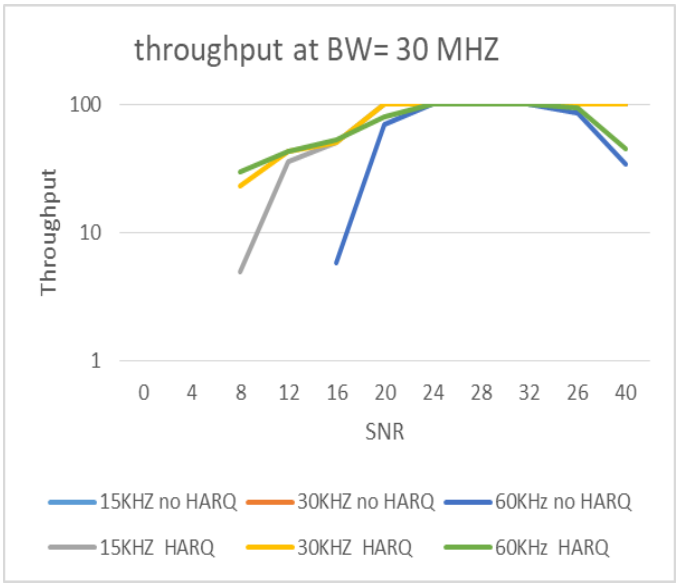

a) Throughput at BW= 15 MHz

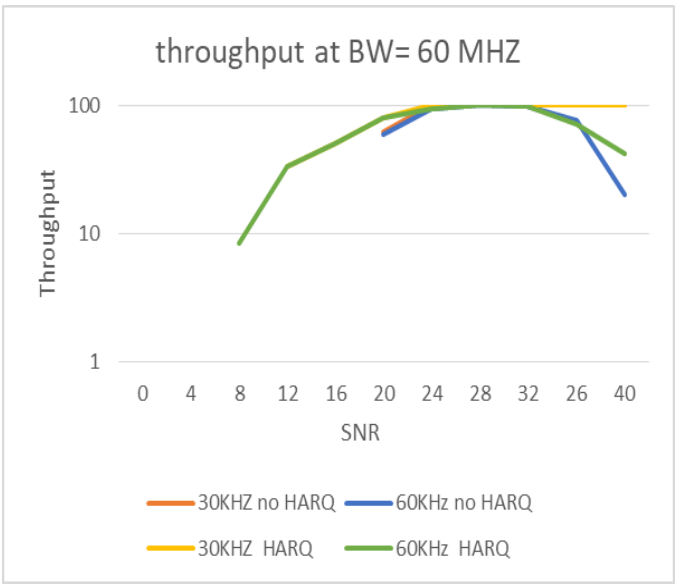

a) Throughput at BW= 15 MHz

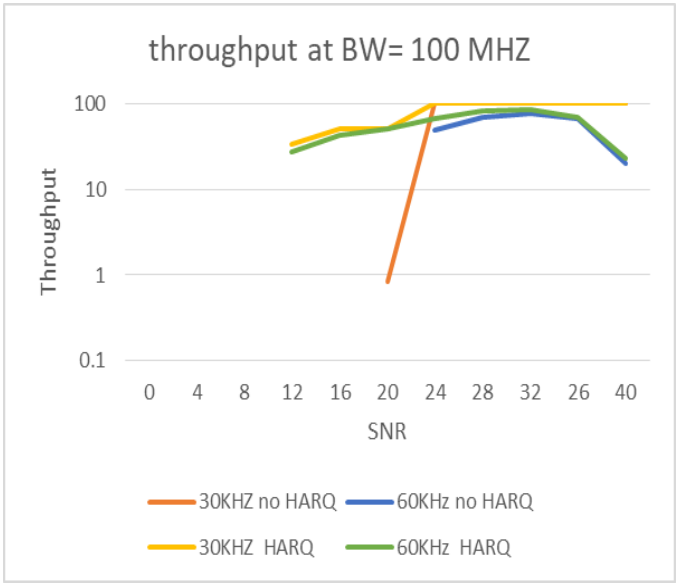

a) Throughput at BW= 15 MHz

Figure 8-9 Throughput for Performance analysis of different subcarrier spacing values

8.1.4.3 -BER at different subcarrier spacing with different delay spread values

Simulation parameters	value
Bandwidth	10MHz
Modulation	64QAM
Delay spread	1ns,300ns,1000ns
Subcarrier spacing	15,30,60

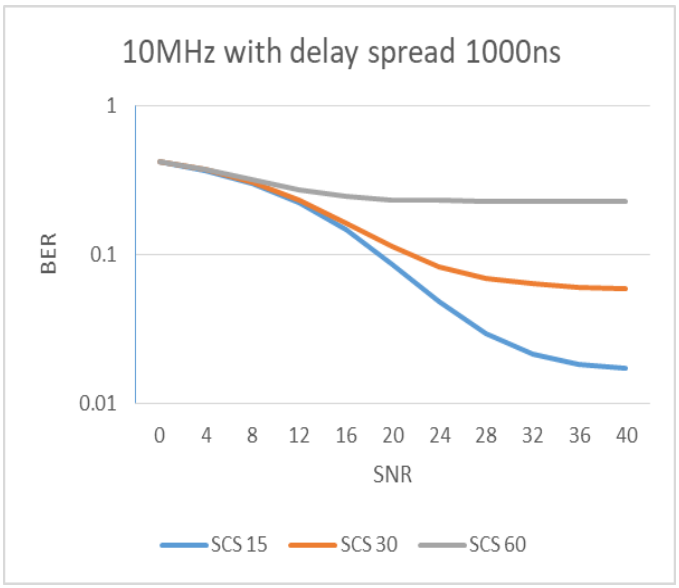

a) BER at BW=10MHz with delay spread 1000ns

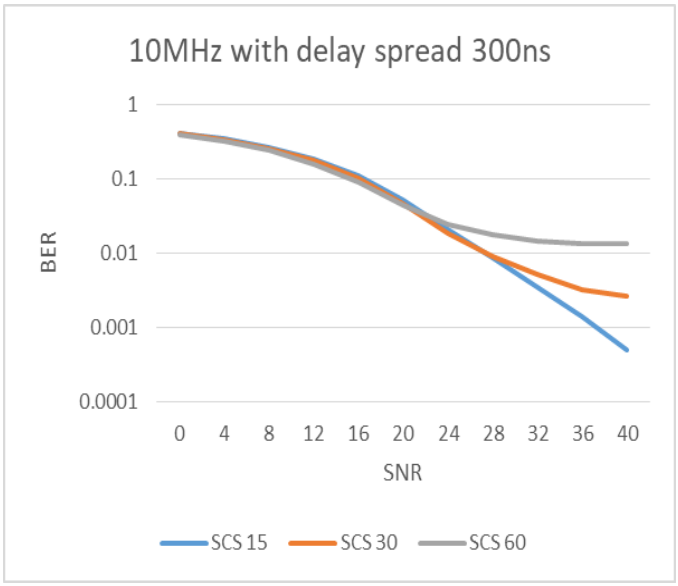

b) BER at BW=10MHz with delay spread 300ns

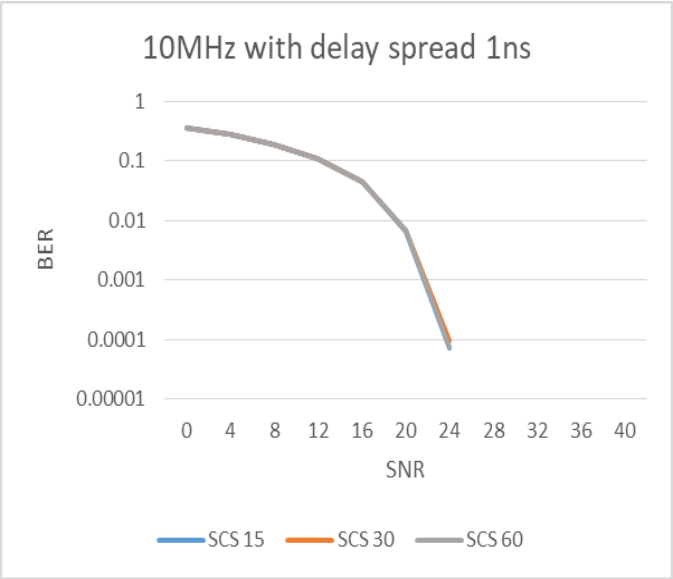

c) BER at BW=10MHz with delay spread 1ns

Figure 8-10: BER versus SNR at different subcarriers spacing with different delay spread values

The two figures above show that:

- In case of 300ns delay spread: the SCS 60 have the least BER at low range of SNR (0:20 dB) while at good SNR value the BER was found to be almost the same.
- In case of 1000 ns delay spread as shown at good SNR value the BER for the SCS 60 is relatively high and totally unacceptable. This shows that the 60 KHz numerology shouldn't be used in delay spread intensive environment.
- In case of 1ns delay spread: the performance of the SCS are considered to be identical, so as a result, no credit for choosing a certain numerology over the rest.

Chapter 9: MIMO simulation results and analysis

9.1 Throughput Performance

In this subsection the throughput performance of 5G Downlink is studied in terms of four major types of Antenna configurations at the GNB side and in terms of different number of data streams. Major among the parameters used for these simulations' subsection is outlined in the Table 1

Table 9-1:Simulation Parameters and values for studying the throughput performance

Parameter	Value
RX antenna	8
Allocated NRB	133
Number of layers	1, 2, 4, 8
Target Code Rate	0.4785
Channel	TDL C
MIMO Configuration	8x8, 16x16, 32x32 and 64x64

9.1.1 In terms of sending different data streams

For the simulations to investigate if the layer variations could affect the throughput performance of 5G communication system, the SNR values were varied for selected number of transmitted layers (1 layer, 2 layers, 4 layers and 8 layers) out of the eight specified available layers, this was done to give valuable analysis.

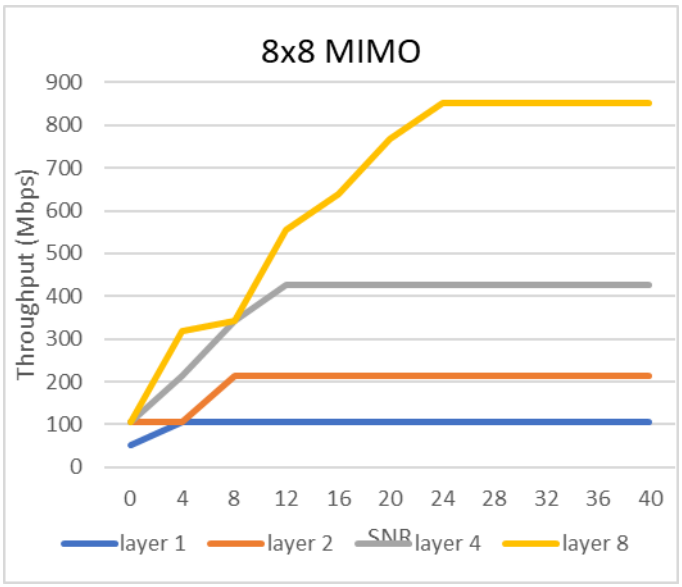

a) 8x8 MIMO

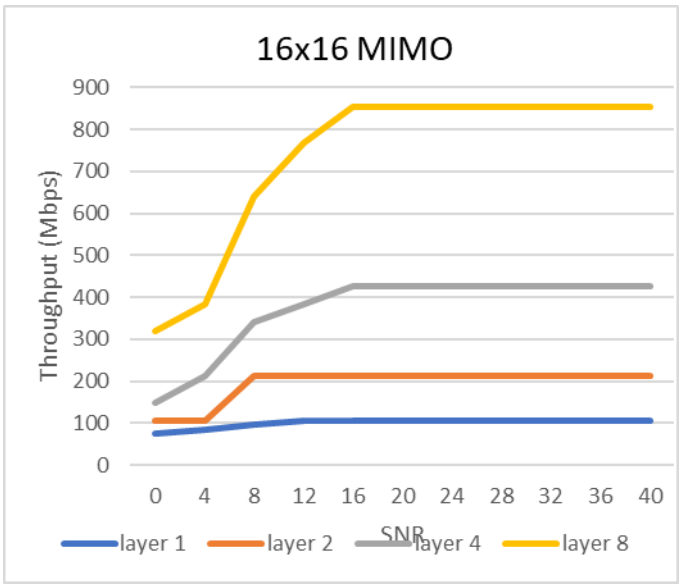

b) 16x16 MIMO

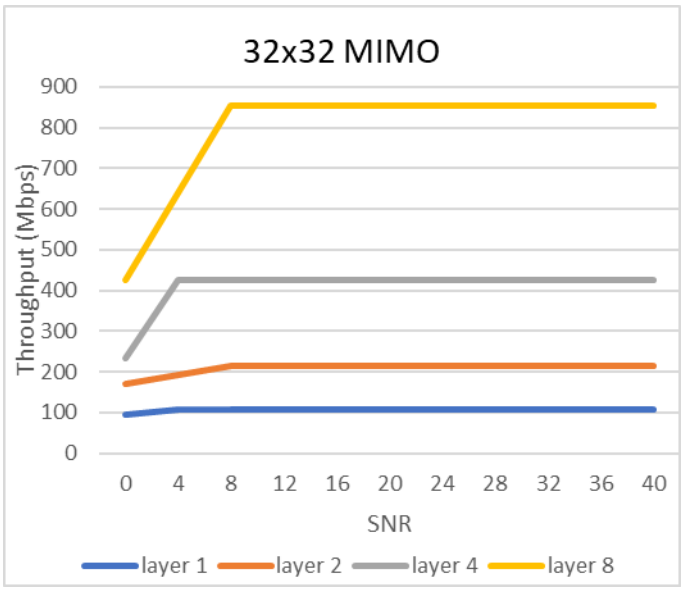

c) 32x32 MIMO

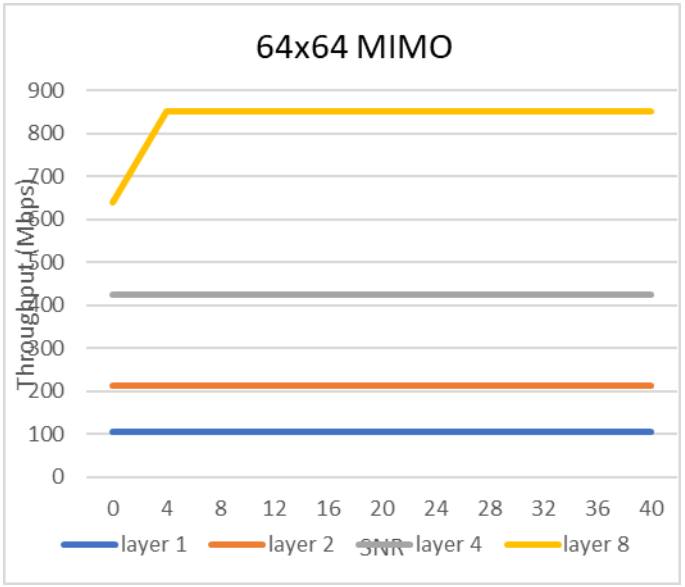

d) 64x64 MIMO

Figure 9-1:Throughput versus SNR for different antenna configurations upon sending 1, 2, 4 and 8 layers

Figure 9-1 demonstrates the throughput values versus SNR on sending 1 layer, 2 layers, 4 layers and 8 layers by four different antenna array configurations: 8x8, 16x16, 32x32 and 64x64. It is observed that for all antenna configurations the value of the achievable maximum throughput for high SNR ranges (>=24 dB) is dependent on the number of sent data streams as the throughput increases by 2x,4x and 8x times when sending 2 layers, 4 layers and 8 layers respectively. Hence it can be deduced that, though employing higher order of layers can offer better spectral efficiency and throughput and this can be visualized numerically in Figure 9-2 and Table 9-2.

Table 9-2:Peak Throughput values versus number of layers

Number of layers	Peak Throughput (Mbps)
1	106
2	213
4	426
8	852

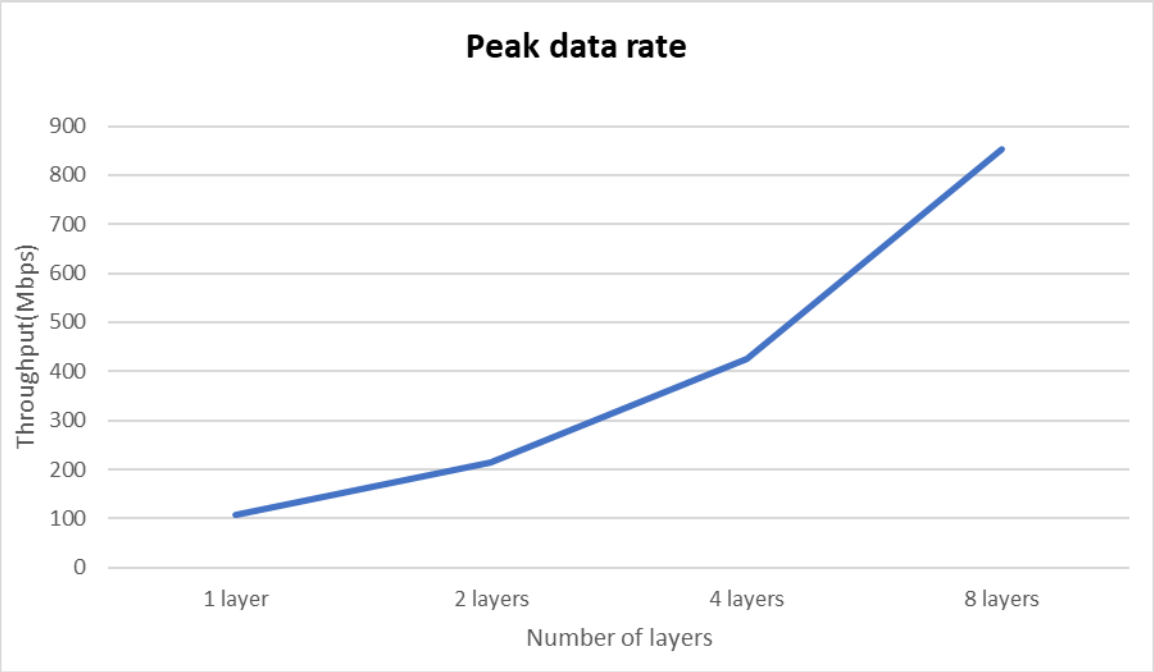

Figure 9-2:Peak data rate versus number of layers

9.1.2 In terms of different antenna configurations

One of the most basic and common factors that controls the spectral efficiency and throughput is the SNR (Signal to Noise Ratio). If the SNR of a network is bad, then that puts a limit on the throughput gain that it can achieve.

Finally, desired relation between SNR and downlink throughput for different antenna configurations at the BS is obtained and presented visually in Figure 9-3.

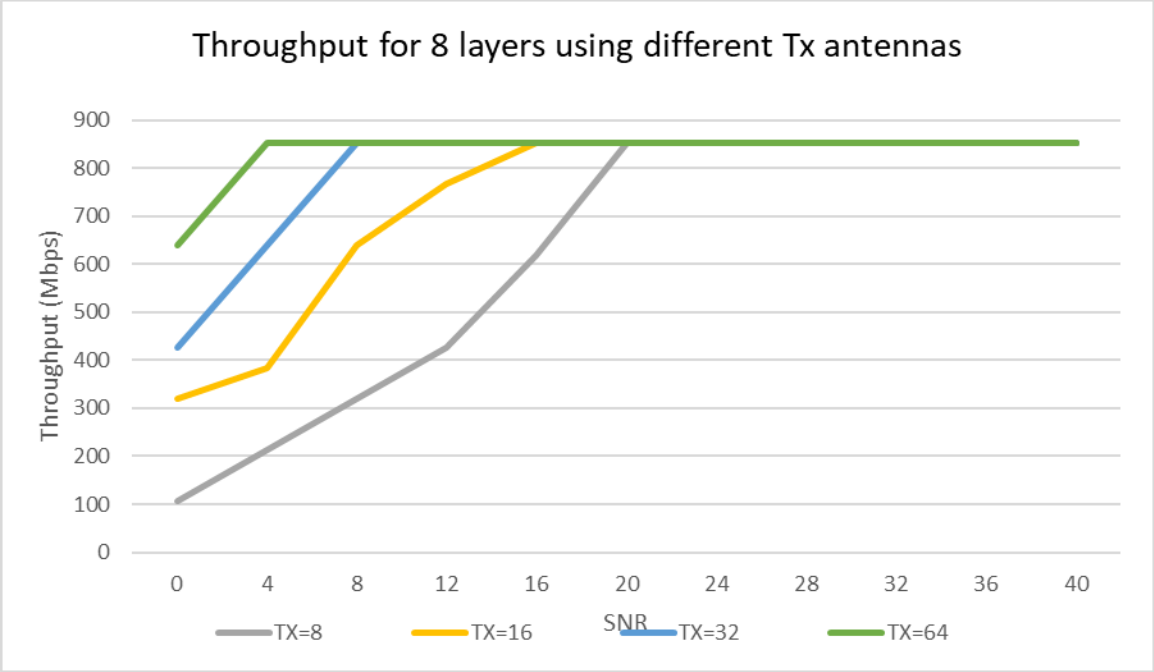

Figure 9-3:Throughput upon sending 8 layers for different antenna configurations at the gNB

The figure above illustrates that the throughput reaches its maximum value when using 64Tx followed by 32 Tx then 16 Tx then finally 8 Tx.

The table below shows the value of SNR where the throughput is at its maximum value for different antenna configurations.

Table 9-3:the value of SNR where the throughput is at its maximum

Antenna Configuration	SNR
8	20
16	16
32	8
64	4

It can be concluded that the throughput performance is behaving similarly in most of the SNR ranges except in range from 0 dB to 20 dB.

Meanwhile, when using a large number of antennas at the gNB side, the throughput dynamically increases and reaches its maximum value at low values of SNR, and almost clear in the case of 64 antennas than any other configurations, where the system reaches its maximum throughput at SNR 4 dB.

Thus, the throughput is maximized earlier even at bad channel conditions as the number of antennas at the gNB increases.

9.2 BER performance for different number of antennas at the gNB side

Antenna arrays have become part of the standard configuration in 5G wireless communication systems. Antenna arrays can help improve the SNR by exploring the redundancy across the multiple transmit and receive channels and Improving the signal-to-noise ratio (SNR) is key to improving data rates. In this subsection the BER performance is studied in terms of four major types of Antenna configurations at the gNB side and in terms of different number of data streams. Major among the parameters used for these simulations' subsection is outlined in the Table 9-4.

Table 9-4: Simulation Parameters and values for studying the BER performance versus number of antennas at the gNB side

Parameter	Value
RX antenna	8
Allocated NRB	10
Number of layers	1, 2, 4, 8
Target Code Rate	0.4785
Channel	TDL C
MIMO Configuration	8x8, 16x16, 32x32 and 64x64

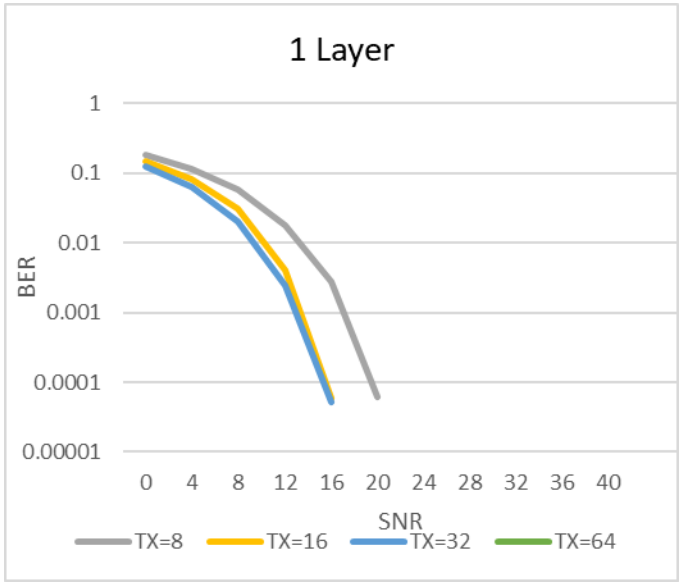

a) 1 layer with different Tx antennas

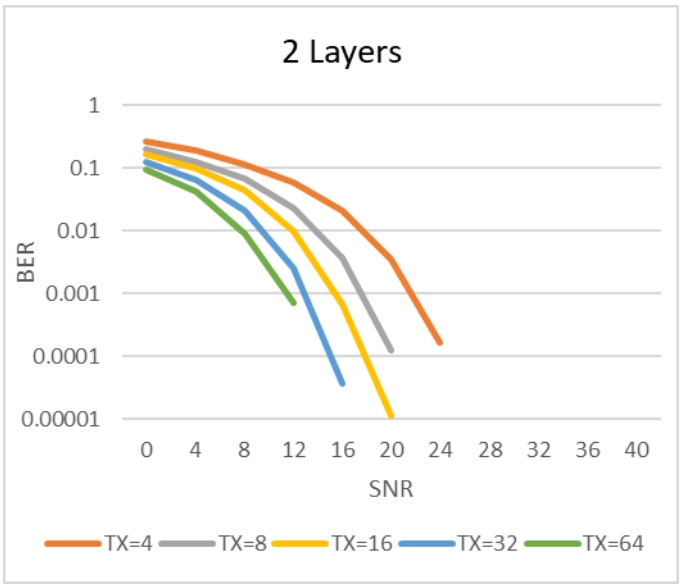

b) 2 layers with different Tx antennas

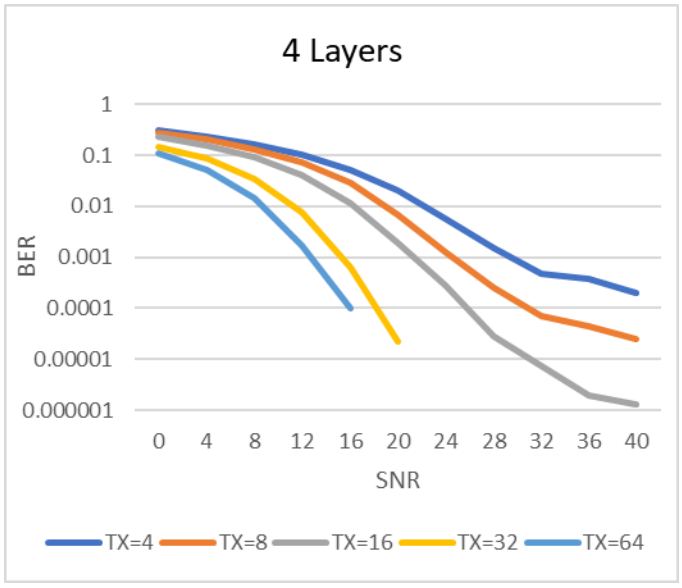

c) 4 layers with different Tx antennas

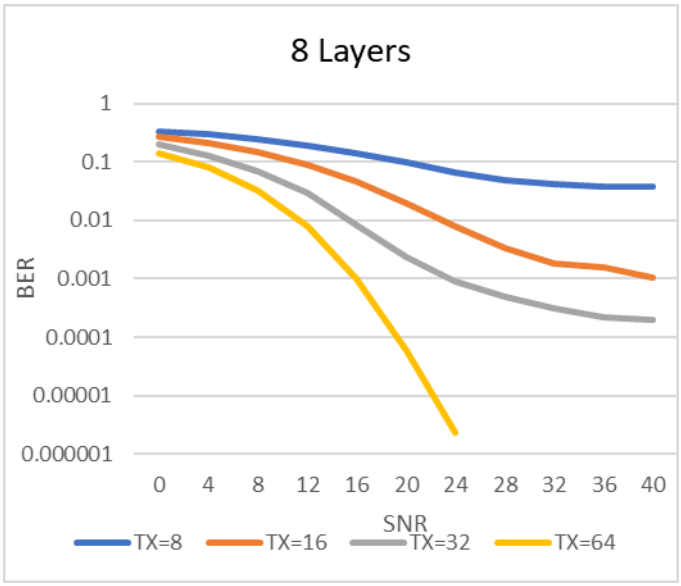

d) 8 layers with different Tx antennas

Figure 9-4:BER versus SNR for different antenna configurations upon sending 1, 2, 4 and 8 layers

The simulation results demonstrate a significant performance improvement using beamforming with higher order antennas. This is because beamforming on the transmit side increases the SNR as well as it eliminates the interference from undesired sources.

With higher order antennas the number of multiple data streams that can be sent simultaneously across the channel will increase and by separating the channel matrix into multiple independent paths the data streams sent from different elements in the transmit array can be independently recovered from the received signal, which will improve the performance in this way.

9.3 BER performance upon sending different number of layers

As shown in subsection 1 the throughput mainly depends on the number of transmitted layers simultaneously to the UE, but this comes at the expense on increasing BER. In this subsection, the BER is studied and analyzed for transmitting different number of layers with different antenna configurations. Major among the parameters used for these simulations' subsection is outlined in the Table 9-5.

Table 9-5:Simulation Parameters and values for studying the BER performance versus number of layers

Parameter	Value
Allocated NRB	10
RX antenna	2,4,8
Channel Model	TDL C
MIMO configuration	4x4, 8x8, 16x16, 32x32 and 64x64
Number of layers	1,2,4,8

Simulations in this subsection as shown in the table are done at different number of receivers at the UE side taking into considerations that the number of layers sent must be less than or equal the number antennas at the UE.

The effect of having different number or receivers at the UE side will be discussed in subsection 9.4.

9.3.1 BER when beamforming with 4x4 MIMO at the gNB

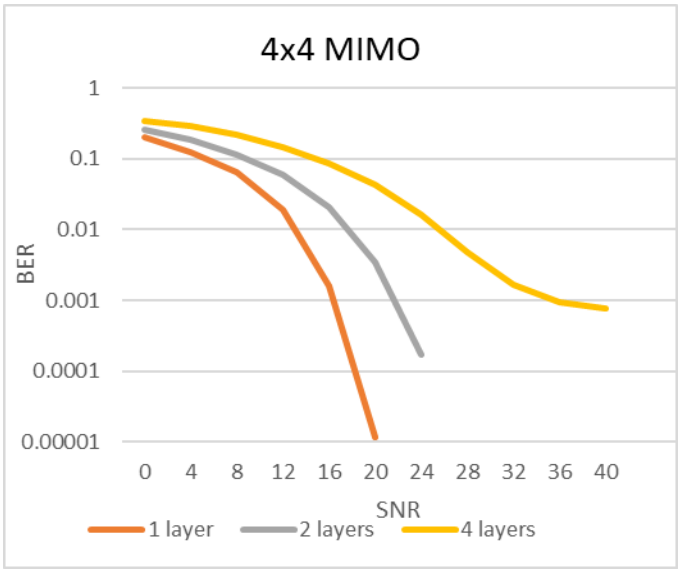

a) BER at RX=2

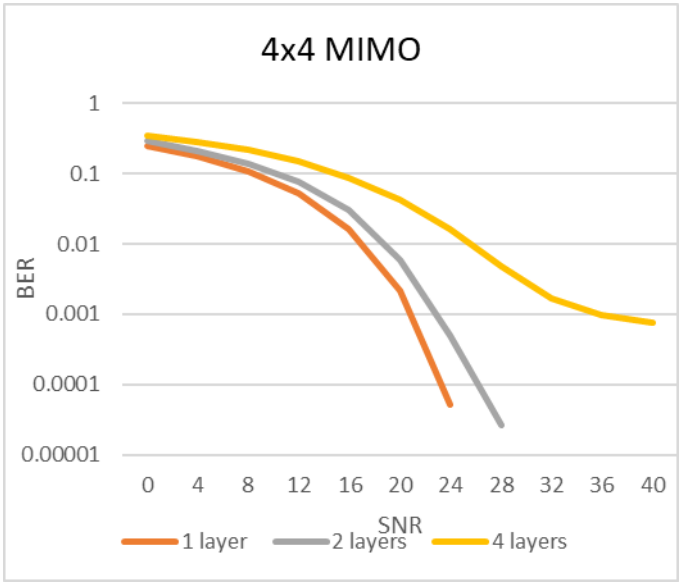

b) BER at RX=4

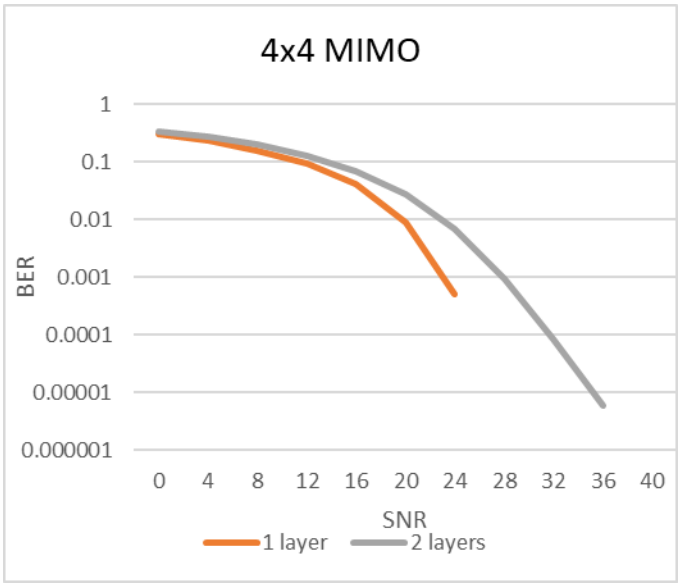

c) BER at RX=8

Figure 9-5:BER using 4x4 at the GNB for RX 2, 4, and 8 at the UE side

9.3.2 BER when beamforming with 8x8 MIMO at the gNB

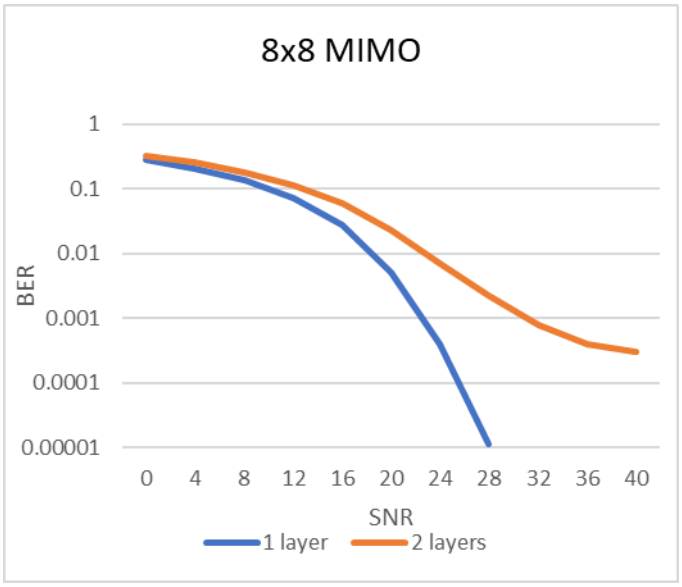

a) BER at RX=2

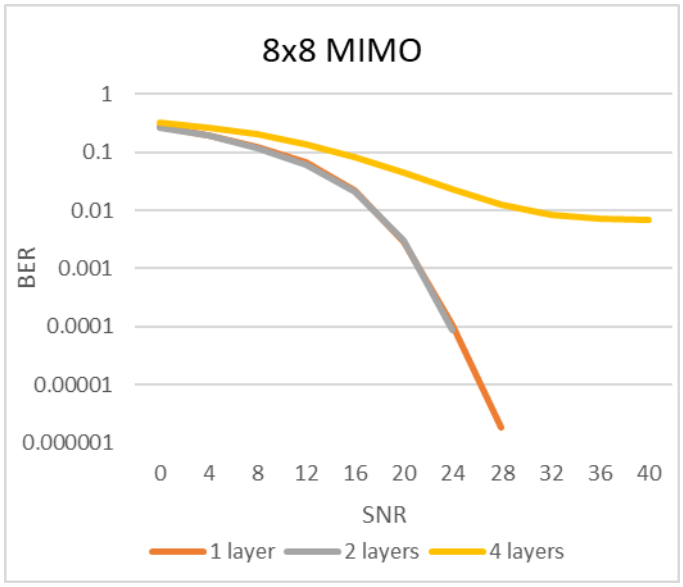

b) BER at RX=4

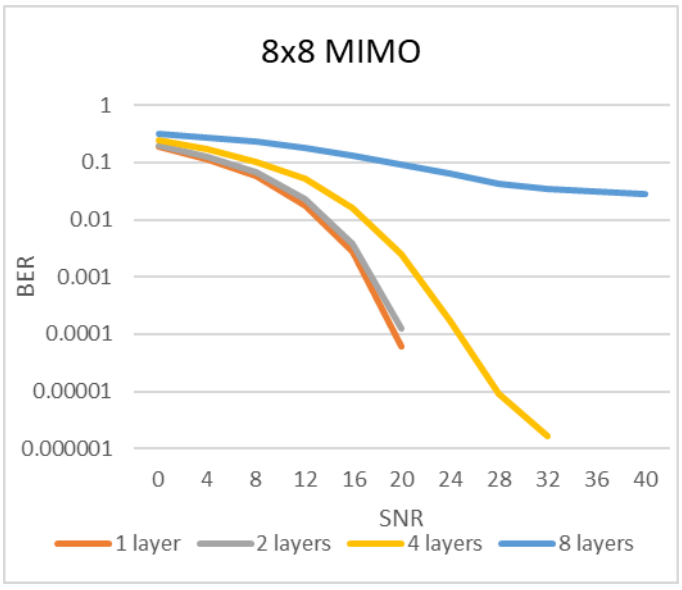

c) BER at RX=8

Figure 9-6:BER using 8x8 at the GNB for RX 2, 4, and 8 at the UE side

9.3.3 BER when beamforming with 16x16 MIMO at the gNB

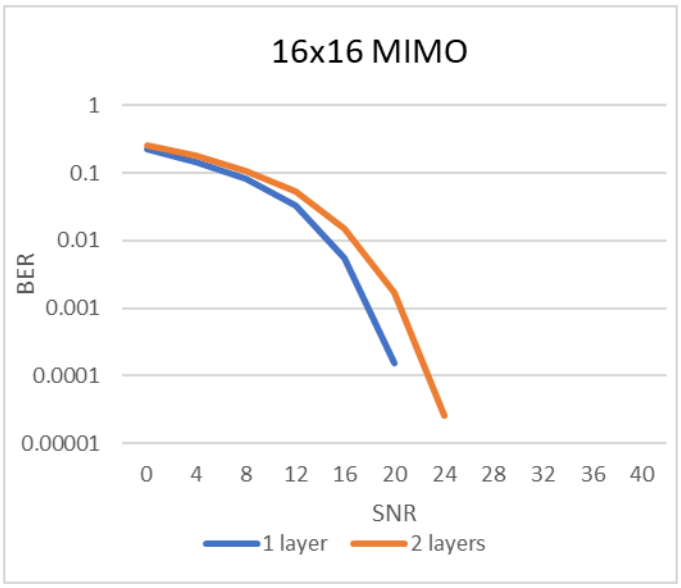

a) BER at RX=2

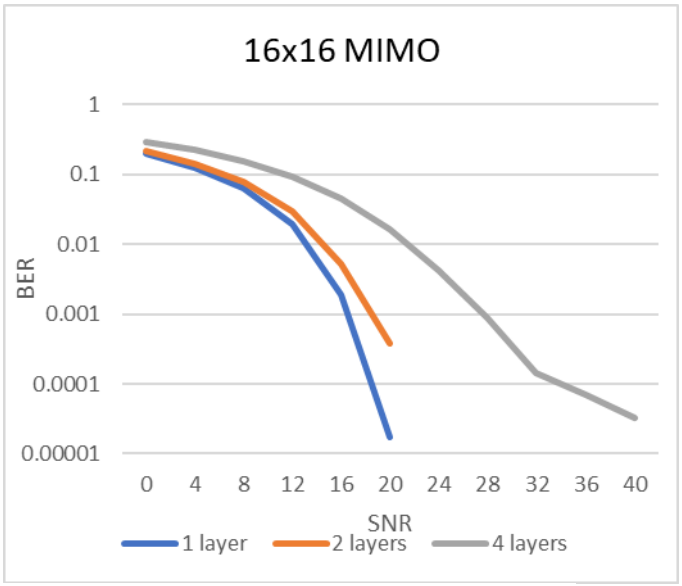

b) BER at RX=4

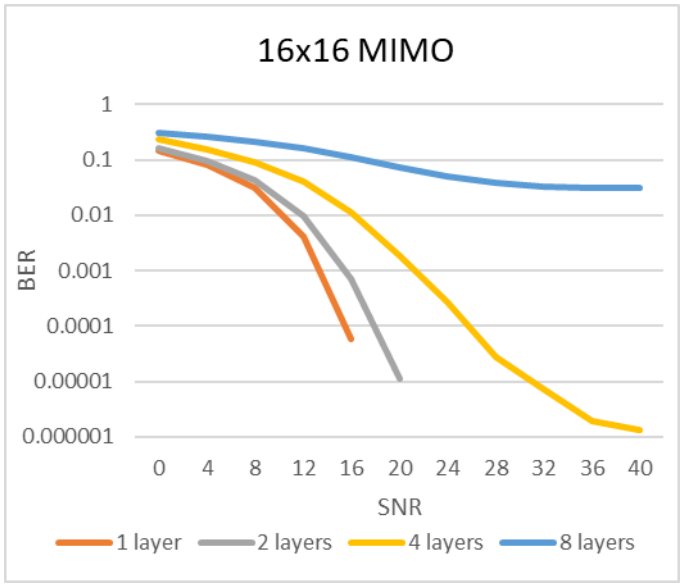

c) BER at RX=8

Figure 9-7:BER using 16x16 at the GNB for RX 2, 4, and 8 at the UE side

9.3.4 BER when beamforming with 32x32 MIMO at the g

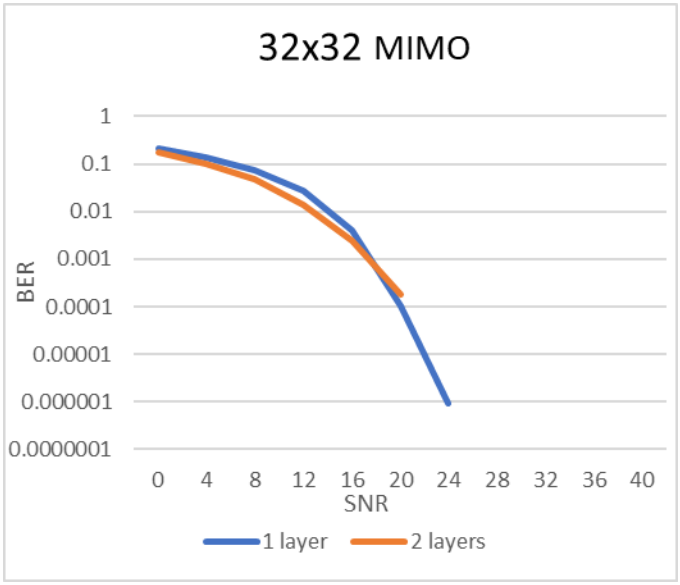

a) BER at RX=2

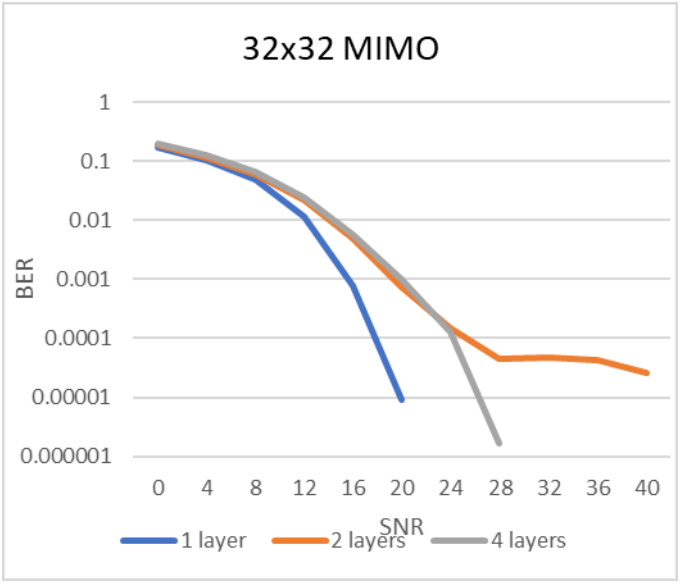

b) BER at RX=4

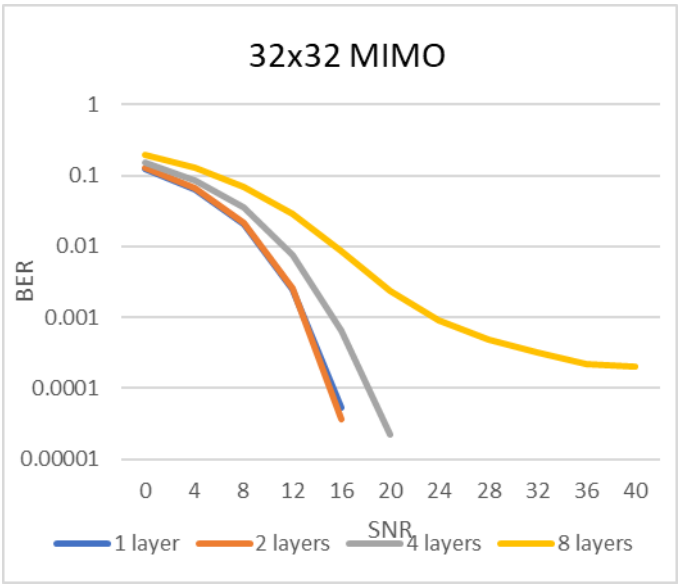

c) BER at RX=8

Figure 9-8:BER using 32x32 at the GNB for RX 2, 4, and 8 at the UE side

9.3.5 BER when beamforming with 64x64 MIMO at the gNB

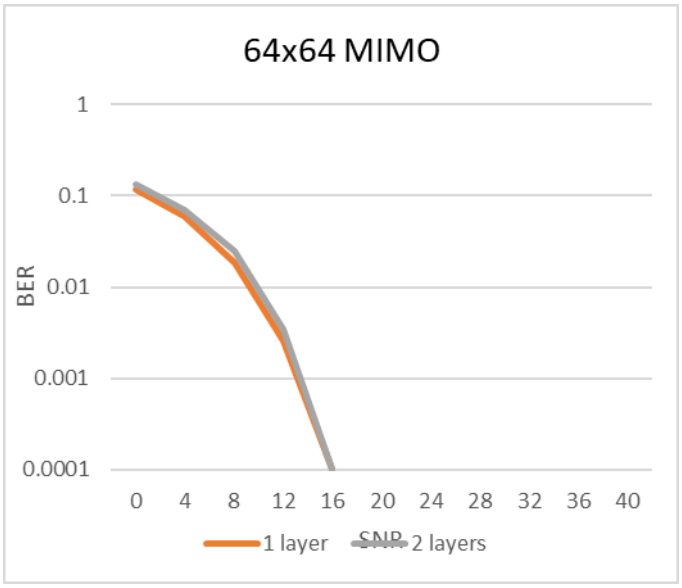

a) BER at RX=2

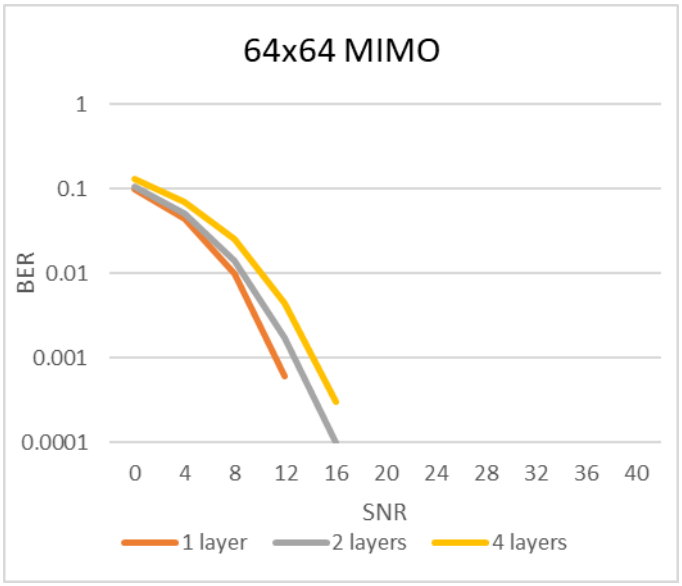

a) BER at RX=4

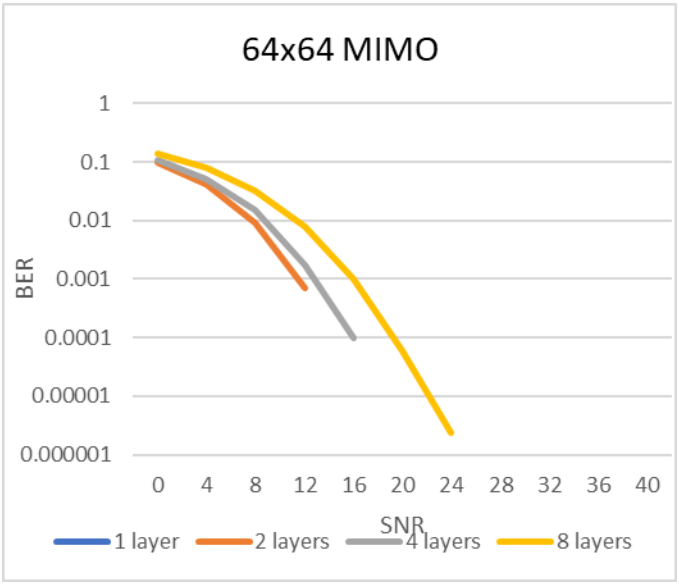

c) BER at RX=8

Figure 9-9:BER using 64x64 at the GNB for RX 2, 4, and 8 at the UE side

Figure 9.5, 9.6, 9.7, 9.8 and 9.9 depict the BER performance on sending multiple layers. The BER increases with increasing the number of layers sent to reach its worst value at 8 layers for different antenna configurations at the GNB.

From Fig.9.6c, Fig.9.7c and Fig.9.8c, the BER seems to be constant at SNR values from 28 dB to 40dB in case of sending 8 layers and this is due to the high interference resulted from each layer on the other layers. So, it can be depicted that the BER upon sending 8 layers even at high antenna configurations seems to be unacceptable at SNR values (<=12dB). Therefore sending 8 layers is an option to efficiently enjoy trade-off between throughput and BER.

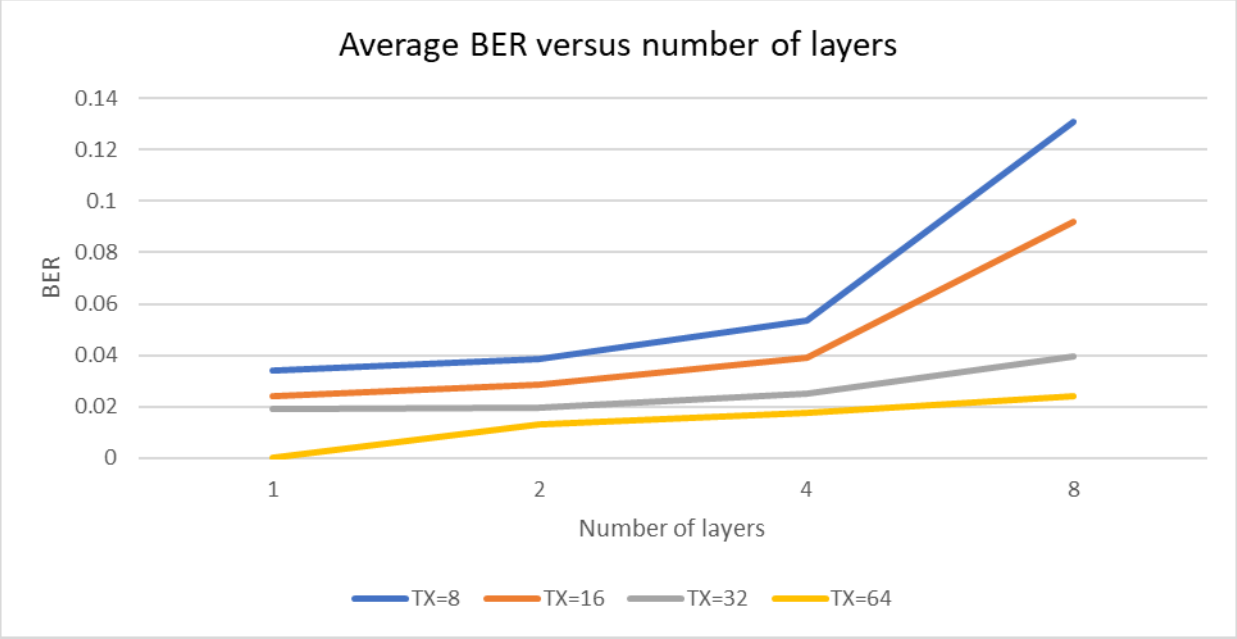

Figure 9-10:Average BER versus number of layers

9.4 BER performance for different number of antennas at the UE side

The standards do not limit the number of antennas at mobile handsets but unfortunately power and cost limitations do instead. It was found that latest mobile phones supporting 4.5G from vendors such as Apple, Samsung, Huawei, Sony, and LG have four antennas for reception and many proposals and trials were made in order to examine the 5G performance with different number of receiving antennas.

In this subsection BER is computed for different antenna configurations at the mobile to analyze the UE performance and whether increasing the number of antennas in mobiles are worthy or not, and if it is, new solutions can be found in order to reduce the cost of the mobile phones and reduce its complexity. The following table shows the parameters of the simulation of this subsection.

Table 9-6:Simulation Parameters and values for studying the BER performance versus number of antennas at the UE side

Parameter	Value
Allocated NRB	10
RX antenna	1,2,4,8
Channel Model	TDL C
MIMO configuration	4x4, 8x8, 16x16, 32x32 and 64x64
Number of layers	1,2,4

9.4.1 BER performance on sending 1 layer and receiving it with different number of antennas at the UE

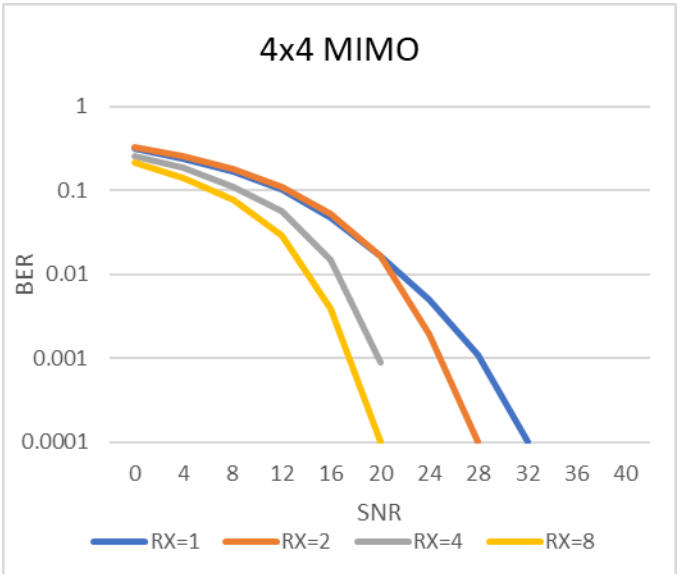

a) BER for 4x4 MIMO

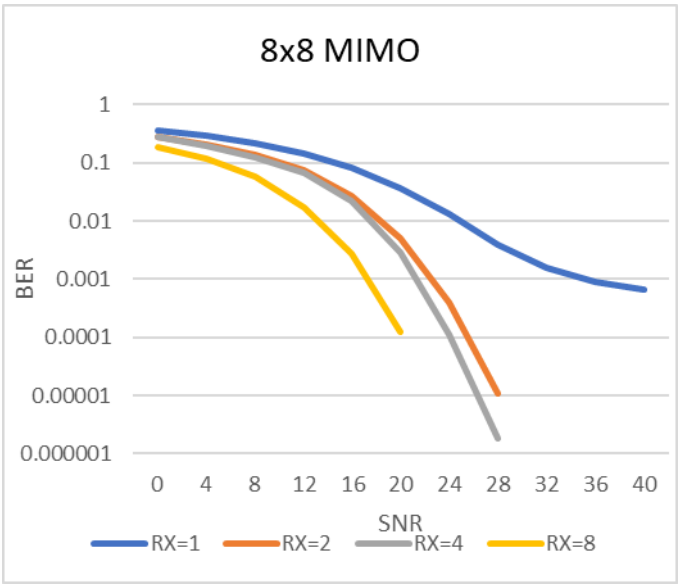

b) BER for 8x8 MIMO

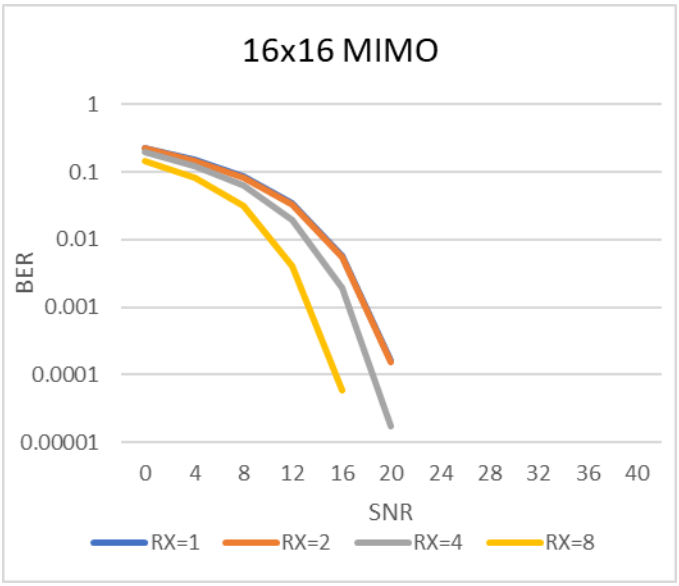

c) BER for 16x16 MIMO

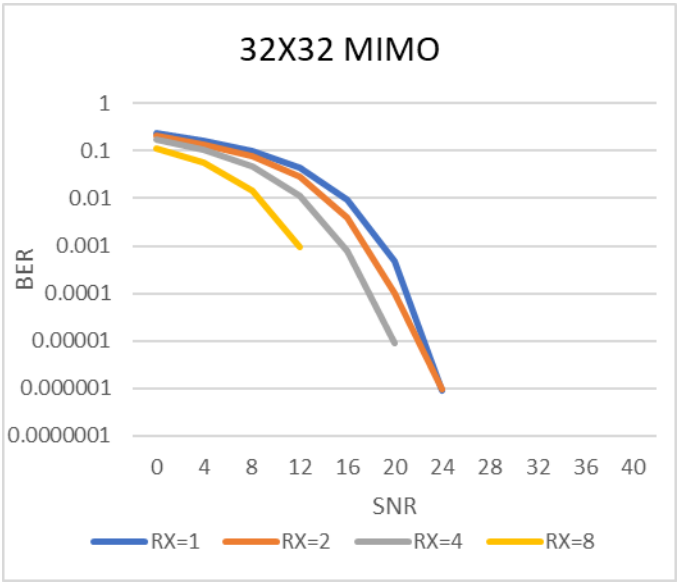

d) BER for 32x32 MIMO

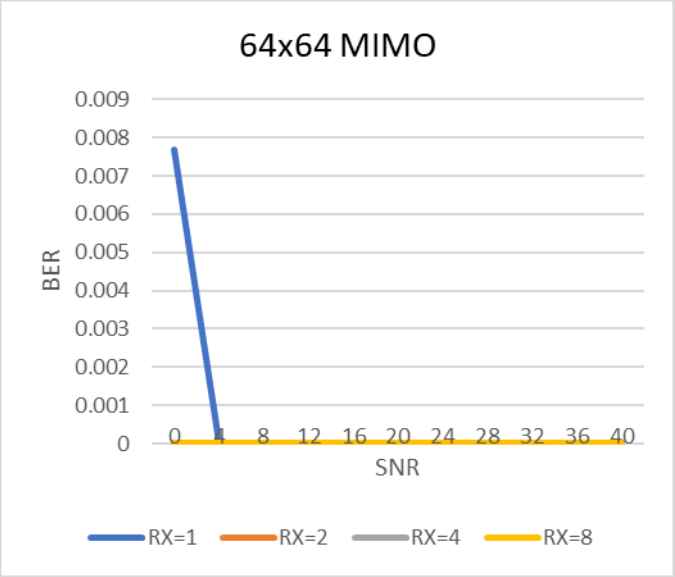

e) BER for 64x64 MIMO

Figure 9-11:BER performance versus different number of receivers at the gNB on sending 1 layer

9.4.2 BER performance on sending 2 layers and receiving it with different number of antennas at the UE

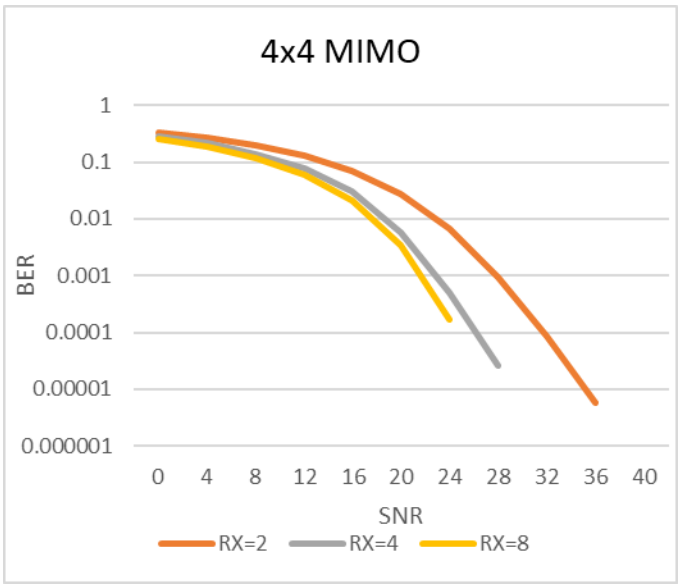

a) BER for 4x4 MIMO

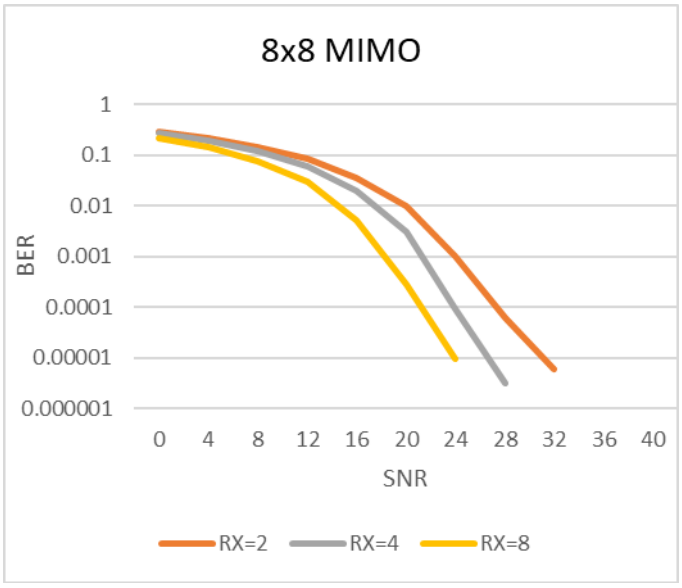

b) BER for 8x8 MIMO

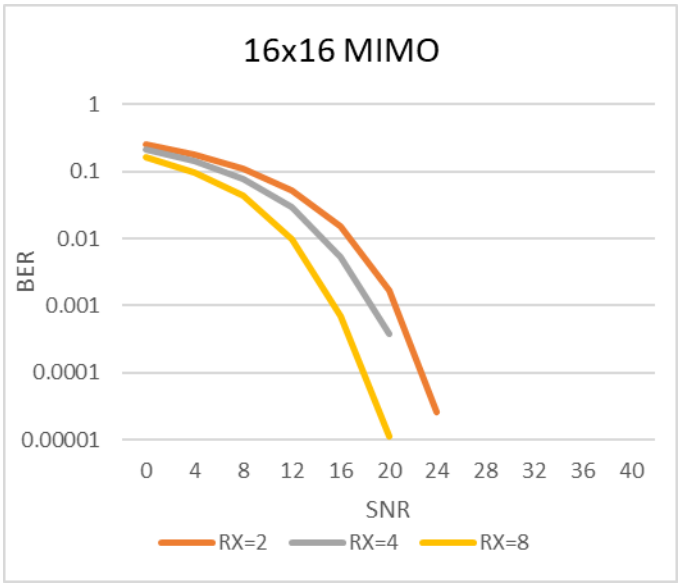

c) BER for 16x16 MIMO

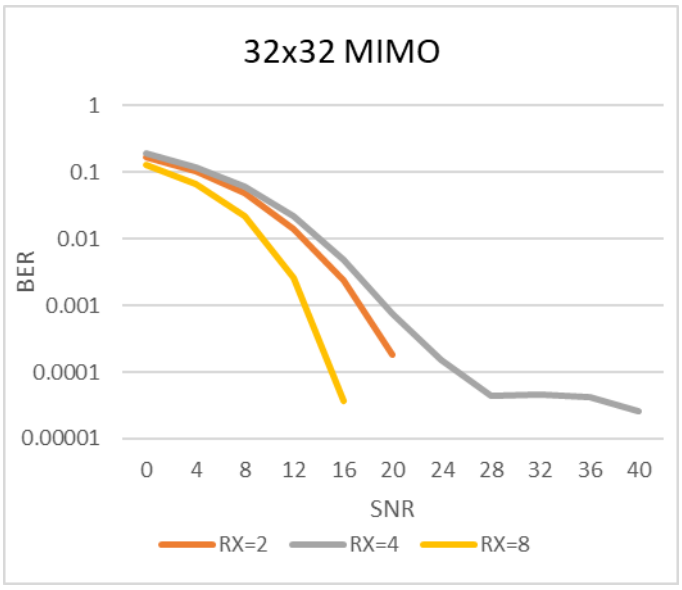

d) BER for 32x32 MIMO

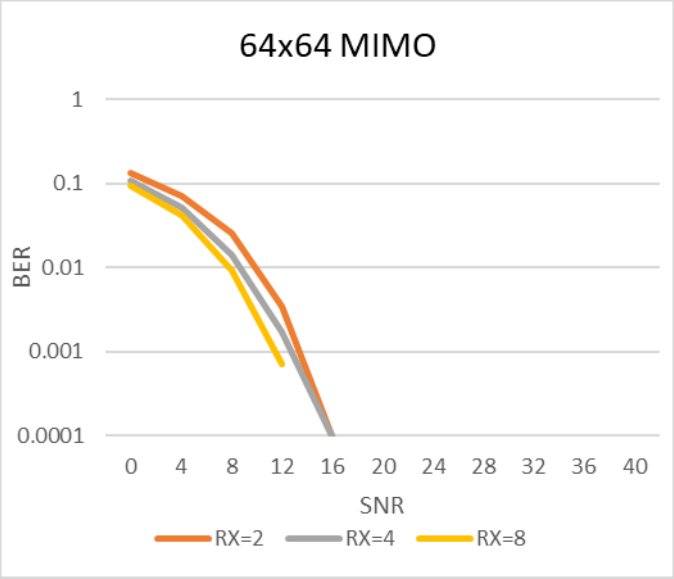

e) BER for 64x64 MIMO

Figure 9-12:BER performance versus different number of receivers at the gNB on sending 2 layers

9.4.3 BER performance on sending 4 layers and receiving it with different number of antennas at the UE

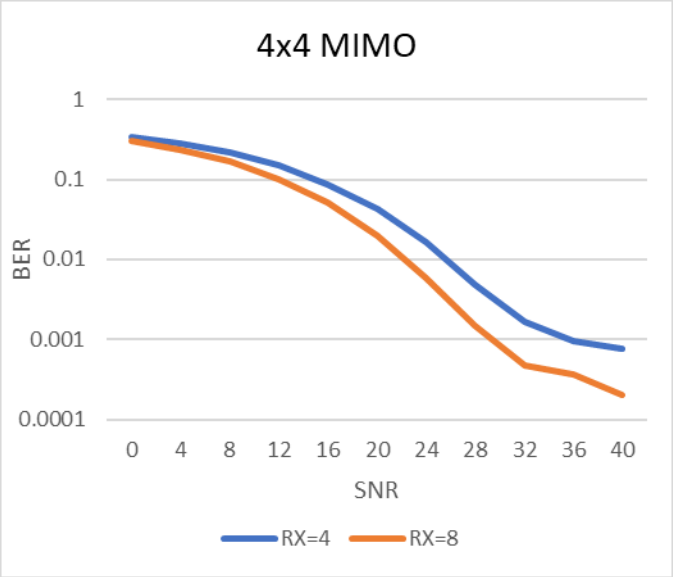

a) BER for 4x4 MIMO

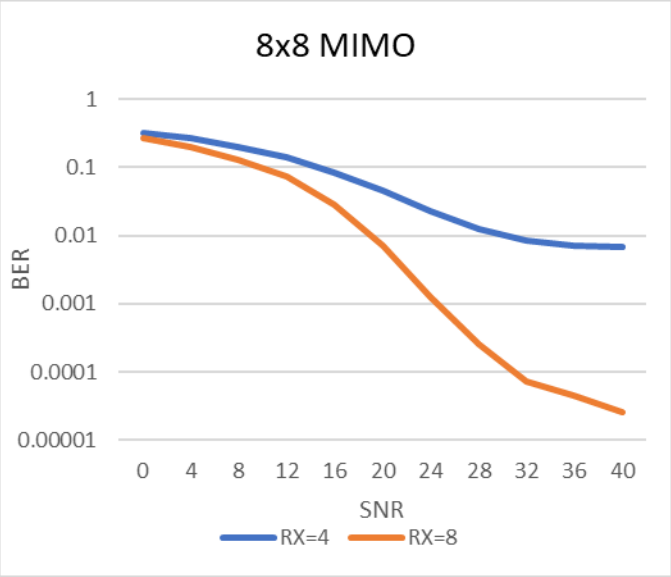

b) BER for 8x8 MIMO

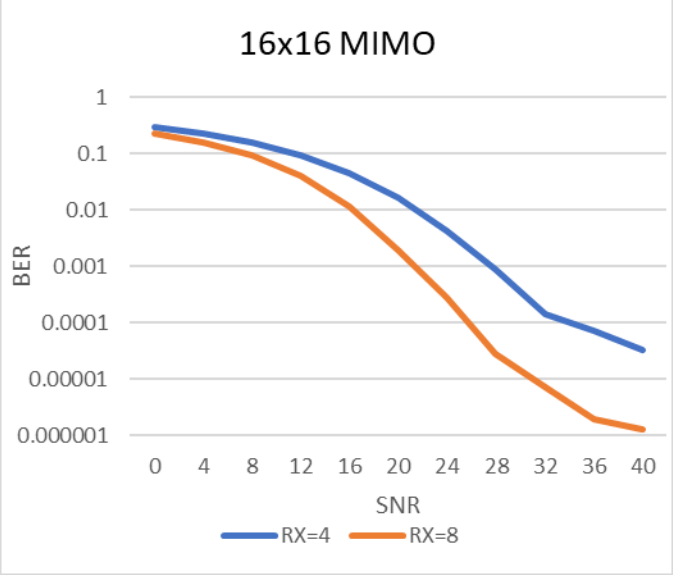

c) BER for 16x16 MIMO

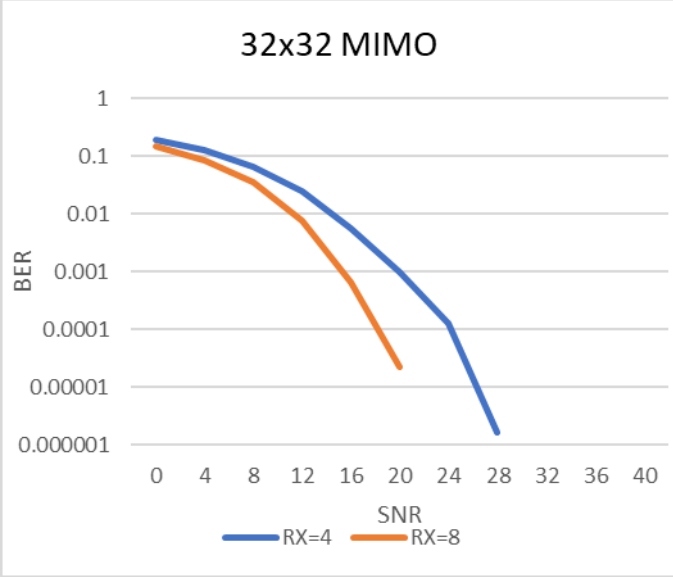

d) BER for32x32 MIMO

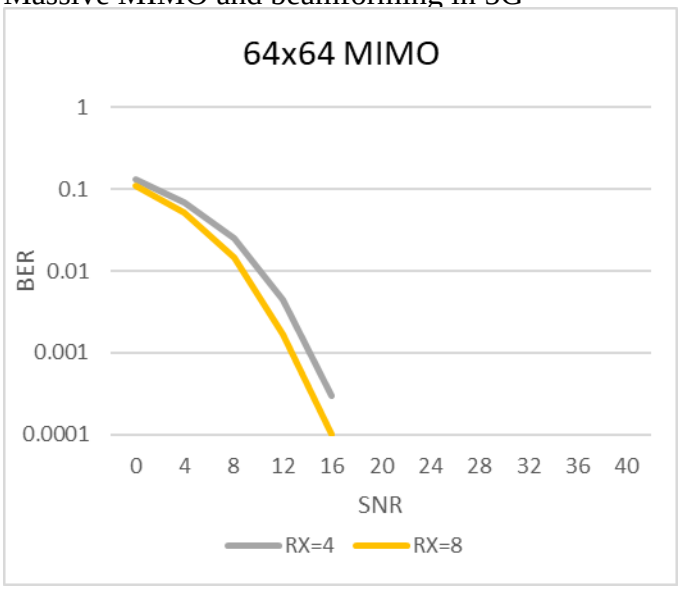

e) BER for 64x64 MIMO

Figure 9-13:BER performance versus different number of receivers at the gNB on sending 4 layers

Figure 9-11, figure 9-12 and figure 9-13 demonstrate the impact of increasing the number of antennas at the UE side. It is observed that varying the number of antennas at the UE side showed insignificant SNR saving and no BER improvement except at SNR values above 16 to 20 dB, so as a result it is not favorable or no need to increase the number of antennas at the UE side for bad channel conditions (low SNR). Instead, for SNR values above 20 dB the BER is clearly improved.

where using multiple receiving antennas improves the link quality and reliability, as it provides diversity that results in receiving slightly different versions of the signal, then combining them to form a better estimate of the transmitted signal than having one receiving antenna.

9.5 BER performance for different TDL models

This subsection mainly focuses on the performance of the BER upon beamforming different number of data streams in two different TDL models; LOS and NLOS. The following table lists the value of parameters used in this subsection simulations.

Table 9-7:Simulation Parameters and values for studying the BER performance for LOS and NLOS

Parameter	Value
Channel	TDL C, TDL E
Allocated NRB	10
Number of layers	1, 2, 4 and 8
RX antennas	1, 2, 4, 8
Number of taps	24, 14

9.5.1 BER for 4x4 antenna configuration

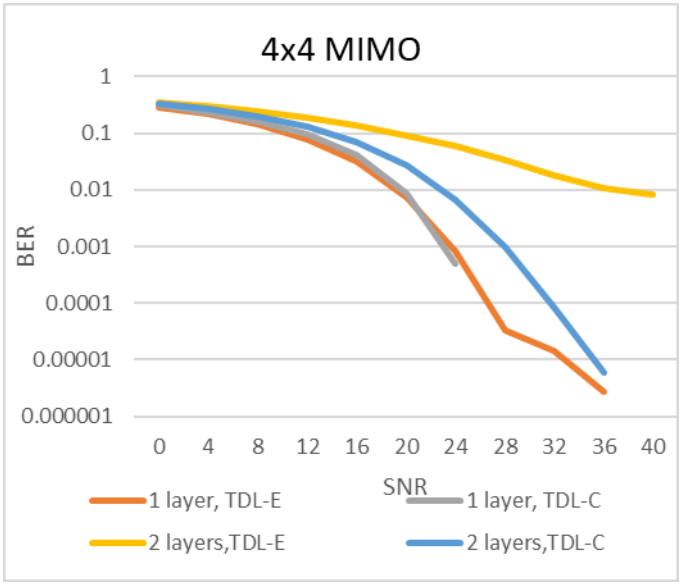

a) BER at RX=2

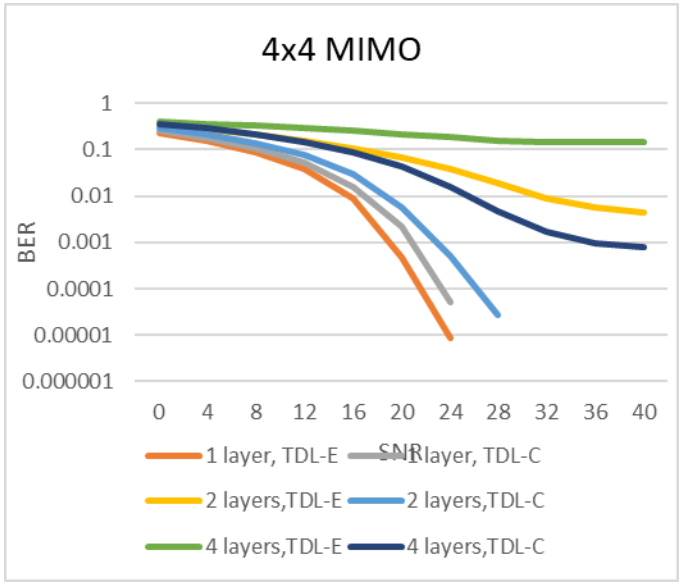

a) BER at RX=4

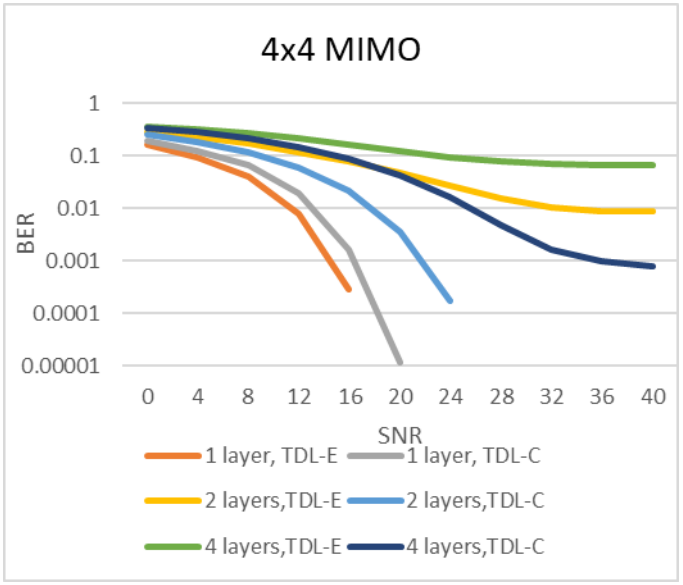

c) BER at RX=8

Figure 9-14:BER performance for LOS and NLOS using 4x4 MIMO

9.5.2 BER for 8x8 antenna configuration

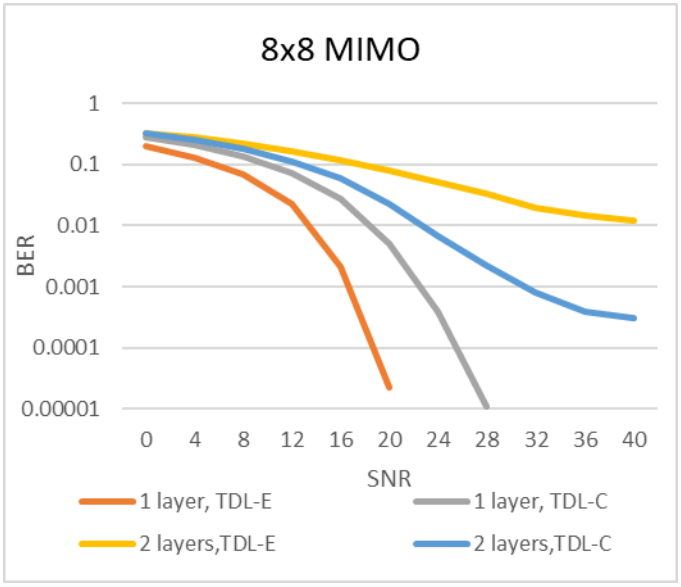

a) BER at RX=2

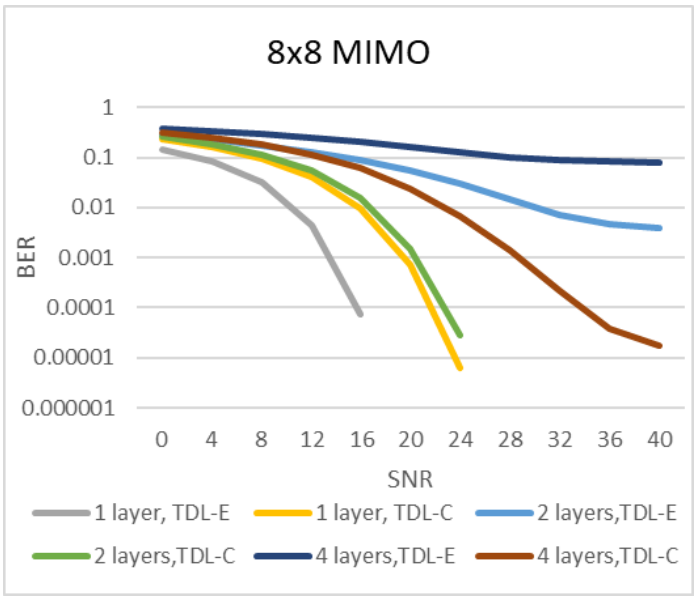

a) BER at RX=4

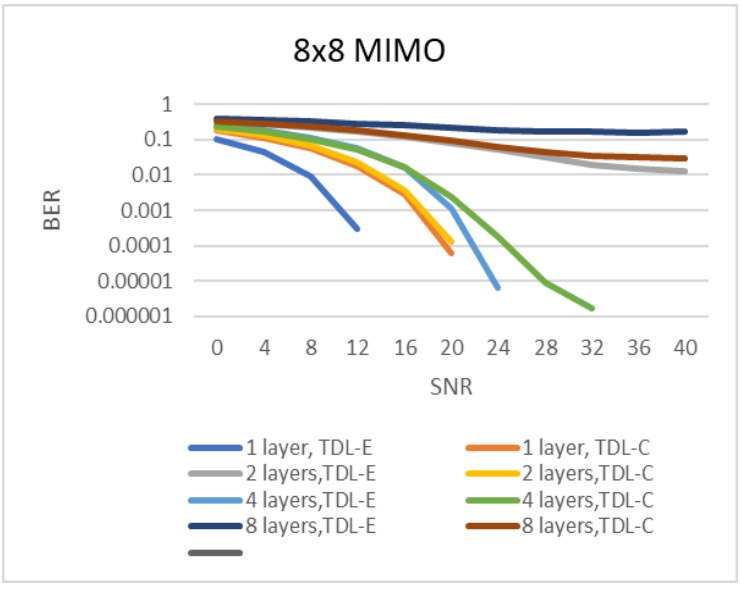

c) BER at RX=8

Figure 9-15:BER performance for LOS and NLOS using 8x8 MIMO

9.5.3 BER for 16x16 antenna configuration

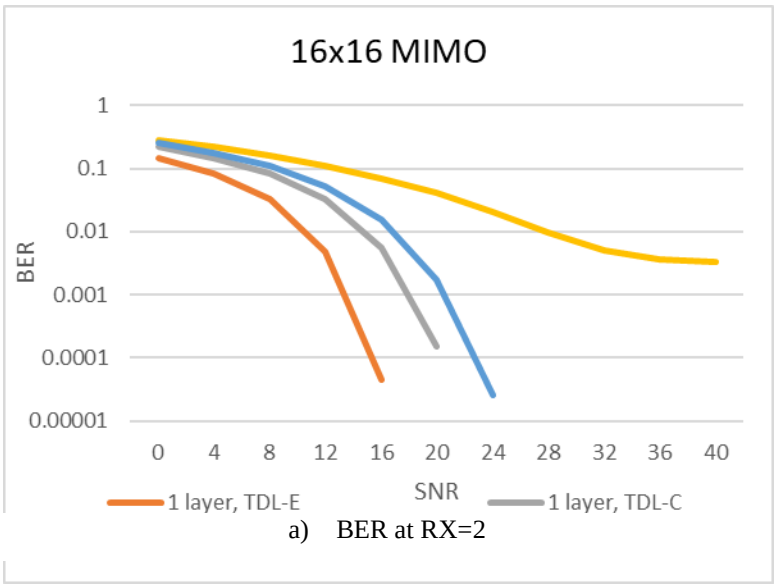

a) BER at RX=2

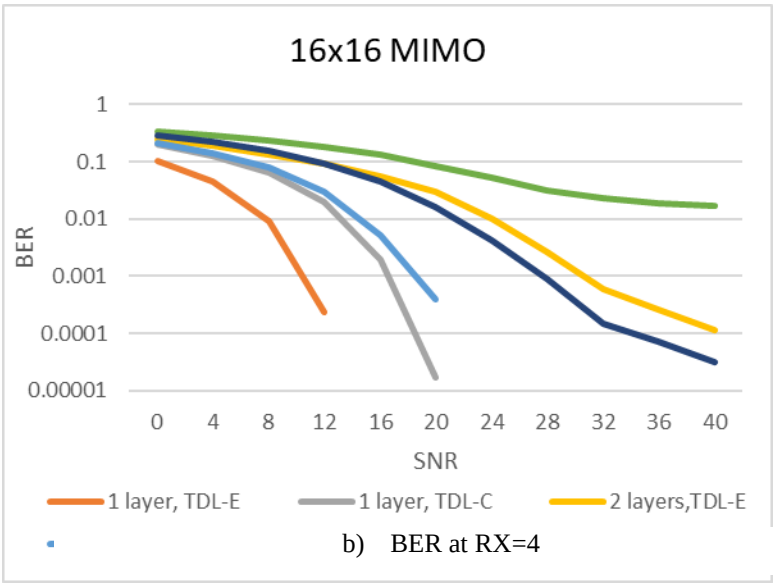

b) BER at RX=4

Figure 9-16:BER performance for LOS and NLOS using 16x16 MIMO

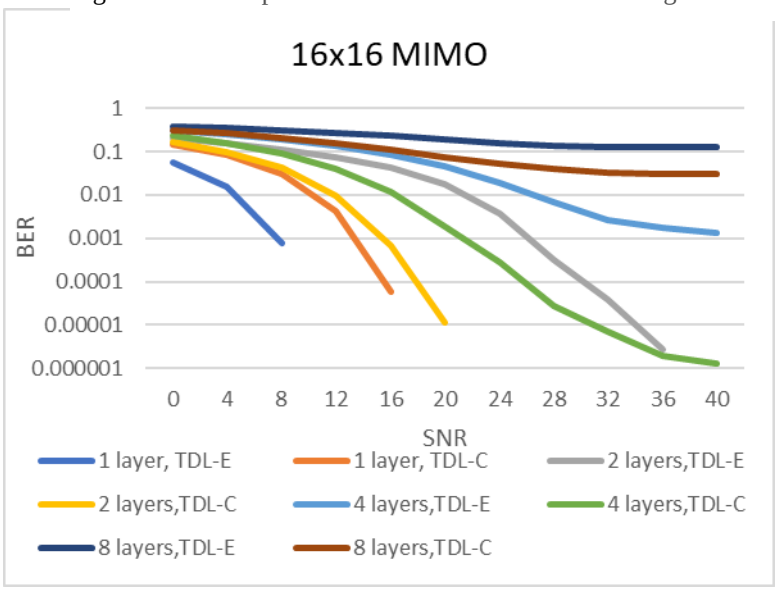

c) BER at RX=8

9.5.4 BER for 32x32 antenna configuration

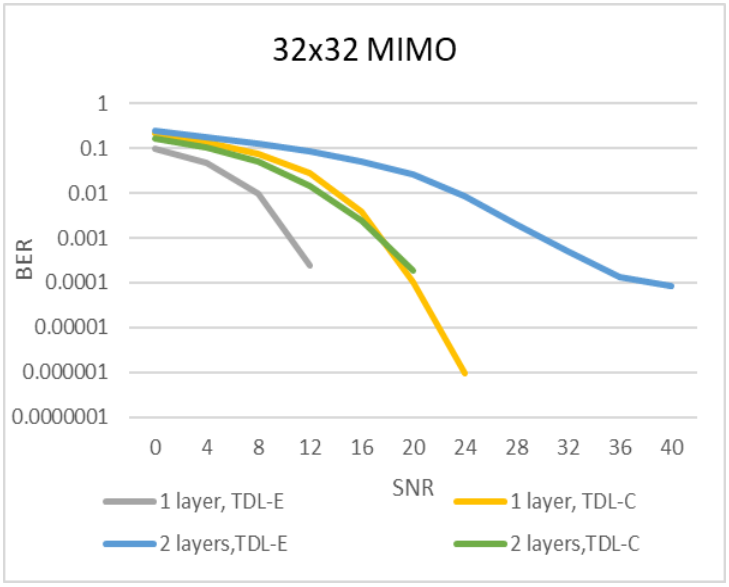

a) BER at RX=2

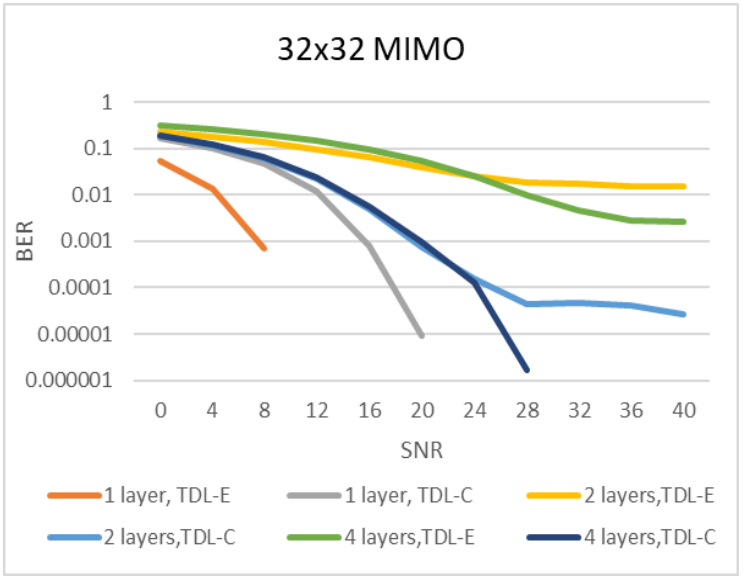

b) BER at RX=4

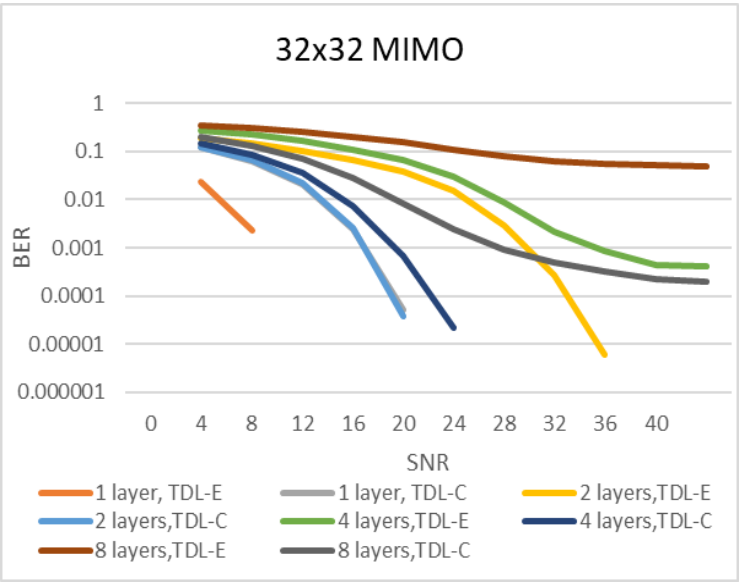

c) BER at RX=8

Figure 9-17:BER performance for LOS and NLOS using 32x32 MIMO

9.5.5 BER for 64x64 antenna configuration

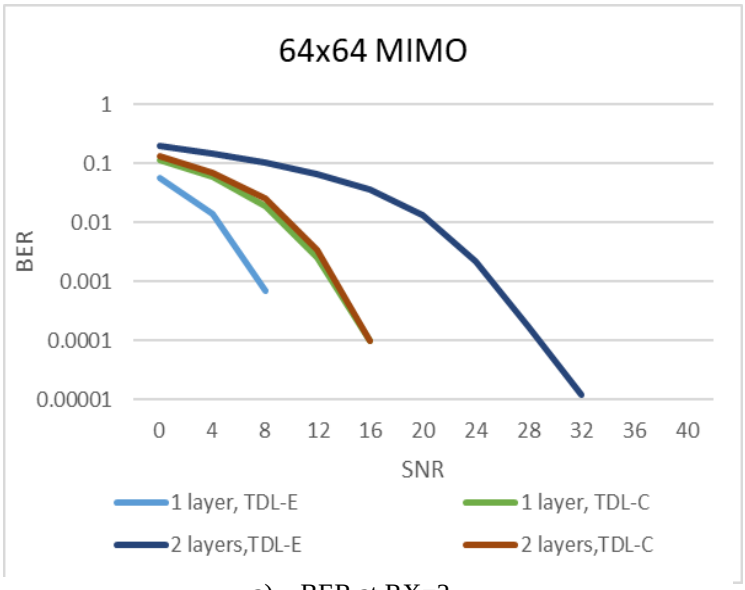

a) BER at RX=2

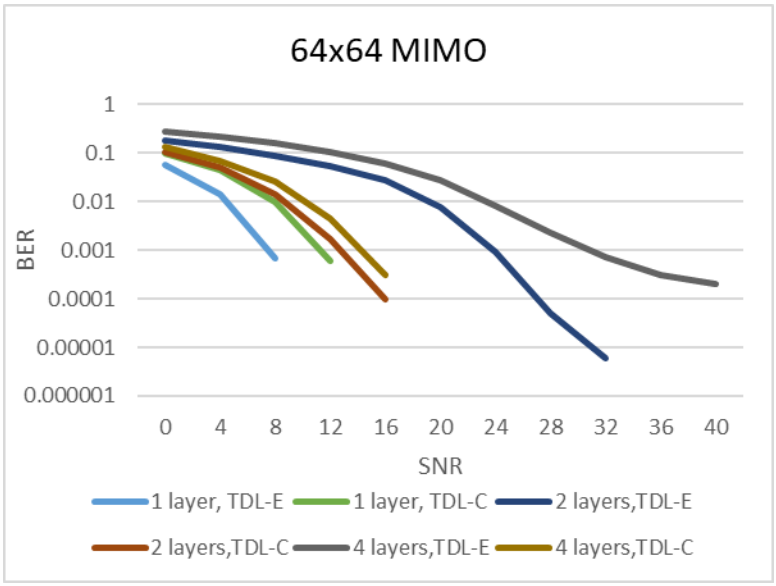

a) BER at RX=4

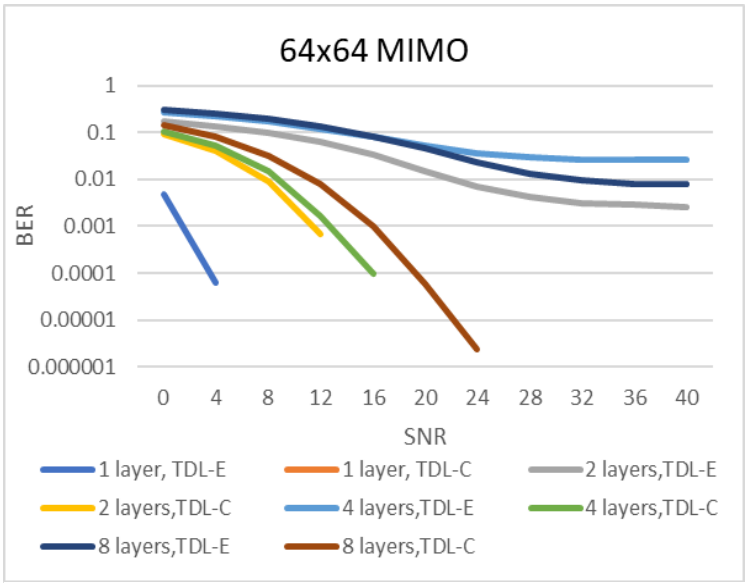

c) BER at RX=8

Figure 9-18:BER performance for LOS and NLOS using 64x64 MIMO

In case of NLOS channel (TDL-C), on increasing the number of antennas at the GNB and the number of receiving antennas at the UE, a significant improvement in the BER performance occurs, while in the case of LOS channel (TDL-E) it is clearly shown that BER is almost constant for SNR range especially when sending 4 and 8 layers and this is due to the high interference that occurs from each layer on the other layers. Fig, 9-14 c and Fig.9-15 c show that even when using 32x32 MIMO or 64x64 MIMO at the GNB side for LOS channel, the BER seems to be unacceptable evet at high SNR values.

From Fig.9-19 it can be concluded that if the channel is LOS (TDL-E) it is advisable to send lower data streams (1 layer)as the number of the taps is lower (only 14) and unexpectedly for NLOS channels it can perform better as the number of data streams increase as it has higher number of tabs (24) and as the number of taps increase, the channel is expected to perform better as there are more reflections and in the multipath channels, reconstruction of the transmitted signal at receiver is higher as probability of having constructive interference is higher

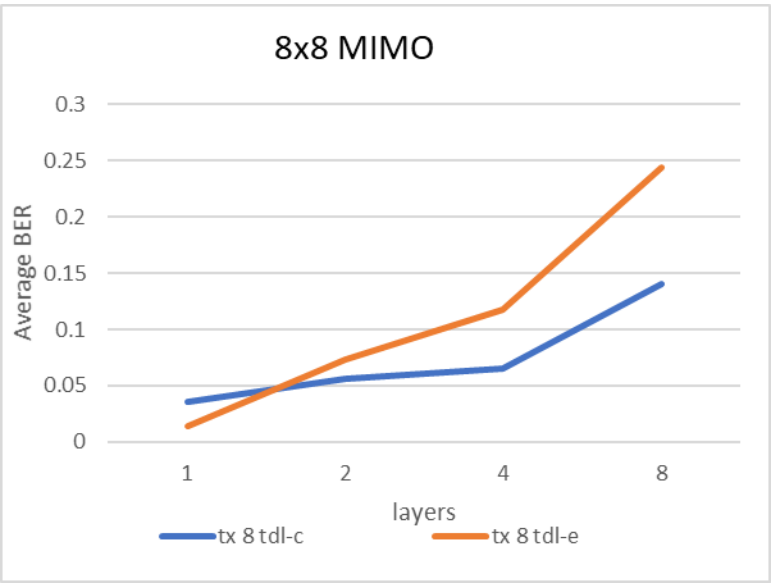

a) Average BER using 64x64 MIMO configuration

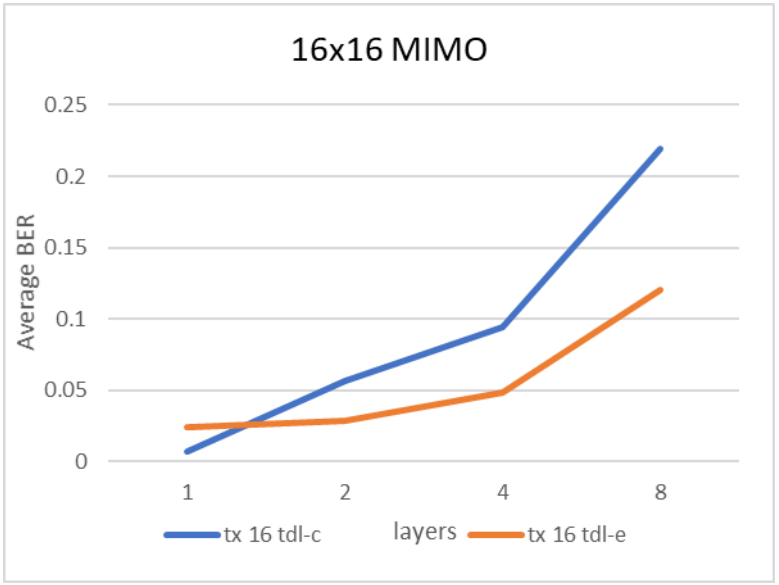

b) Average BER using 16x16 MIMO configuration

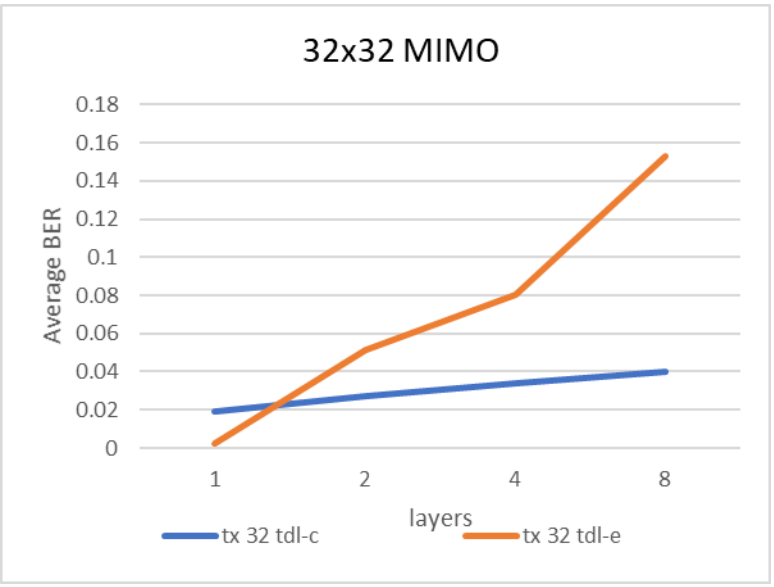

c) Average BER using 32x32 MIMO configuration

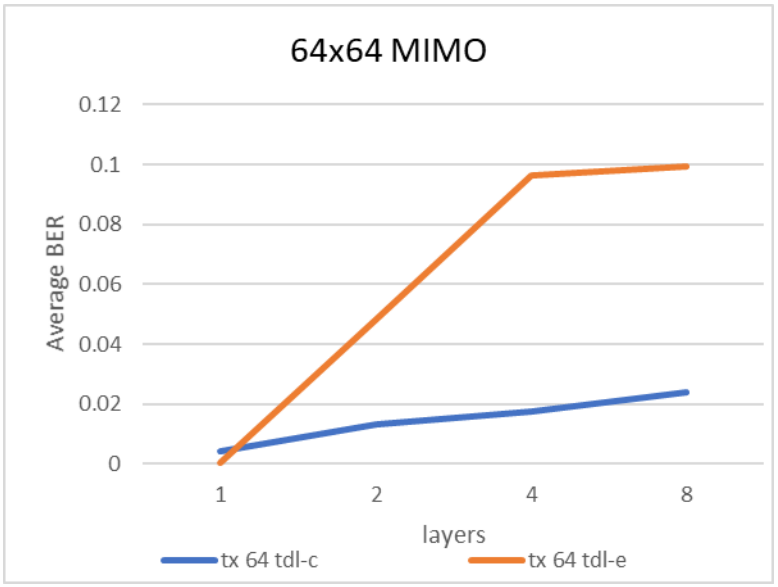

d) Average BER using 8x8 MIMO configuration

Figure 9-19:The average BER performance versus sending different number of layers for different antenna configurations

9.6 Perfect and Imperfect channel estimation:

Unfortunately, channel estimates are never perfect, which leads to performance degradations if these channel estimates, instead of perfect channel knowledge. In this subsection a comparative analysis is done to chow the difference and the impact of not knowing the perfect channel in the BER. Major among the parameters used for these simulations' subsection is outlined in the Table 9-8.

Table 9-8:Simulation Parameters and values for studying the BER performance for perfect and imperfect channel estimation

Parameter	Value
RX antenna	8
Allocated NRB	10
Number of layers	1, 2, 4
Channel	TDL C
MIMO Configuration	8x8, 16x16, 32x32 and 64x64

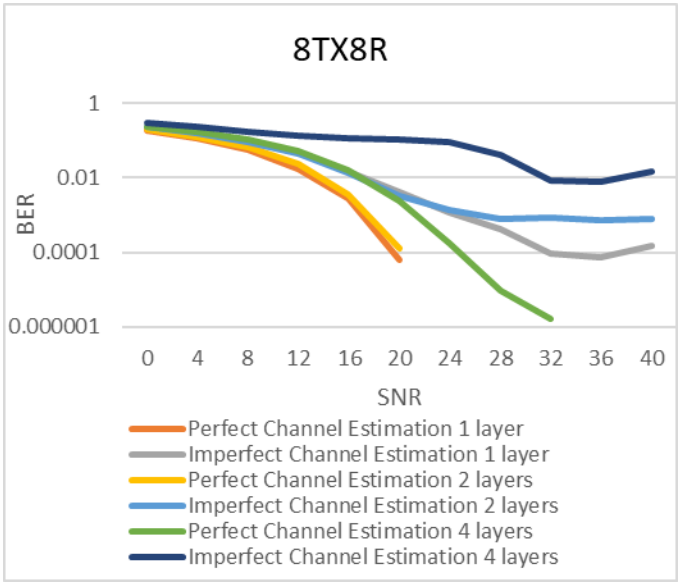

a) BER at 8 TX

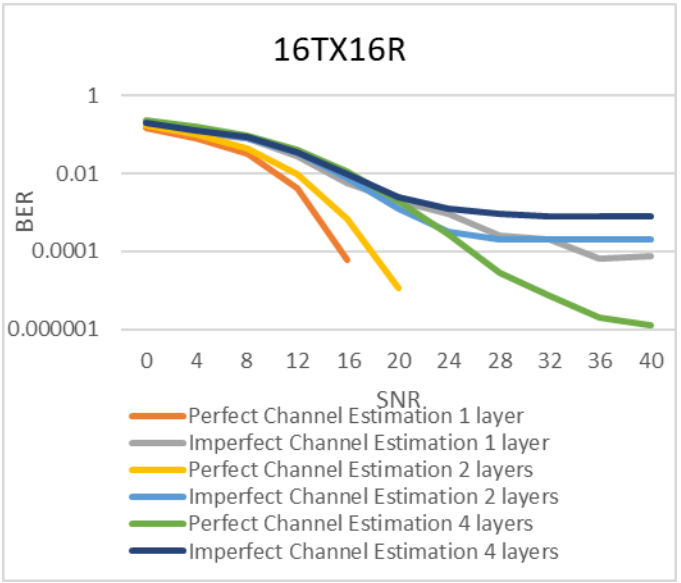

b) BER at 16 TX

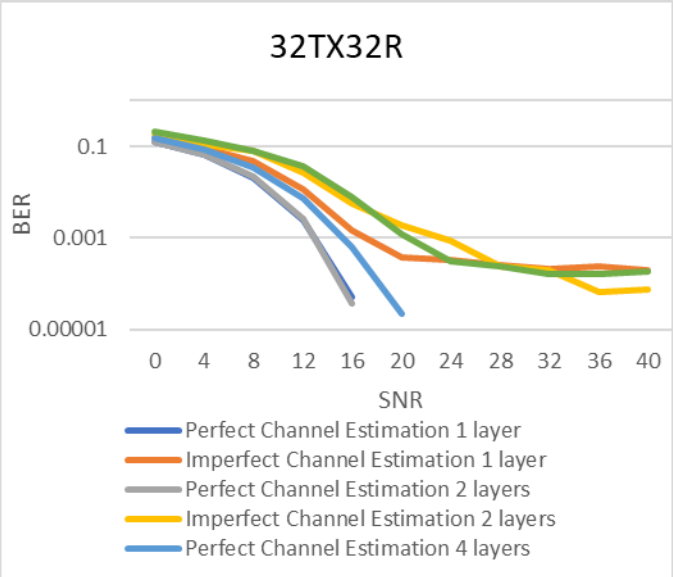

c) BER at 32 TX

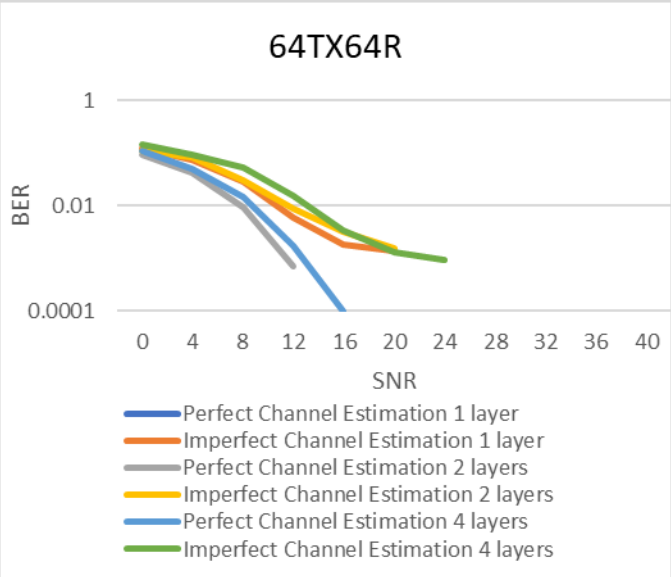

d) BER at 64 TX

Figure 9-20: perfect vs imperfect channel estimation

Figure 9-20 depicts the impact of the imperfect channel estimation. MMSE equalizer is used at the UE side to reduce inter symbol interference and combat the distortive channel effects hence maximizes the probability of correct decision.

Conclusion

To conclude this thesis aimed to identify the 5G NR physical layer. No doubts that the 5G is going nowadays through a massive deployment to support not only the telecommunication field as it is expected to drive global economic growth.

Our role in this project was to study the physical layer which is the start of network creation between devices. Throughout our work, we studied the impact of different parameters in the BER and throughput performance for a SISO case then after that we took into consideration that the 5G NR will be mainly be dealing with massive number of antennas so, an analysis is also made for the MIMO case with beamforming technology. The results achieved in this thesis represents a solid starting point for a future vision in the performance of the 5G system.

Future work

In this thesis all simulations that we explained and discussed based on release15 from GPP in which only (eMBB) use case was covered, but now the work to further enhance the 5G NR Release15 technology has already begun, and will not only bring even better mobile broadband efficiencies and experiences, but also cover enhancement Ultra-Reliable Low-Latency Communications (URLLC) support in the 5G Core network, and 5G New radio (NR) support for Industrial Internet of Things.

In response to COVID-19, 3GPP has delayed the next two 5G standards releases 16 and 17 – by three months.

References

[1] Mathworks.com. 2020. *5G New Radio Design With MATLAB*. [online] Available at: <https://www.mathworks.com/campaigns/offers/5g-technology-ebook.html> [Accessed 16 March 2020].

[2] Etsi.org. 2020. [online] Available at: <https://www.etsi.org/deliver/etsi_ts/138200_138299/138211/15.02.00_60/ts_138211v150200p.pdf> [Accessed 16 March 2020].

[3] Sharetechnote.com. 2020. *5G - What Is 5G ? - Sharetechnote*. [online] Available at: <https://www.sharetechnote.com/html/5G/5G_Definition.html> [Accessed 5 April 2020].

[4] Sharetechnote.com. 2020. *5G | Sharetechnote*. [online] Available at: <https://www.sharetechnote.com/html/5G/5G_CSI_RS_Codebook.html#What_is_Codebook> [Accessed 5 April 2020].

[5] Remcom. 2020. *Massive MIMO Beamforming, Spatial Multiplexing And Diversity — Remcom*. [online] Available at: <https://www.remcom.com/wireless-insite-mimo-beamforming-spatial-multiplexing-and-diversity> [Accessed 5 April 2020].

[6] Ali, E., Ismail, M., Nordin, R. and Abdulah, N., 2017. Beamforming techniques for massive MIMO systems in 5G: overview, classification, and trends for future research. *Frontiers of Information Technology & Electronic Engineering*, 18(6), pp.753-772.

[7] M, R. and P, M., 2011. SVD-BASED TRANSMIT BEAMFORMING FOR VARIOUS MODULATIONS WITH CONVOLUTION ENCODING. *ICTACT Journal on Communication Technology*, 02(03), pp.393-399.

[8] 3gpp.org. 2020. *LTE-Advanced*. [online] Available at: <https://www.3gpp.org/technologies/keywords-acronyms/97-lte-advanced?fbclid=IwAR12qLhVd6cg-eaYKXtUvQKMqRs1NoBAhCZNwb3SXRQhNx-eu4OhuKaiJBQ> [Accessed 16 May 2020].

[9] notes, e., 2020. *4G LTE MIMO: Multiple Input Multiple Output » Electronics Notes*. [online] Electronics-notes.com. Available at: <https://www.electronics-notes.com/articles/connectivity/4g-lte-long-term-evolution/mimo.php?fbclid=IwAR1OOyubrvWt7cdP7zukrXskE5xQU2jZEMonCD3sOYGTy5LVT5klPLzUAEE> [Accessed 16 May 2020].

[10] Ctw2018.ieee-ctw.org. 2020. [online] Available at: <http://ctw2018.ieee-ctw.org/files/2018/05/5G-NR-CTW-final.pdf> [Accessed 16 May 2020].

[11] Arxiv.org. 2020. [online] Available at: <https://arxiv.org/pdf/1804.01908.pdf> [Accessed 16 May 2020].

[12] Sharetechnote.com. 2020. *5G | Sharetechnote*. [online] Available at: <http://www.sharetechnote.com/html/5G/5G_FrameStructure.html> [Accessed 16 May 2020].

[13] DAHLMAN, E., PARKVALL, S. and PEISA, J., 2015. 5G Wireless Access. *IEICE Transactions on Communications*, E98.B(8), pp.1407-1414.

[14] Zaidi, A., Baldemair, R., Tullberg, H., Bjorkegren, H., Sundstrom, L., Medbo, J., Kilinc, C. and Da Silva, I., 2016. Waveform and Numerology to Support 5G Services and Requirements. *IEEE Communications Magazine*, 54(11), pp.90-98.

[15] Stepanets, I. and Fokin, G., 2018. FEATURES OF MASSIVE MIMO IN 5G NETWORKS. *LastMile*, (1), pp.46-52.